



THÈSE / UNIVERSITÉ DE RENNES 1

sous le sceau de l'Université Bretagne Loire

pour le grade de

DOCTEUR DE L'UNIVERSITÉ DE RENNES 1

Mention : Traitement du signal et télécommunications

Ecole doctorale MATISSE

présentée par

Nahed Jalloul

préparée à l'unité de recherche LTSI - INSERM U1099

Laboratoire Traitement du Signal et de l'Image
Université de Rennes 1

**Development of
a System of
Acquisition and
Movement Analysis:
Application on
Parkinson's Disease**

Thèse soutenue à Rennes

le 12 Décembre 2016

devant le jury composé de :

M. VESIN Jean-Marc

MER, PhD, EPFL, Lausanne Suisse / Rapporteur

M. ELBADAoui Mohamed

Pr, Université de Saint Etienne / Rapporteur

M. DUCHENE Jacques

Pr, Université de Technologie de Troyes /
Examineur

Mme PORÉE Fabienne

MCU, Université de Rennes 1 / Co-Directrice

M. CARRAULT Guy

Pr, Université de Rennes 1 / Directeur

Acknowledgments

First and foremost, I would like to extend my sincere gratitude to my advisors, Prof. Guy Carrault and Dr. Fabienne Porée. They have been wonderful mentors over the past three years and it has been a true pleasure working with them. I would also like to thank the team at Biotrial, whose members have contributed immensely to the success of this project. Their efforts were essential in the advancement of this work. I gratefully acknowledge Biotrial's role as a funding source that made my PhD possible. I would like to express my heartfelt appreciation to the volunteers participating in this study for offering their time and efforts, and without whom this work would not have been possible. Finally, I would like to thank the members of the jury who took the time to review this work.

Contents

Résumé	xvii
Introduction	1
I Clinical context	7
I Parkinson’s Disease and Levodopa Therapy	9
1 Epidemiology and Pathophysiology	9
2 Clinical Diagnosis	12
3 Motor Symptoms and Therapeutic Measures	13
3.1 Major Motor Symptoms of PD	13
3.2 Deep Brain Stimulation	14
3.3 Treatment by Medication: Levodopa Therapy	16
4 Rating Scales	20
5 Conclusion	21
II Ambulatory Monitoring of Levodopa Induced Dyskinesia and PD Motor Sympt-	
toms	27
1 Wearable Sensors and Systems	27
2 Movement Analysis and Objective Assessment of PD	30
2.1 Measuring Human Motion Through IMUs	30
2.2 Objective Measurement of PD Motor Symptoms and Complications	34
3 Objectives of the Thesis	36
II Automated, Objective Quantification of Levodopa Induced Dyskinesia	45
III Materials and Measurement Protocol	47
1 Activity Monitoring and Recognition using IMUs	47
2 Ambulatory Monitoring System	49
2.1 Shimmer3 Inertial Measurement Units	49
2.2 System Architecture	50

3	Acquisition Protocol, Database and Measurement Technique	51
3.1	Laboratory Setting	51
3.2	Sensor Placement	53
3.3	Presentation of the Database	54
3.4	Data Acquisition	55
4	Conslusion	59
IV Pattern Recognition for Activity Classification and Dyskinesia Detection		65
1	Data Processing Methods	65
1.1	Preprocessing	68
1.2	Activity Classification	69
1.3	Dyskinesia Detection	73
2	Results	74
2.1	Performance Measures	75
2.2	Activity Classification	75
2.3	Dyskinesia Detection	77
2.4	Towards a Simplified System: Reduction of Number of Modules	80
2.5	Conclusion	83
V Complex Network Analysis for Activity Classification and Dyskinesia Detection		89
1	Graph Theory: Definitions and Methodology	89
1.1	Definitions	90
1.2	Directed Graphs and Weighted Graphs	91
2	Complex Network Analysis	91
2.1	Definitions	91
2.2	Network Measures: Mapping from a Complex Network to a Feature Vector	92
3	Methods	93
3.1	Network Construction	94
3.2	Data Processing	94
3.3	Network representation and computation of measures	96
3.4	Statistical Significance and Classification	100
4	Results	101
4.1	Activity Classification Network	101
4.2	Dyskinesia Detection Network	104
4.3	Overcoming the Limitation of a Low Number of Observations	107
5	Conclusion	111
III Evaluation of the Ambulatory Monitoring System		115
VI Unsupervised, At-Home Patient Monitoring		117
1	Protocol and Measurement Method	117
2	Data processing	119
2.1	Dyskinesia Detection Using the Global Approach	120
2.2	Dyskinesia Detection Using the Subject-Specific Approach	120

3	Results	123
3.1	Dyskinesia Detection Using the Global Approach	123
3.2	Dyskinesia Detection Using the Subject-Specific Approach	126
4	Conclusion	131
VIIPARADYSE : Platform of Activity Recognition and Dyskinesia Evaluation		133
1	Introduction to PARADYSE	133
1.1	Objectives	133
1.2	Development	134
1.3	Elements	135
2	Main Interface	135
3	Feature Extraction Interface	138
4	Classification Interface	141
4.1	Activity Classification	142
4.2	Dyskinesia Detection	145
5	Future Prospects	147
Conclusion and perspectives		151
List of publications		157
A Reduction by Feature Selection		159

List of Figures

I.1	James Parkinson's Essay on the Shaking Palsy.	10
I.2	Pathophysiology of the basal ganglia in Parkinson's disease [10].	11
I.3	Timeline of disease progression according to the Braak staging system, and the Hoehn&Yahr staging scale. The healthcare system requirements are shown relative to disease stage [12].	12
I.4	Diagnostic criteria for Parkinson's disease as set by the UK Brain Bank and NINDS.	13
I.5	(A) Example of Archimedes spirals drawn by a PD patient in comparison with a normal subject and a patient suffering from essential tremor. The spirals drawn by the PD patient becomes smaller and more cramped [24]. (B) Handwriting sample of a PD patient showing micrographia as a result of bradykinesia [25]. (C) Pull test normally performed by a trained examiner to assess the patient's ability to react to postural imbalance and recover [26].	15
I.6	Components of Deep Brain Stimulation surgery.	15
I.7	Mechanism of action of Levodopa in the brain.	17
I.8	Motor fluctuations associated with Levodopa therapy [31].	18
II.1	Diagram showing the different categories of wearable sensors, common body fixed positions based on sensor type, and a general summary of health related applications [5].	28
II.2	Uniaxial accelerometer measurement for a sensor attached to a leg segment.	31
II.3	Uniaxial gyroscope angular velocity measurement for a sensor attached to a rotating plate.	32
II.4	Uniaxial magnetometer measurement for a sensor attached to a a leg segment.	33
III.1	General scheme of development of an activity recognition system.	48
III.2	Shimmer3 IMU: (A) enclosed module, (B) default axis position, (C) exploded view showing individual components.	50
III.3	(A): Simplified schema of the Shimmer3 <i>LogAndStream</i> operational hierarchy. (B): Shimmer Dock - enclosure view.	51
III.4	General scheme of programming, configuration, and data logging for the system of acquisition.	52

III.5	Room layout in the laboratory where patients and healthy individuals performed the protocol of activities.	52
III.6	Placement of the sensing modules on the subject's body.	54
III.7	Signals collected from the Ankle module of a healthy individual.	56
III.8	Signals collected from the Ankle module of a PD patient in absence of LID.	57
III.9	Signals collected from the Ankle module of a PD patient in presence LID.	58
IV.1	Schema of the preprocessing and activity classification procedures performed on the data collected from the healthy individuals.	66
IV.2	The algorithms applied on the data collected from the PD patients. First Approach: dyskinesia detection without activity classification. Second Approach: dyskinesia detection for manually separated activities. Third Approach: dyskinesia detection for automatically classified activities.	67
IV.3	Performance of the classifiers for seven or four groups of activities showing the classification accuracy of the healthy subjects' TestSet (RF: Random Forest, KNN: K Nearest Neighbour, DT: Decision Tree, NB: Naive Bayes).	76
IV.4	Activity classification results in terms of Se and Sp for the healthy subjects' TestSet and Valset (A), and the PD patients' TestSet (B). The overall accuracy Acc is displayed in the titles.	77
IV.5	Overall accuracy of the classifiers in detecting dyskinesia for the PD patients' dataset as described in <i>App1</i> (RF: Random Forest, KNN: K Nearest Neighbour, DT: Decision Tree, NB: Naive Bayes).	78
IV.6	Overall performance of single module dyskinesia detection arranged by decreasing order of accuracy.	82
IV.7	Overall performance of the three best performing modules, Ankle, Hip and Thigh, in both AC and DD phases versus the performance obtained when using all the modules when applying <i>App3</i>	83
V.1	Example of a graph, formed by vertices and edges [3].	90
V.2	Example of a directed graph, formed by vertices and directed edges [3].	91
V.3	Mapping from a complex network to a feature vector, which is used to obtain a characterisation of the network through a set of measures. If the mapping is invertible, then it is considered a complete representation of the original structure [9].	93
V.4	Flow chart representing the steps carried out in order to classify the activities performed by HS in the case of Activity Classification Network, or to detect presence of LID in PD patients in the case of Dyskinesia Detection Network.	95
V.5	An example of the correlation matrix calculated for a segment of $\Delta t = 7$ seconds between the nodes.	96

V.6	Example of the complex network representation using a circular graph showing the nodes (module position and channel), the links (correlation between the channels) and the weights (correlation coefficients represented by link thickness).	97
V.7	Example of the circular graph visualisation for the Activity Classification Network taken from the same individual while performing the activities of standing (A), and walking (B).	98
V.8	Example of the circular graph visualisation for the Dyskinesia Detection Network taken from the same PD patient while performing the same activity of Lying in the absence of LID (A), and in the presence of LID (B).	98
V.9	Ranking of network measures computed for the Activity Classification Network in decreasing order using the ReliefF feature selection method.	102
V.10	Biplot showing the projection of observations belonging to the four activity classes along with the selected network measures. Each group of observations belonging to the same category forms a distinct cluster.	103
V.11	Ranking of network measures computed for the dyskinesia detection network in decreasing order using the ReliefF feature selection method.	106
V.12	Biplot showing the projection of observations belonging to the two motor states, dyskinetic and non-dyskinetic, along with the selected network measures. Each group of observations belonging to the same category forms a somewhat distinct cluster.	106
V.13	Flow chart representing the steps carried out in order to classify the activities performed by HS in the case of Activity Classification Network, or to detect presence of LID in PD patients in the case of Dyskinesia Detection Network. In this case, the total number of observations is increased by computing the mean correlation per minute instead of the the mean correlation of the total number of observations.	108
V.14	Ranking of network measures computed for the Activity Classification Network in decreasing order using the ReliefF feature selection method: case of MeanR per minute.	109
V.15	Ranking of network measures computed for the Dyskinesia Detection Network in decreasing order using the ReliefF feature selection method: case of MeanR per minute.	111
VI.1	Some of the daily life activities performed by the patient at her home during the long duration, free acquisition.	118
VI.2	Self-evaluation survey taken by the patient to assess her motor symptoms.	119
VI.3	Triaxial gyroscope signals collected from the Ankle module of patient M01 during Day 01, Day 02 and the long-duration acquisitions.	122
VI.4	Global approach results for dyskinesia detection in <i>App1</i> and <i>App3</i> versus the patient's self-evaluation survey. Each spike represents one instance, which is a 7 second time window.	125

VI.5	Subject-specific approach results for dyskinesia detection in <i>App1</i> and <i>App3</i> versus the patient's self-evaluation survey, using TrainSet1 as the training set. Each spike represents one instance, which is a 7 second time window.	127
VI.6	Subject-specific approach results for dyskinesia detection in <i>App1</i> and <i>App3</i> versus the patient's self-evaluation survey, using TrainSet3 as the training set. Each spike represents one instance, which is a 7 second time window.	129
VII.1	Diagram of the elements comprising the developed platform.	134
VII.2	Main interface of the GUI.	136
VII.3	Main interface of the GUI: Load raw data and plot example.	137
VII.4	Main interface of the GUI: (A) selection of sampling frequency, (B) selection of sensor data. . .	137
VII.5	Main interface of the GUI: Extraction and plot of a segment of data.	138
VII.6	Feature Extraction Interface.	139
VII.7	Feature Extraction Interface: Preprocessing user input.	140
VII.8	Feature Extraction Interface: Feature extraction and sensor order based on the IMU's configuration.	140
VII.9	Feature Extraction Interface: Arranging features by sensor order.	141
VII.10	Classification Interface.	142
VII.11	Classification Interface: Load and plot data, and load corresponding feature matrix.	142
VII.12	Classification Interface: Activity classification options.	143
VII.13	Classification Interface: Activity classification train using existing data.	144
VII.14	Classification Interface: Activity classification example for training criteria using existing data.	144
VII.15	Classification Interface: Confusion matrix variable output to the command window.	145
VII.16	Classification Interface: Dyskinesia detection example for training criteria using existing data. .	146
VII.17	Classification Interface: Selection of data to include in the training set for dyskinesia detection.	146
VII.18	Classification Interface: Confusion matrix variable output to the command window.	147
A.1	The distribution of selected features with respect to the module position by each method for the data collected from HS.	160
A.2	Overall accuracy of activity classification obtained using the different feature selection methods, and by reducing the size of the selected subset of features.	160
A.3	The distribution of selected features with respect to the module position by each method for the data collected from PD patients.	162
A.4	Overall accuracy of dyskinesia detection obtained using the different feature selection methods, and by reducing the size of the selected subset of features.	162

List of Tables

I.1	Currently Used Scales for Monitoring and Evaluating Disease Progression	21
II.1	Selection of Studies on the Objective Measurement of PD Motor Symptoms.	35
II.2	Selection of Studies on the Objective Measurement of Dyskinesia.	36
III.1	Review of Recent Literature on Activity Recognition.	49
III.2	Technical Specifications of the Shimmer3 Modules.	50
III.3	Protocol of Simple Daily Life Activities.	53
III.4	Parkinson’s Disease Patients	54
IV.1	Healthy Subjects Data Split.	72
IV.2	Number of Instances per Activity for Healthy Subjects: Case of Seven Classes.	73
IV.3	Number of Instances per Activity for Healthy Subjects: Case of Four Classes.	73
IV.4	Patient Data Split.	73
IV.5	Number of Instances per Motor State.	74
IV.6	Performance Measures for Classifier Performance Evaluation (* indicates the predicted class).	75
IV.7	An Example of the Contingency Table Obtained for the Healthy Subjects TestSet.	76
IV.8	Performance Measures Obtained for the Healthy Subjects TestSet.	77
IV.9	An Example of the Contingency Table Obtained for the PD Patients TestSet Without Separation of Activities.	78
IV.10	Dyskinesia Detection Results for <i>App2</i> Computed for Each Activity Dataset.	79
IV.11	Dyskinesia Detection Results for <i>App3</i> Computed for Each Predicted Activity Dataset.	79
IV.12	Dyskinesia Detection Results for the 3 Approaches.	80
IV.13	Overall Performance of DD Using Combinations of the Top Three Modules for <i>App1</i>	82
IV.14	Overall Performance of DD Using Combinations of the Top Three Modules for <i>App2</i>	82
V.1	Statistically Significant Network Measures for Activity Classification.	102
V.2	An Example of the Contingency Table Obtained for the TestSet.	104

V.3	Performance Measures Obtained for the TestSet.	104
V.4	Overall Performance Measures (%) Obtained for the Activity Classification Network.	104
V.5	Statistically Significant Network Measures for Dyskinesia Detection.	105
V.6	An Example of the Contingency Table Obtained for the TestSet and the Computed Performance Measures.	107
V.7	Number of Observations per Category for Healthy Subjects.	108
V.8	Statistically Significant Network Measures for Activity Classification for MeanR per Minute. . .	109
V.9	Overall Performance Measures (%) Obtained for the Activity Classification Network: Case of MeanR per Minute.	109
V.10	Number of Observations per Category for PD patients.	110
V.11	Statistically Significant Network Measures for Dyskinesia Detection for MeanR per Minute. . .	110
V.12	Overall Performance Measures (%) Obtained for the Dyskinesia Detection Network: Case of MeanR per Minute.	110
VI.1	Patient Data Split: Global Approach.	120
VI.2	Patient Data Split: Subject-Specific Approach.	123
VI.3	Overall Performance of Dyskinesia Detection For Short Duration Acquisition Data Using the Ankle Module Only.	123
VI.4	Global Approach: Number of Instances per Motor State.	124
VI.5	Global Approach: Performance Measures Obtained for the TestSet. "*" Indicates Predicted State.	124
VI.6	Subject-Specific Approach (TrainSet1): Number of Instances per Motor State.	126
VI.7	Subject-Specific Approach: Performance Measures Obtained for the TestSet When Using TrainSet1. "*" Indicates Predicted State.	128
VI.8	Subject-Specific Approach (TrainSet2): Number of Instances per Motor State.	128
VI.9	Subject-Specific Approach: Performance Measures Obtained for the TestSet When Using TrainSet2. "*" Indicates Predicted State.	130
VI.10	Performance of Dyskinesia Detection in <i>App1</i> Using the Short-Duration Protocol Data vs. Global and Subject-Specific (TrainSet1) Approaches Using Short and Long-Duration Acquisition Data.	131
VI.11	Performance of Dyskinesia Detection in <i>App3</i> Using the Short-Duration Protocol Data vs. Global and Subject-Specific (TrainSet1) Approaches Using Short and Long-Duration Acquisition Data.	131
VII.1	Variables Exported to MATLAB Workspace.	141

List of acronyms

ACC Accelerometer

Acc Accuracy

ADL Activities of Daily Living

AIMS Abnormal Involuntary Movement Scale

ANN Artificial Neural Network

BDM Bayesian Decision Making

Cfs Correlation-Based Feature Subset

CIFRE Conventions Industrielles de Formation

DBS Deep Brain Stimulation

DCAA Central Aromatic Acid Decarboxylase

DT Decision Tree

DTM Decision Table Majority

DWT Discrete Wavelet Transform

ECG Electrocardiography

EEG Electroencephalography

EMG Electromyography

FBF Fuzzy Basis Function

FD Frequency Domain

LIST OF ACRONYMS

FDA Food and Drug Administration

FN False Negative

FP False Positive

gdi Gini's Diversity Index

GPe Globus Pallidus Externa

GPI Globus Pallidus Interna

GYRO Gyroscope

HS Healthy Subjects

ID3 Iterative Dichotomiser 3

IMU Inertial Measurement Unit

IPG Impulse Generator

LDA Linear Discriminant Analysis

LID Levodopa Induced Dyskinesia

MAG Magnetometer

MDS Movement Disorders Society

MDS-UPDRS Movement Disorders Society Unified Parkinson's Disease Rating Scale

MEMS Micro-Electro-Mechanical Systems

NINDS National Institute of Neurological Disorders and Stroke

PCA Principal Component Analysis

PD Parkinson's Disease

QL Quality of Life

RF Random Forest

Se Sensitivity

SNc Substantia Nigra Pars Compacta

Sp Specificity

SR Sparse Representation

STN Subthalamic Nucleus

SVM Support Vector Machine

TD Time Domain

TN True Negative

TP True Positive

UDysRS Unified Dyskinesia Rating Scale

UPDRS Unified Parkinson's Disease Rating Scale

VL Ventrolateral

WHO World Health Organisation

Résumé

La maladie de Parkinson (MP) est une maladie neurodégénérative progressive qui se caractérise par la manifestation d'un dysfonctionnement moteur qui s'aggrave avec la progression de maladie. La prise en charge du patient implique soit une intervention chirurgicale pour la mise en place d'une Stimulation Cérébrale Profonde, soit la prise de médicaments visant à rétablir la fonction dopaminergique au niveau du système nerveux central.

Dans ce dernier cas, la Levodopa est considérée comme la molécule de référence pour soulager les troubles moteurs de la MP. Cependant, un traitement prolongé par Levodopa induit des effets secondaires indésirables et invalidants. Il est en effet observé chez de nombreux patients que l'effet positif du médicament diminue après une période de deux à cinq ans et qu'un effet secondaire appelé Levodopa Induced Dyskinesia (LID) commence à apparaître. Ces dyskinésies se traduisent par des mouvements involontaires et anormaux particulièrement gênants pour les patients.

La nécessité de prolonger la période effective de Levodopa et de retarder la manifestation et la gravité des LID est donc importante. Cependant, le diagnostic, l'évaluation et par conséquent le traitement de la MP sont basés sur des échelles d'évaluation cliniques, qui ont été critiquées pour leur subjectivité et le manque de fiabilité. Il importe donc de développer des méthodes objectives d'évaluation des symptômes moteurs et des complications de la MP.

C'est l'objet de ce mémoire de thèse de proposer, par l'utilisation de capteurs portables, un dispositif permettant d'évaluer et de quantifier le plus objectivement possible le mouvement et le dysfonctionnement moteur des patients MP. Ce développement a été financé par la société Biotrial, spécialisée dans l'évaluation de médicaments et la recherche pharmacologique. L'objectif est de proposer un système complet d'acquisition, capable de détecter les LID, afin de mieux évaluer les effets de la Levodopa et de gérer le plan thérapeutique, de manière à améliorer la période effective du médicament.

Succinctement, ce mémoire est divisé en trois grandes parties :

La première partie concerne le **contexte clinique** et est composée de deux chapitres :

- Le Chapitre I présente la Maladie de Parkinson et le Traitement par Levodopa

Ce chapitre présente les symptômes moteurs associés à la maladie de Parkinson et décrit les méthodes conventionnelles de traitement à base de Levodopa et les effets secondaires qu'elle entraîne. Il montre qu'il existe un véritable besoin pour la proposition d'une méthode d'évaluation objective et automatisée, fournissant des informations continues et quantifiables, pour mieux guider les cliniciens dans leur stratégie thérapeutique.

- Le Chapitre II s'intéresse à la Mesure Ambulatoire de LID et Symptômes Moteurs de la MP

Ce chapitre présente les technologies de capteurs portables et montre comment les derniers progrès technologiques fournissent un moyen objectif de surveiller, quantifier et évaluer le mouvement humain. L'objet principal de ce chapitre est la présentation des Unités de Mesure Inertielle (IMU). Les différentes composantes de ces unités sont décrites et les principes de mesure des mouvements humains sont présentés. L'utilisation de ces capteurs portables dans l'évaluation clinique des dysfonctionnements moteurs de la MP est réalisée par une revue de la littérature récente. Ce travail repose sur certains des aspects présentés dans la littérature mentionnée et vise à améliorer spécifiquement la capacité à détecter correctement les LID chez les patients parkinsoniens dans un contexte réaliste.

La seconde partie traite de la **Quantification Objective et Automatisée de LID**. Cette partie présente le matériel et les méthodes utilisées dans le développement de notre système d'acquisition au travers de trois chapitres :

- Le Chapitre III concerne le Matériel et le Protocole de Mesure

Le principal objectif de cette thèse est de concevoir et valider un système de surveillance ambulatoire capable de détecter objectivement les LID chez les patients parkinsoniens. Notre choix s'est porté sur un système basé sur des unités de mesure inertielle, parfaitement appropriées pour l'enregistrement des mouvements corporels.

Notre dispositif est composé de dispositifs Shimmer3. L'architecture du système et les positions des IMUs sur le corps des sujets sont détaillés dans la première section. Le protocole mis en

place pour évaluer le dispositif est ensuite décrit. L'acquisition des données a eu lieu dans un laboratoire, qui a été configuré pour ressembler à un environnement domestique. Des sujets sains ainsi que des patients parkinsoniens ont effectué un protocole d'activités de la vie quotidienne, décrites dans ce chapitre. La méthode d'acquisition de données, les avantages et les limites du système sont également présentés.

- Le Chapitre IV présente la Reconnaissance de Formes Pour la Classification des Activités et la Détection de la Dyskinésie

Cette chaîne de reconnaissance se compose de plusieurs étapes : la segmentation, l'extraction de caractéristiques et la classification. Tout d'abord, dans l'étape de segmentation, les signaux recueillis ont été répartis en fenêtres temporelles de courte durée. Ensuite, des caractéristiques, extraites de la littérature, dans le domaine temporel et fréquentiel, ont été calculées pour chaque fenêtre temporelle. Pour la classification, notre démarche a été de comparer différentes stratégies à base de KNN (K Nearest Neighbor), de Naive Bayesian, des Decision Trees, et des Random Forest. Conscient que l'activité du patient pouvait influencer la détection des phases de dyskinésie, notre stratégie a été de confronter trois approches différentes.

Pour la première approche, la détection des périodes de dyskinésie se fait sans séparation des activités. Dans ce cas, le détecteur de dyskinésie a été utilisé pour détecter si une certaine période est dyskinétique ou non-dyskinétique, à partir de l'ensemble des données recueillies auprès des patients. Pour la seconde approche, la détection des périodes de dyskinésie se fait sur des activités séparées manuellement (en d'autres termes on suppose qu'il n'y aucune erreur de classification de l'activité). Enfin, la troisième approche est l'application de notre algorithme complet, qui consiste d'abord à classer automatiquement les activités, puis à détecter la présence de la dyskinésie en fonction de la classe d'activité identifiée.

Le classifieur d'activités a d'abord été validé également sur une base de données de sujets sains ayant suivi le même protocole que les patients parkinsoniens. Les résultats obtenus montrent que le classifieur d'activité conçu, s'appuyant sur les Random Forest, fournit des résultats tout à fait satisfaisants sur les données recueillies auprès des sujets sains, en fournissant une précision globale de 98.5%. Ce classifieur atteint une précision globale de 93.6% lors de la classification des activités exercées par les patients parkinsoniens. Les résultats obtenus à partir des trois approches montrent que l'étape de classification d'activité offre une légère amélioration dans la

détection de la dyskinésie.

Dans une ultime partie, nous avons essayé de proposer un dispositif comprenant un nombre réduit d'IMUs. Nous avons montré qu'il est possible d'utiliser trois modules, placés au niveau de la cheville, la hanche et de la cuisse du patient. En utilisant le système réduit, les résultats montrent que la précision globale de classification des activités et la détection des dyskinésies (en se fondant dans les deux cas toujours sur les Random Forest) restent très satisfaisantes avec un taux de 94.2% et 94.8%, respectivement.

- Le Chapitre V offre un nouveau regard et propose l'Analyse des Réseaux Complexes Pour la Classification des Activités et la Détection de la Dyskinésie

L'ensemble de nos dispositifs formant un réseau de capteurs, il était naturel d'analyser le mouvement en se basant sur la théorie des graphes. À notre connaissance, cette approche n'a jamais été utilisée dans le cadre des capteurs inertiels. L'analyse de réseau complexe est une nouvelle approche multidisciplinaire combinant la théorie des graphes et des mesures statistiques pour l'analyse de bases de données réelles. Ces bases de données comprennent classiquement des réseaux avec des connexions anatomiques ou fonctionnelles. Ce type d'analyse vise à caractériser les réseaux avec un nombre limité de mesures significatives et simples. Dans ce chapitre, ce principe d'analyse est repris et appliqué à un réseau composé des IMUs.

Cette méthode est composée de quatre étapes : la segmentation, la construction du réseau, l'extraction de ses caractéristiques et la classification. La segmentation des signaux recueillis a été effectuée exactement comme décrit dans le chapitre IV. Le réseau est construit sur la base de la mesure de corrélation entre les différentes unités inertielles. L'extraction de ses caractéristiques implique le calcul de mesures correspondant aux réseaux construits telles que degré, force, densité, etc. Comme précédemment, la classification des activités de sujets sains et la détection de la dyskinésie chez les patients parkinsoniens ont été abordées en comparant plusieurs stratégies de classification. Ceci a conduit à la construction d'un réseau complexe pour les sujets sains pour la classification des activités et d'un réseau, pour les patients parkinsoniens, pour la détection des dyskinésies.

En utilisant le réseau de classification des activités, nous avons montré qu'il est possible de classer, en utilisant toujours les Random Forest, les activités exercées par des sujets sains avec une précision globale de 84.69%. D'autre part, en utilisant le réseau de détection de la dyskinésie,

nous avons été capables de classer des phases de dyskinésie avec une précision globale de 78.6%.

Les résultats obtenus en utilisant cette nouvelle approche sont discutés et comparés à ceux de la méthode présentée dans le Chapitre IV. Les résultats, certes inférieurs à ceux obtenus avec la première approche, restent prometteurs et l'évaluation de cette technique sur une plus grande population sera nécessaire afin de valider son utilisation spécifiquement dans le but de la détection de la dyskinésie.

La Partie III aborde l'**Évaluation du Système de Surveillance Ambulatoire**. Dans cette partie, le système d'acquisition proposé a été testé en effectuant une acquisition de longue durée non supervisée. Les résultats de ce test sont présentés et discutés dans le Chapitre VI. Enfin, ce travail s'inscrivant dans un contexte industriel, il était également important de développer une plateforme embarquant les solutions méthodologiques qui ont été développées dans le cadre de ce travail. C'est l'objet du Chapitre VII de la présenter. En d'autres termes :

- Le Chapitre VI aborde le Monitoring Non Supervisée à Domicile des Patients

L'objectif du système développé est de fournir une détection fiable et précise des LID chez les patients parkinsoniens dans un environnement de la vie quotidienne. Par conséquent, une acquisition non supervisée de longue durée a été réalisée sur l'un des patients parkinsoniens à son domicile. La capacité du système à identifier correctement les périodes de dyskinésie est évaluée ici dans des conditions réelles et l'évaluation des performances se fait sur la base de l'auto-évaluation du patient de la dyskinésie au cours de l'acquisition.

Dans ce contexte, nous avons testé et comparé l'intérêt d'un apprentissage global et d'un apprentissage patient-spécifique des classes afin d'évaluer la détection de la dyskinésie, avec et sans la classification des activités. Les résultats obtenus montrent qu'en réalisant la détection de dyskinésie sur des activités séparées automatiquement, et dans le cas d'un apprentissage patient-spécifique, nous sommes capables d'identifier correctement des périodes de dyskinésie avec une précision globale de 82%. Ces résultats très encourageants et montrant le bien-fondé de notre dispositif doivent bien sûr une nouvelle fois être considérés comme préliminaires étant donné que cette expérimentation, même réalisée sur plusieurs heures, ne l'a été que pour un seul patient.

- Le Chapitre VII décrit la plateforme PARADYSE (Platform of Acquisition, Recognition of Activities and DYSkinesia Evaluation)

L'intérêt de cette plateforme est de faciliter la relecture des données, la sélection des IMUs à analyser, le choix des variables de représentation des segments à classer et le choix des méthodes de classification. Cette plateforme permet donc l'exploitation directe des données acquises, la classification des activités et la détection des phases de dyskinésie. Elle répond en cela à l'objectif initial fixé. Elle permet la recherche des variables les plus pertinentes mais aussi de mieux appréhender l'intérêt d'un apprentissage global ou patient-spécifique. Dans ce chapitre, l'idée fondamentale et le fonctionnement de cette plateforme sont présentés et son rôle dans l'avancement des capacités globales du système est expliqué.

Introduction

Parkinson's disease is a neurodegenerative disorder of the brain [1]. It occurs when certain neurons in the substantia nigra, which is an area of the basal ganglia responsible for controlling voluntary movements and regulating the mood, die or become impaired. The loss of these dopaminergic cells leads to the inhibition of the direct pathway of movement, which in turn leads to a hypokinetic movement disorder [2]. This disease mainly affects the motor system and its cardinal symptoms are tremor, rigidity, akinesia, bradykinesia, postural abnormalities and gait impairments [4]. Currently, there is no known cure for Parkinson's disease and the principal treatment methods are based on medication that aim to compensate the brain's dopamine deficiency, through mimicking, creating or inhibiting the breakdown of dopamine in the brain [5]. Some of the non-motor symptoms include depression or psychosis, and autonomic or gastrointestinal dysfunction. These non-motor symptoms [3] are part of a prodromal stage of the disease which can occur up to twenty years before the prevalence of the first motor symptom.

The gold standard of treatment through medication is a drug called Levodopa [6]. It acts as a dopamine precursor, able to cross the blood brain barrier, and is converted to dopamine by dopamine-producing cells thereby directly replacing the dopamine deficiency in the brain [7]. The use of Levodopa for relieving motor symptoms of Parkinson's disease is highly effective and almost all patients demonstrate significant improvement in motor symptoms after Levodopa intake.

However, a major disadvantage of Levodopa is the manifestation of motor complications that typically begin after two to five years of treatment [8]. The motor complications associated with Levodopa are motor fluctuations and dyskinesias [9]. Motor fluctuations are dramatic variations in the patient's motor ability associated with the effectiveness of the medication. Dyskinesia, on the other hand, is defined as random, involuntary jerking movements which are a direct result of chronic Levodopa therapy. In many cases, Levodopa Induced Dyskinesia (LID) can be severe and interferes

with the patient's day to day life.

There is a need to better evaluate the effects of Levodopa and manage the therapeutic plan in such a way to ameliorate the beneficial period of the drug. Currently, methods used to evaluate the severity of LID are based on self assessment diaries and rating scales such as the Abnormal Involuntary Movement (AIM) rating scale. However, there are several major issues concerning these methods, including lack of objectivity and assessment based on short-period tests performed in clinical settings [10]. As a result, recent research has been aimed towards finding more objective, and automated methods for the detection and evaluation of Levodopa Induced Dyskinesia, as well as other Parkinson's disease motor symptoms [11]. On the other hand, recent advances in wearable sensor technology, signal processing and pattern recognition have lead to major breakthroughs in the fields of human activity recognition and rehabilitation [12]. Consequently, these advances have presented the possibility of transitioning towards objective methods of assessment of Parkinson's disease motor symptoms and complications [13].

The work done in this thesis was funded by Biotrial, a drug development and pharmacology research group based in Rennes. The project required the development of a complete system of acquisition capable of detecting LID. For this reason, the focus of this thesis was on PD patients suffering from LID in varying severities. Patients who participated in this study had been following Levodopa treatment for several years and had not had DBS or other related surgeries. Other motor symptoms of PD were not investigated as they were not in the scope of the study.

This thesis is divided into three major parts. Part I (Chapter I-II) serves as an introduction to the clinical context and the problem statement. In Part II (Chapter III-V), the design of the ambulatory monitoring system is presented and the developed algorithms are detailed. A novel method based on complex network analysis is introduced and the results obtained are discussed. While in Part III (Chapter VI-VII), we introduce the preliminary results of a long-duration, at-home acquisition performed on one of the PD patients, and present a platform developed to incorporate the applied analysis methods. A synthesis of the contents of each chapter is in the following:

- **Chapter I: Parkinson's Disease and Levodopa Therapy**

This chapter introduces the pathophysiology of Parkinson's disease and the currently pursued therapeutic measures, with a main focus on treatment through Levodopa. The motor symptoms associated with the disease are described and current methods of assessment, which are based

mostly on clinical scales, are presented. The mode of functioning and effectiveness of Levodopa are also presented, followed by the problem statement which is the manifestation of motor fluctuations and LID, causing a deterioration of the patient's motor condition and quality of life.

- **Chapter II: Ambulatory Monitoring of Levodopa Induced Dyskinesia and PD Motor Symptoms**

The wearable sensing technologies that have provided an objective means of monitoring, quantifying and evaluating human movement are presented in this chapter. A focus is given on the principles behind describing human movement through the use of Inertial Measurement Units (IMUs), which are devices that combine a number of different sensors. A review of recent literature shows how these devices provide an objective means of assessment of PD motor symptoms and complications.

- **Chapter III: Materials and Measurement Protocol**

In this chapter, the ambulatory monitoring system developed to objectively detect LID in PD patients is presented. The system is composed of wearable Inertial Measurement Units designed to collect movement data from subjects. The pilot system, initially set up to record the widest possible movement patterns is detailed in this section. The individuals participating in the study as well as the acquisition protocol are also described.

- **Chapter IV: Pattern Recognition for Activity Classification and Dyskinesia Detection**

This chapter details the methods used to evaluate the system's capabilities in detecting LID using pattern recognition approaches. The processing steps and classification techniques implemented on the collected signals, from healthy individuals and PD patients, are explained here along with the basic scheme of analysis. The results obtained are presented and the evaluation of the system and techniques applied under different conditions is discussed. Finally, we propose a system with a minimal number of modules, after assessing the performance obtained using individual IMUs.

- **Chapter V: Complex Network Analysis for Activity Classification and Dyskinesia Detection**

This chapter introduces a novel approach for the classification of activities and LID detection using complex network analysis. This type of analysis is a new multidisciplinary approach

that combines graph theory and statistical measures. The system comprised of several Inertial Measurement Units is represented as a network structure and computed network measures are used to perform activity classification and LID detection on the collected data. The results obtained using this type of analysis are compared to those obtained using the more conventional pattern recognition approach described in Chapter IV.

- **Chapter VI: Unsupervised, At-Home Patient Monitoring**

The developed system is evaluated in a long duration, non-dictated and unsupervised acquisition which was performed at the home of one of the PD patients. This serves to validate the system's capabilities to provide reliable and accurate detection of LID in an unsupervised daily life environment. The proposed method of analysis in Chapter IV is applied on the collected data and the obtained results are presented and discussed.

- **Chapter VII: PARADYSE: Platform of Activity Recognition and Dyskinesia Evaluation**

A platform for the implementation of the processing methods and approaches applied in this work has been developed as part of the final system to be proposed. This platform is a graphical user interface developed in MATLAB and aimed to provide faster and more efficient manipulation of the collected data using the monitoring system. The concept and functioning of this platform are presented in this chapter through provided examples. The main objective of this platform is to advance the overall capabilities of the monitoring system and allow for quick and standardised analysis of future acquisitions.

A general conclusion regarding the work done during this thesis accompanies the three parts, highlighting the objectives achieved, providing a synthesis of the main results, and introducing the future prospects of the developed system.

Bibliography

- [1] J. JANKOVIC AND E. TOLOSA. *Parkinson's disease and movement disorders*. Lippincott Williams & Wilkins (2007).
- [2] D. J. MOORE, A. B. WEST, V. L. DAWSON, AND T. M. DAWSON. *Molecular pathophysiology of Parkinson's disease*. *Annu. Rev. Neurosci.* **28**, 57–87 (2005).
- [3] K. R. CHAUDHURI, D. G. HEALY, AND A. H. SCHAPIRA. *Non-motor symptoms of Parkinson's disease: diagnosis and management*. *The Lancet Neurology* **5**(3), 235–245 (2006).
- [4] J. SHAHED AND J. JANKOVIC. *Motor symptoms in Parkinson's disease*. *Handbook of clinical neurology* **83**, 329–342 (2007).
- [5] B. S. CONNOLLY AND A. E. LANG. *Pharmacological treatment of Parkinson's disease: a review*. *Jama* **311**(16), 1670–1683 (2014).
- [6] P. S. GROUP ET AL. *Levodopa and the progression of Parkinson's disease*. *N Engl J Med* **2004**(351), 2498–2508 (2004).
- [7] P. RIEDERER, M. GERLACH, T. MÜLLER, AND H. REICHMANN. *Relating mode of action to clinical practice: dopaminergic agents in Parkinson's disease*. *Parkinsonism & related disorders* **13**(8), 466–479 (2007).
- [8] B. THANVI AND T. LO. *Long term motor complications of levodopa: clinical features, mechanisms, and management strategies*. *Postgraduate medical journal* **80**(946), 452–458 (2004).
- [9] G. FABBRINI, J. M. BROTHIE, F. GRANDAS, M. NOMOTO, AND C. G. GOETZ. *Levodopa-induced dyskinesias*. *Movement disorders* **22**(10), 1379–1389 (2007).
- [10] C. RAMAKER, J. MARINUS, A. M. STIGGELBOUT, AND B. J. VAN HILTEN. *Systematic evaluation of rating scales for impairment and disability in Parkinson's disease*. *Movement Disorders* **17**(5), 867–876 (2002).
- [11] W. MAETZLER, J. KLUCKEN, AND M. HORNE. *A clinical view on the development of technology-based tools in managing Parkinson's disease*. *Movement Disorders* (2016).
- [12] S. PATEL, H. PARK, P. BONATO, L. CHAN, AND M. RODGERS. *A review of wearable sensors and systems with application in rehabilitation*. *Journal of neuroengineering and rehabilitation* **9**(1), 1 (2012).
- [13] C. OSSIG, A. ANTONINI, C. BUHMANN, J. CLASSEN, I. CSOTI, B. FALKENBURGER, M. SCHWARZ, J. WINKLER, AND A. STORCH. *Wearable sensor-based objective assessment of motor symptoms in Parkinson's disease*. *Journal of Neural Transmission* **123**(1), 57–64 (2016).

Part I

Clinical context

Parkinson's Disease and Levodopa Therapy

The first chapter of this thesis serves as an introduction to Parkinson's disease, its pathophysiology and therapeutic measures, namely focusing on Levodopa. In this chapter, we present the different motor symptoms associated with Parkinson's disease, the motor complications that occur as a result of Levodopa therapy, and the current methods of assessment. The objective here is to provide clinical context with regards to the disease, its development and the impairments that are induced as a result of the therapeutic measures.

First, the epidemiology and pathophysiology of Parkinson's disease are explained through the disease's onset, diagnosis and currently applied therapeutic measures. This is followed by defining the major motor symptoms that occur as a result of disease progression. We then discuss the disease's treatment through Levodopa, highlighting the mechanism of action of this drug, its effects on the motor symptoms of Parkinson's disease and the motor complications it induces.

1 Epidemiology and Pathophysiology

Parkinson's Disease: Onset and Disease Progression

Parkinson's disease (PD) is a slowly progressive neurological disorder that affects an area of the basal ganglia known as the substantia nigra. PD is the second most common neurodegenerative disease today, following Alzheimer's disease. According to the Parkinson's Disease Foundation, an estimated seven to ten million people worldwide are living with PD, including as many as one million in America and one point two million in Europe [1]. This disease was first discovered by Dr. James Parkinson in 1817, who was the first to document its syndromes in his famous monograph titled *An Essay on the Shaking Palsy* (Figure 1.1, [2]).

The cardinal signs of PD mainly relate to motor dysfunction represented by symptoms such as resting tremor, bradykinesia, and loss of postural reflex, usually referred to as Parkinsonism. However, Parkinsonism is a broader term and in some cases can be related to other causes such as intoxication, tumors, infection, trauma, and vascular diseases. PD is the most common form of Parkinsonism and its major pathological abnormalities include neuronal cell loss, gliosis, and loss of pigment in the substantia nigra [3].

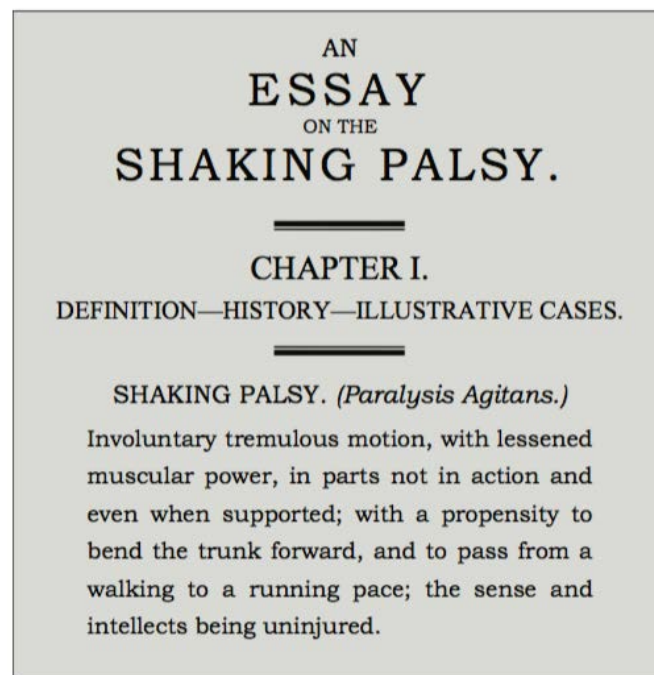


Figure I.1 – James Parkinson's Essay on the Shaking Palsy.

The causes of PD are still largely unknown. Recently, several causative monogenetic mutations were discovered [4–6], but seemed to explain only a small percentage of PD and around 90% of all cases are believed to be sporadic. Remarkably, however, only a few environmental causes or triggers have so far been identified [7–9]. Current beliefs about the origin of PD is that major genetic mutations have a role in PD pathogenesis and that these processes are also induced by non-genetic factors interacting with susceptibility genes.

The pathological hallmark of PD is the selective loss of dopaminergic neurons from the pars compacta of the substantia nigra. Figure I.2 shows the normal functioning of the basal ganglia versus the effect of striatal dopamine loss in PD. In the case of normal functioning, dopamine from the substantia nigra pars compacta (SNc) controls both the "indirect" and "direct" pathways of the neostriatum. Two families of receptors mediate the action of dopamine through the basal ganglia. The striatal neurons belonging to the indirect pathways are inhibited by dopamine via D2 receptors. These striatal neurons send inhibitory fibers to the globus pallidus externa (GPe) which in turn sends inhibitory fibers to the subthalamic nucleus (STN). The STN sends excitatory fibres to the globus pallidus interna (GPi), which sends inhibitory fibers to the ventrolateral (VL) and ventral anterior nuclei of the thalamus. On the other hand, the striatal neurons belonging to the direct pathway are excited by dopamine via D1 receptors. These neurons then send inhibitory fibers directly to the GPi. Therefore, the purpose of dopamine acting through the striatum via both the direct and indirect pathways is to inhibit the activity of the GPi. Hence, the loss of striatal dopamine as a result of the

degeneration of the SNc neurons, causes an increase in the activity of the GPi neurons via both the direct and indirect pathways [3]. This imbalance in the motor networks that stimulate and/or inhibit the initiation of movement is the primary cause of motor dysfunction in PD.

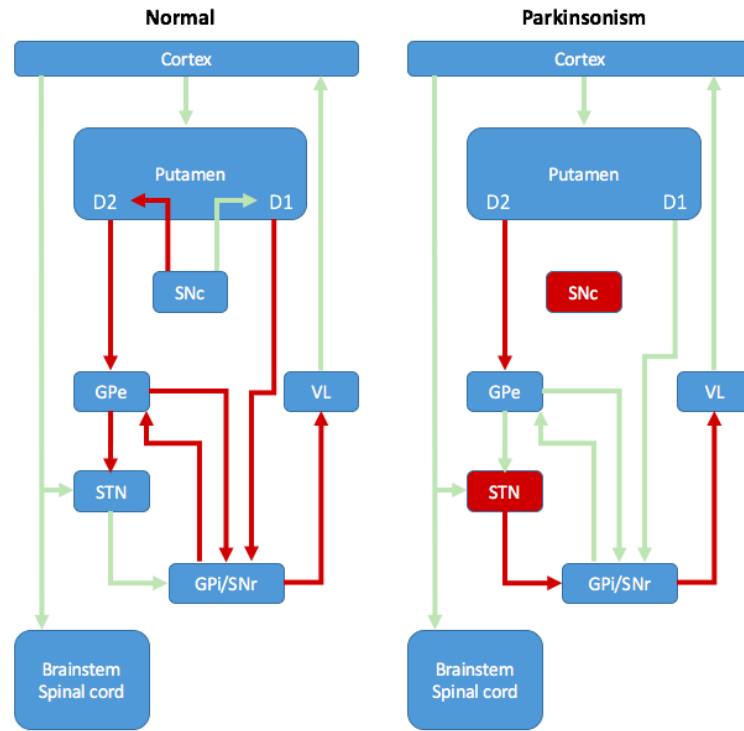


Figure I.2 – Pathophysiology of the basal ganglia in Parkinson's disease [10].

The timeline of PD is directly related to the rate of loss of dopaminergic cells in the brain. The progression in cell damage was translated into six stages of the disease by Dr. Heiko Braak, and lead to the Braak staging system [11] which is still used today. Figure I.3 (Top) shows the timeline of PD progression from onset till death and the symptoms of the different stages of the disease. According to the Braak staging system, stage 1 is a pre-symptomatic stage where cell loss is occurring but not significantly enough to produce any symptoms. The first premotor symptoms appear at the end of stage 1 and stage 2. The symptoms might include a diminished sense of smell, or hyposmia, constipation and REM sleep behaviour disorder. The first motor symptoms, such as tremor and akinesia, begin to appear in stage 3. The manifestation of motor symptoms suggests a significant loss (over 50%) of dopaminergic cells specifically in the substantia nigra. The function of the striatum is disrupted as described earlier and by stage 4, cell loss would have reached the mesocortex. Stages 5 and 6 involve cell loss in the higher cortical centers of the brain, responsible for controlling emotion and cognition, which causes confusion and dementia. Other common neuropsychiatric disorders during these stages are depression, anxiety, apathy and hallucinations.

Following diagnosis, a descriptive staging scale, known as the Hoehn&Yahr staging scale [13], is used

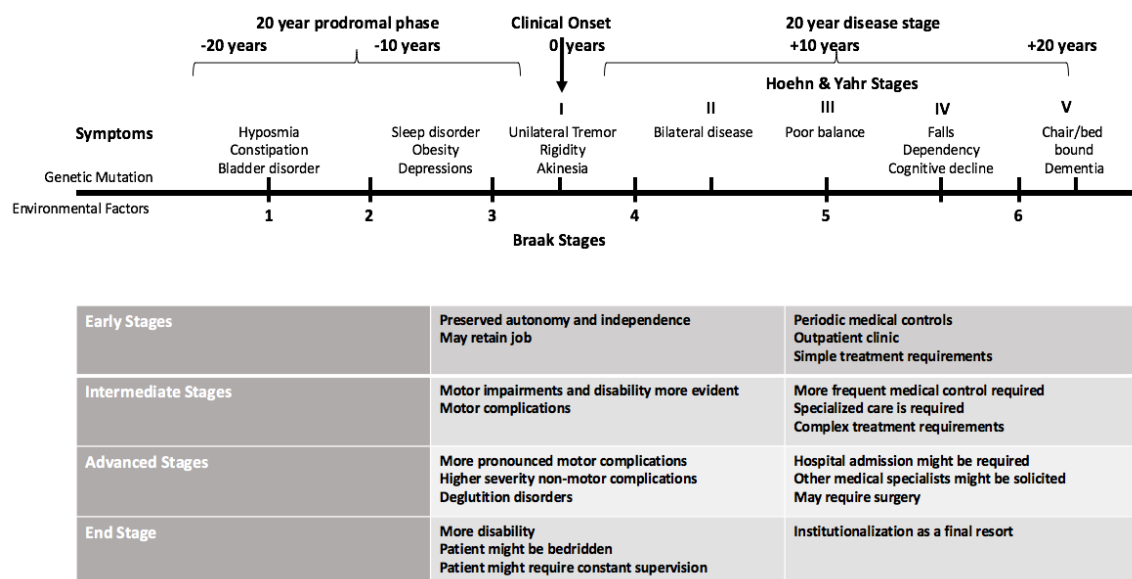


Figure I.3 – Timeline of disease progression according to the Braak staging system, and the Hoehn&Yahr staging scale. The healthcare system requirements are shown relative to disease stage [12].

to provide context of clinical function in PD. This scale was first developed in 1967 by Dr. Margaret Hoehn and Dr. Melvin Yahr, to be a simple staging scale used to describe functional deficits and objective signs of PD, and contains five different stages (Figure I.3 Top). The associated healthcare system requirements, defined by the WHO, relative to the disease stages are presented in Figure I.3 (Bottom).

2 Clinical Diagnosis

At the present time, there is no definitive test for the diagnosis of PD. Instead, diagnosis of the disease is based on the presence of certain clinical features and by exclusion criteria. In most cases, the physician reviews the medical history of the patient and performs clinical examination. Other tests are also performed in order to ensure the absence of clinical, laboratory, or radiologic abnormalities that could contribute to the patient's symptoms.

Diagnostic criteria have been developed by the UK Parkinson's Disease Society Brain Bank [14] and the National Institute of Neurological Disorders and Stroke (NINDS) [15] (Figure I.4). However, the validity and accuracy of these criteria have not yet been clearly established. No single feature definitively guarantees or excludes the presence of PD. Although diagnosis of PD can be considered straightforward when patients display classical PD symptoms that differentiate the disease from other forms of Parkinsonism, misdiagnosis can still occur. In [14], up to 25% of clinically diagnosed PD were found to be misdiagnosed at autopsy. These misdiagnosis rates are most commonly caused by essential tremor, Alzheimer's disease, vascular parkinsonism, and lack of response to antiparkinsonian

UK Parkinson's Disease Society Brain Bank Clinical Criteria		National Institute of Neurological Disorders and Stroke Criteria	
Step 1	Bradykinesia At least one of the following: • Rigidity • 4-6 Hz rest tremor • Postural instability not caused by primary visual, vestibular, cerebellar or proprioceptive dysfunction	Group A Features (characteristics of PD)	Resting tremor Bradykinesia Rigidity Asymmetric onset
Step 2	Exclude other causes of parkinsonism	Group B Features (suggestive of alternative diagnosis)	Unusual features early in the clinical course Prominent postural instability in the first 3 years after onset Freezing phenomenon in the first 3 years Hallucinations unrelated to medications in the first 3 years Dementia preceding motor symptoms or in the first year Supranuclear gaze palsy or slowing of vertical saccades Severe, symptomatic dysautonomia unrelated to medications
Step 2	At least three of the following: • Unilateral onset • Rest tremor • Progressive disorder • Persistent asymmetry primarily affecting side of onset • Severe Levodopa Induced Dyskinesia • Levodopa response for five years or more • Clinical course of ten years or more	Criteria for definite PD	All criteria from probable Parkinson's are met Histopathological confirmation of the diagnosis is obtained at autopsy
		Criteria for probable PD	At least three of the four features in group A are present None of the features in group B is present Substantial and sustained response to Levodopa or dopamine agonist
		Criteria for possible PD	At least two of the four features in group A are present: at least one of these is tremor or bradykinesia None of the features in group B is present Symptoms have been present for less than 3 years and none of the features in group B is present Substantial response to Levodopa or dopamine agonist has been documented

Figure I.4 – Diagnostic criteria for Parkinson's disease as set by the UK Brain Bank and NINDS.

medication [16, 17]. More recently, the Movement Disorders Society (MDS) Task Force defined newly updated criteria for the clinical diagnosis of PD[18] that are in line with the current understanding of the neurodegeneration process, onset of symptoms and differing phenotypes and genotypes. The newly outlined criteria introduces the first ever produced criteria for prodromal PD, which is also quite unique in its design as it is based on mathematical calculations to estimate the probability of the disease.

3 Motor Symptoms and Therapeutic Measures

Despite continuous research, the cure for PD has yet to be found. The major treatment methods today aim to relieve motor and non-motor symptoms of PD. Over the course of this thesis, we will be focusing on the detection of motor complications associated with the therapeutic plan of PD. As an overview, the next section details the major motor symptoms of the disease and the currently adopted therapeutic measures.

3.1 Major Motor Symptoms of PD

- **Resting Tremor** is a shaking or oscillatory movement that appears when a person's muscles are relaxed or at rest, characteristically disappearing with action or during sleep (Figure I.5 (A)). It is considered to be the most common, with 70% of PD patients display rest tremor in early stages of the disease, and easily recognised symptom of PD. It occurs at a frequency of 4-6 Hz and affects asymmetrically upper and lower limbs [19].
- **Bradykinesia** refers to general slowness of movement and is the most defining clinical feature

of PD. It includes a general reduction in spontaneous movement, difficulty with initiating and executing movement, and difficulty with performing simultaneous tasks. Bradykinesia can affect the person's daily life as the patient may have difficulties performing everyday activities such as getting dressed or handling utensils (Figure I.5 (B)). Other manifestations of bradykinesia include slow walking with shuffled steps, impaired swallowing, and loss of facial expressions [20].

- **Rigidity** describes stiffness and inflexibility of the limbs, neck, and trunk. It is usually accompanied by "cogwheel" phenomenon that manifests as shortened range of flexion, extension, or rotation of a limb. Rigid muscles may be painful, and shoulder, calf and thigh pain are the most common early symptoms of PD [21].
- **Postural Instability** commonly appears in the later stages of the disease, after the onset of other clinical features. This symptom encompasses loss of postural reflexes and is the most common cause of falls in PD patients, posing a serious risk of injuries. Postural stability is usually evaluated through a "pull test" (Figure I.5 (C)), where an experienced examiner stands behind the patient and briskly pulls the patient backwards in order to test the patient's ability to recover [22].
- **Freezing of Gait** is a characteristic feature and one of the most disabling symptoms of PD. The term freezing refers to a motor block that occurs and prohibits the patient from moving the feet in certain situations such as turning or walking through a narrow passageway. While it occurs most commonly in the legs, freezing can affect the arms and eyelids. It is also one of the most common causes of falls in PD patients [23].

3.2 Deep Brain Stimulation

Deep Brain Stimulation (DBS) is a surgical treatment of PD reserved for patients suffering from disabling motor complications despite maximal drug therapy [27]. During this surgery, electrodes are implanted in a target site in the brain, most commonly the subthalamic nucleus and the globus pallidus, and connected to a pacemaker-like device called the impulse generator (IPG). The IPG is usually implanted under the collarbone and provides electrical impulse to the area of the brain where the electrodes are present. Although the effects of this surgery are quite substantial in relieving motor symptoms and complications of PD, it is not accessible for every PD patient. Indications that qualify the patient for this type of surgery include:

- A diagnosis period of five to ten years.
- Patients experiencing significant disabilities, such as severe tremors, wearing-off and LID.
- Patients without cognitive impairment or dementia.

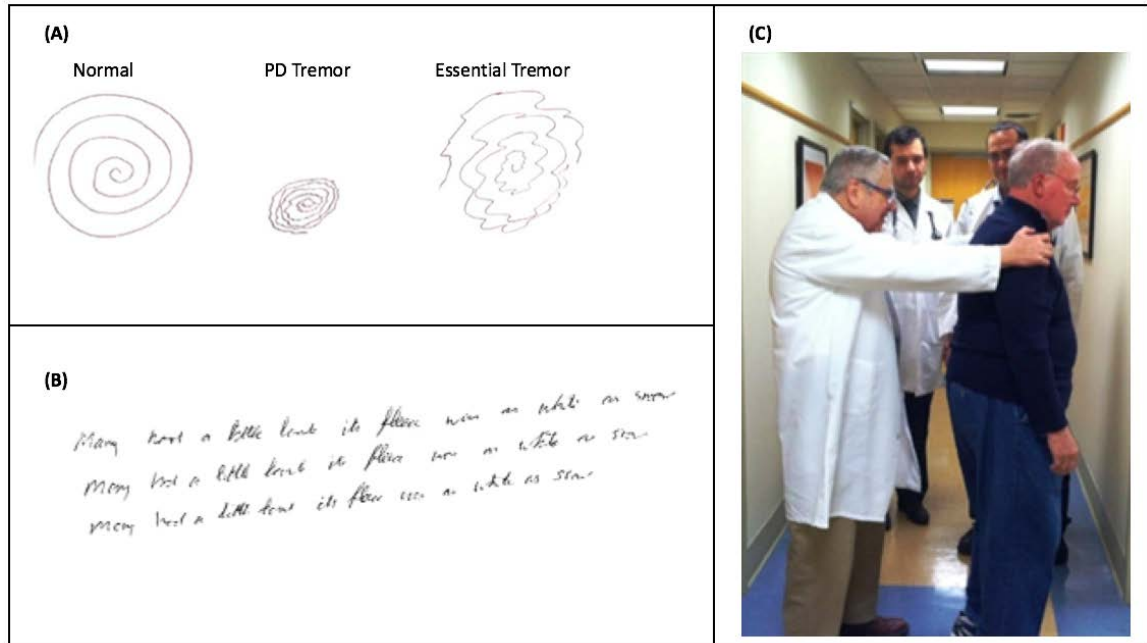


Figure I.5 – (A) Example of Archimedes spirals drawn by a PD patient in comparison with a normal subject and a patient suffering from essential tremor. The spirals drawn by the PD patient becomes smaller and more cramped [24]. (B) Handwriting sample of a PD patient showing micrographia as a result of bradykinesia [25]. (C) Pull test normally performed by a trained examiner to assess the patient's ability to react to postural imbalance and recover [26].

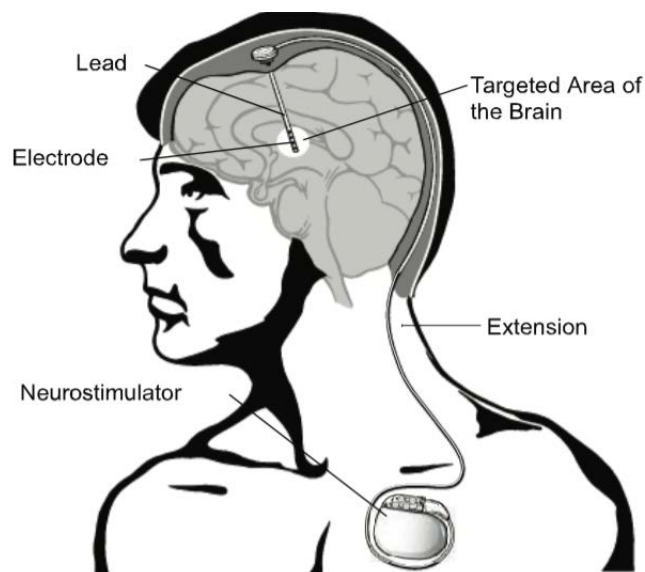


Figure I.6 – Components of Deep Brain Stimulation surgery.

- Consideration of age and life expectancy play a significant role.

The risks associated with any brain surgery, such as infection, stroke and bleeding, are also present in this case. Some patients have also been reported to experience cognitive decline following DBS. While this surgery can improve the quality of life, it is worth noting that it does not prevent disease progression in any way. In addition, this surgery is not accessible to all patients [28, 29].

3.3 Treatment by Medication: Levodopa Therapy

The therapeutic plan used to treat each PD patient is usually customised to that patient specifically based on an evaluation of symptom presentation and health issues. This plan includes medications that act to replace the dopamine deficiency in the brain through mimicking its function, or compounds to create dopamine in the brain, or inhibit the breakdown of dopamine. The types of medications used to treat PD symptoms currently can be summarised into the following classes:

- **Cardiopa/Levodopa** is considered to be the most effective treatment of PD motor symptoms today. Levodopa on its own causes severe nausea and vomiting, and therefore is usually combined with cardiopa in a formulation normally called Sinemet.
- **COMT Inhibitors** are used to prolong the effect of Levodopa and do not actually affect the symptoms of PD. These drugs are usually administered to block COMT, catechol-o-methyltransferase, which is an enzyme that metabolises Levodopa in the periphery or outside the brain.
- **MAO-B Inhibitors** can have a modest effect on PD symptoms if taken alone, but are mainly used to reduce the wearing-off effects of Levodopa. MAO-B, monoamine oxidase type B, is an enzyme that also metabolises Levodopa in the brain and the inhibitors can have a positive effect on motor fluctuations.
- **Dopamine Agonists** are artificial chemicals able to directly cross into the brain and stimulate areas influenced by dopamine by binding to dopamine receptors. These drugs are not as effective as Levodopa, and are commonly used in combination with Levodopa to improve motor fluctuations.
- **Anticholinergics** were the main treatment of PD symptoms before the discovery of Levodopa. The medications mainly affect rest tremor and have a less significant effect on bradykinesia and gait symptoms. They have been found to cause negative effects on memory.
- **Amantadine** is also one of the first treatments proposed for PD, but has only a mild effect on PD symptoms. It was recently found that these drugs can be useful in reducing dyskinesia associated with dopaminergic drugs, such as Levodopa and are currently used in advanced PD treatment specifically for that purpose.

Mechanism of Action of Levodopa

Levodopa is the precursor of dopamine in dopaminergic neurons and is transformed to dopamine in the central nervous system by decarboxylation via central aromatic acid decarboxylase (DCAA). After the synthesis of dopamine from Levodopa has occurred, D1-like and D2-like family receptors are activated (Figure I.7). This in turn restores the movement in PD patients as a result of regulation of dopamine function in the brain [30].

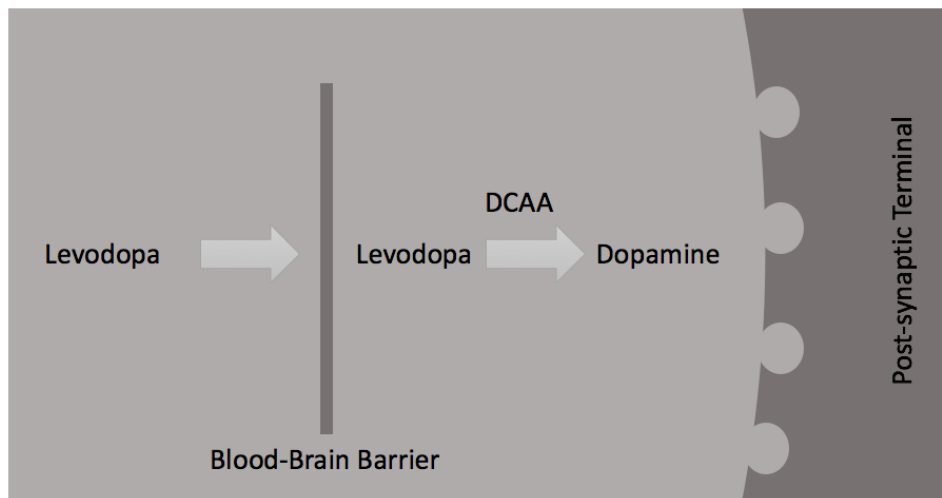


Figure I.7 – Mechanism of action of Levodopa in the brain.

Levodopa is still considered the most effective and powerful treatment method for symptoms of PD, and almost all PD patients will be prescribed this treatment at one point or another. The significance of this treatment method lies in the fact that almost all PD patients are responsive and experience important symptomatic relief after intake, such that it is one of the criteria for diagnosis of PD (section I.2). In most cases, the effect of the drug is more powerful on bradykinesia and rigidity, but still offers some improvement in tremor. Another major advantage of Levodopa is the rapid response, where most patients see significant improvement in symptoms within the first few days which gradually builds up over several weeks.

Motor Fluctuations and Levodopa Induced Dyskinesia

Once Levodopa is described as the main treatment method for PD symptoms, most patients go through an average period of two to five years where the drug functions properly. This is usually referred to as "Levodopa-honeymoon" phase, and response is described as stable and smooth. However, after this phase, the side effects of Levodopa start to appear and many patients begin to experience motor fluctuations that gradually worsen.

During this stage of the disease, Levodopa is usually prescribed in three or four daily divided dosages. The response to Levodopa stops being stable and smooth, and instead patients begin to respond to

each individual dose separately. This fluctuation in response manifests as motor complications and the patient experiences different motor states based on the onset, duration and termination of each dose (Figure I.8).

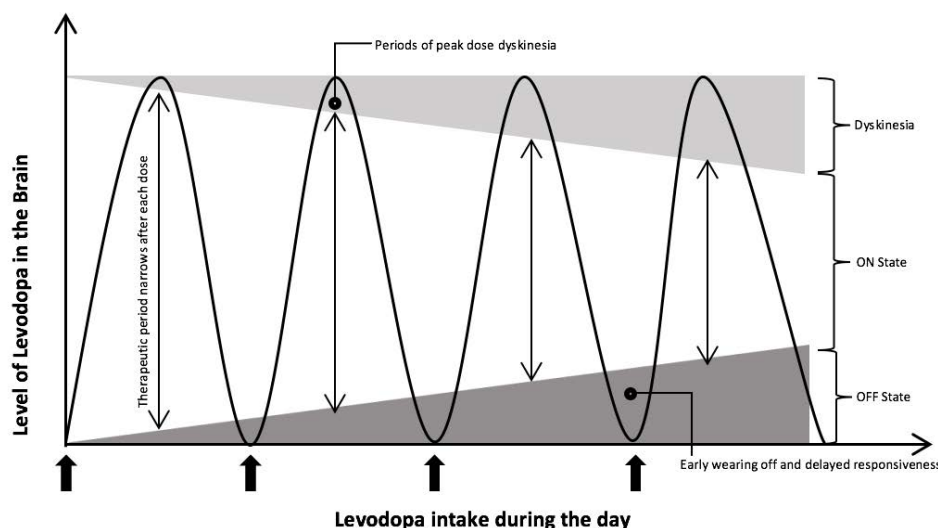


Figure I.8 – Motor fluctuations associated with Levodopa therapy [31].

The prevalence of motor complications associated with Levodopa therapy increases gradually with disease progression and duration of treatment. In most severe cases, the fluctuations experienced by the patient are described as "yo-yo" phenomenon, where the patient transitions rapidly between different motor states [32]. These motor states are characterised as:

- **On State:** describes the period in which the drug is functioning properly. This signifies that the patient is relieved from PD motor symptoms and is not experiencing any motor complications as a result of Levodopa itself.
- **Off State:** refers to the period in which the drug is not functioning at all. During this period, patients experience severe worsening of PD symptoms and motor deterioration. In advanced stages of the disease, the patient becomes absolutely disabled, unable to move and trembles while experiencing freezing. Other alarming symptoms associated with this phenomenon include severe depression, autonomic dysfunction and tachycardia.
- **Wearing-off:** signifies shortening of the therapeutic period of clinical benefit after each dose. At the beginning of treatment, the therapeutic window during which the patient is in the "on state" lasts about four to six hours. However, in later stages, the duration of "on state" shortens reaching an average of one to two hours. Wearing off phenomenon may be abrupt or gradual and may be associated with "off" period dystonia.
- **Dyskinesia:** include peak-dose dyskinesia or "on" period dyskinesia, diphasic dyskinesia and "off" period dystonia. This phenomenon is described as random, chorea-like movements that can

be quite debilitating and interfere with the patient's ability to perform daily functions. Peak-dose dyskinesia occurs when plasma levels of the drug are at their highest. Diphasic dyskinesia usually appears before the response to the drug occurs, disappear during the "on" period when the drug is functioning properly, and then reappear as the response to the drug starts to fade. Off period dystonia, however, is described as prolonged muscle spasms that could affect different body segments, and are usually associated with pain.

Despite the negative side-effects, Levodopa remains to be the drug of choice for treatment of PD motor symptoms. The prevention of development of these motor fluctuations is therefore a crucial issue [33]. So far, different attempts have been made to delay the prevalence of these motor fluctuations that include prescribing COMT inhibitors along with Levodopa medication, and delaying the initiation of Levodopa therapy in younger patients for as long as possible. Another viable option is management of dosage, where the smallest possible daily dose is prescribed, to ensure sustained non-pulsatile action of Levodopa.

Clinical Features of Levodopa Induced Dyskinesia

While the underlying pathophysiology of LID remains incompletely understood, it has been established that dyskinesia appears only after the administration of dopaminergic therapy. In general terms, dyskinesia is described as random, spastic, involuntary movements that appear shortly after the administration of Levodopa. Clinical observations, however, have led to the identification of several types of dyskinesias. The clinical features associated with the different types of LID are distinct and can be associated to Levodopa dosing.

LID in PD patients is described as clinically heterogeneous. This phenomenon is presented as abnormal movements, most commonly characterised as chorea or choreoathetosis. In most PD patients, LID begins in the side most affected by PD and generally in the lower limbs before transitioning to the upper limbs as well. The clinical term *chorea* is used to describe LID that manifests as a series of flowing movements from one side of the body to another, that are involuntary, rapid, irregular, and non-sustained. These movements can have varying severities, from mild twitching and squirming, to violent large amplitude flinging and flailing arm movements, otherwise known as *ballism*. Generally, this type of dyskinesia is not painful, and in mild cases does not incur discomfort in the patient. Many patients even prefer the sense of mobility during this case to the immobility experienced in the absence of dyskinesia.

Another term used to describe LID is *dystonia*. This is the second most common form of LID, and presents itself as sustained muscle contractions. This type of LID can occur on its own or in combination with *chorea*, and is observed as twisting of the leg while walking or the arm being pulled behind the back. *Dystonia* is commonly associated with pain, specifically when it occurs in the morning, and accounts for greater discomfort in patients than *chorea*. Other less common forms of LID exist and include overshooting gait, rapid abnormal movements and mixed pattern movements.

Levodopa Induced Dyskinesias and Quality of Life

In most patients suffering from mild dyskinesias induced by Levodopa, Quality of Life (QL) is not majorly affected [34]. However, as the disease progresses into advanced stages, the severity of dyskinesias increases, introducing more disabling abnormal movements that could be painful. For the majority of patients in the advanced stages, QL is reported to be poorer [35].

Physicians are aware that a more aggressive treatment with Levodopa will most likely induce motor complications at an earlier stage. In many cases, this leads to treatment with conservative doses of Levodopa that are insufficient to provide the patient with relief from PD symptoms. Interestingly, a comparison between QL scores of patients prescribed adequate doses of Levodopa and suffering from LID and patients prescribed lesser doses that are insufficient to suppress PD motor symptoms, found that patients suffering from LID presented higher QL scores [36].

On the other hand, QL scores of patients in more advanced stages of the disease worsen as a direct result of higher severity LID. QL scores in areas of activities of daily living, emotional well-being, communication and bodily discomfort have been reported to significantly decrease [35, 37]. Clinicians therefore need to find a balance between sufficient dosage able to reduce PD motor symptoms, prolonging the beneficial effect of Levodopa and managing the severity of LID to ensure better QL for the patients.

4 Rating Scales

Current methods of assessment of motor symptoms and complications of PD in clinical practice are based on clinician rated scales and patient diaries (Table I.1). These scales are frequently criticised for being subjective, short-period based assessments that lack the ability to properly detect or quantify the symptoms [38].

On the other hand, assessment of LID in the existing scales doesn't provide the necessary objective information required to define the severity of this phenomenon. According to [39], LID assessment should be based on anatomical distribution, severity of abnormal movements and impact on activities of daily living. The AIMS scale is predominantly psychiatric, placing emphasis on lingual-facial-buccal movements. The fourth section of the UPDRS scale dealing with involuntary movements disregards anatomical distribution and lacks objective assessment of global disability and duration of dyskinesias. Patient self-evaluation diaries are accepted by the FDA as an end point for regulatory purposes but introduce serious challenges due to subjectivity, lack of compliance to completion by the patients, and unreliability in advanced stages as a result of declined cognitive abilities.

As a result, research has been aimed towards the development of quantitative instrumental techniques that would be able to objectively measure dyskinesias and other PD motor symptoms. These techniques will help clinicians in the future prospects of treating and managing LID offering guidance in dose adjustment to reduce already existing LID and potentially prevent it from happening.

Table I.1 – Currently Used Scales for Monitoring and Evaluating Disease Progression

Ref.	Scale	Overview of Assessment
[40]	Unified Parkinson's Disease Rating Scale (UPDRS)	Rater and patient evaluation form of cognitive state, activities of daily living, general motor function and complications of treatment
[41]	Unified Dyskinesia Rating Scale (UDysRS)	Rater and patient assessment questionnaires to evaluate motor symptoms of PD
[42]	Abnormal Involuntary Movements Scale (AIMS)	Clinician rated scale based on observations of patient movements to assess tardive dyskinesia
[13]	Hoehn and Yahr Scale	Clinician rated scale based on the patients motor symptoms severity to determine stage of the disease
[43]	Hauser Diary	A patient filled diary to chronologically list episodes of motor fluctuations throughout the day
[44]	Movement Disorders Society Unified Parkinson's Disease Rating Scale (MDS-UPDRS)	Rater and patient evaluation form of cognitive state, an edited/updated version of the UPDRS in which ambiguities were defined and important additions of non-motor symptom assessment were added

5 Conclusion

Parkinson's disease is devastating neurological disorder of unknown aetiology that affects a vast number of the population. Its projected increase due to an ageing population in Europe will incur an economic and social burden on society. PD progresses relentlessly and the current treatment methods revolve around managing motor and non-motor symptoms of the disease. Levodopa is considered to be the gold standard for treatment of PD motor symptoms. However, motor fluctuations and dyskinesias induced by the drug can be important problems for PD patients, often resulting in the deterioration of quality of life. The unreliability of current assessment methods of PD motor symptoms and complications introduces serious issues for clinicians in terms of managing the prescribed therapeutic plan. This also implies the necessity to develop new devices capable of providing an objective assessment of PD motor symptoms and as such producing a better structured therapeutic plan.

Bibliography

- [1] P. D. FOUNDATION. Statistics on Parkinson's, (2016).
- [2] J. PARKINSON. *An essay on the shaking palsy*. Archives of Neurology **20**(4), 441 (1969).
- [3] S. FAHN, P. E. GREENE, B. FORD, S. B. BRESSMAN, AND S. J. FRUCHT. Movement disorders. In *Atlas of Clinical Neurology*, pages 341–394. Springer (2009).
- [4] C. PAISAN-RUIZ, S. JAIN, E. W. EVANS, W. P. GILKS, J. SIMON, M. VAN DER BRUG, A. L. DE MUNAIN, S. APARICIO, A. M. GIL, N. KHAN, ET AL. *Cloning of the gene containing mutations that cause park8-linked Parkinson's disease*. Neuron **44**(4), 595–600 (2004).
- [5] D. G. HEALY, M. FALCHI, S. S. O'SULLIVAN, V. BONIFATI, A. DURR, S. BRESSMAN, A. BRICE, J. AASLY, C. P. ZABETIAN, S. GOLDWURM, ET AL. *Phenotype, genotype, and worldwide genetic penetrance of lrrk2-associated Parkinson's disease: a case-control study*. The Lancet Neurology **7**(7), 583–590 (2008).
- [6] J. HARDY, P. LEWIS, T. REVESZ, A. LEES, AND C. PAISAN-RUIZ. *The genetics of Parkinson's syndromes: a critical review*. Current opinion in genetics & development **19**(3), 254–265 (2009).
- [7] C. M. TANNER, R. OTTMAN, S. M. GOLDMAN, J. ELLENBERG, P. CHAN, R. MAYEUX, AND J. W. LANGSTON. *Parkinson's disease in twins: an etiologic study*. Jama **281**(4), 341–346 (1999).
- [8] K. TAYLOR, C. COUNSELL, C. HARRIS, AND J. GORDON. *Screening for undiagnosed parkinsonism in people aged 65 years and over in the community*. Parkinsonism & related disorders **12**(2), 79–85 (2006).
- [9] F. D. DICK, G. DE PALMA, A. AHMADI, N. SCOTT, G. PRESCOTT, J. BENNETT, S. SEMPLE, S. DICK, C. COUNSELL, P. MOZZONI, ET AL. *Environmental risk factors for Parkinson's disease and parkinsonism: the geoparkinson study*. Occupational and Environmental Medicine **64**(10), 666–672 (2007).
- [10] J. A. OBESO, M. C. RODRIGUEZ-OROZ, M. RODRIGUEZ, J. L. LANCIEGO, J. ARTIEDA, N. GONZALO, AND C. W. OLANOW. *Pathophysiology of the basal ganglia in Parkinson's disease*. Trends in neurosciences **23**, S8–S19 (2000).
- [11] H. BRAAK, K. DEL TREDICI, U. RÜB, R. A. DE VOS, E. N. J. STEUR, AND E. BRAAK. *Staging of brain pathology related to sporadic Parkinson's disease*. Neurobiology of aging **24**(2), 197–211 (2003).
- [12] W. H. ORGANIZATION. *Neurological disorders: public health challenges*. World Health Organization (2006).
- [13] M. M. HOEHN, M. D. YAHR, ET AL. *Parkinsonism: onset, progression, and mortality*. Neurology **50**(2), 318–318 (1998).
- [14] A. J. HUGHES, S. E. DANIEL, L. KILFORD, AND A. J. LEES. *Accuracy of clinical diagnosis of idiopathic Parkinson's disease: a clinico-pathological study of 100 cases*. Journal of Neurology, Neurosurgery & Psychiatry **55**(3), 181–184 (1992).

BIBLIOGRAPHY

- [15] D. J. GELB, E. OLIVER, AND S. GILMAN. *Diagnostic criteria for Parkinson's disease*. Archives of neurology **56**(1), 33–39 (1999).
- [16] E. TOLOSA, G. WENNING, AND W. POEWE. *The diagnosis of Parkinson's disease*. The Lancet Neurology **5**(1), 75–86 (2006).
- [17] J. MEARA, B. K. BHOWMICK, AND P. HOBSON. *Accuracy of diagnosis in patients with presumed Parkinson's disease*. Age and ageing **28**(2), 99–102 (1999).
- [18] R. B. POSTUMA, D. BERG, M. STERN, W. POEWE, C. W. OLANOW, W. OERTEL, J. OBESO, K. MAREK, I. LITVAN, A. E. LANG, ET AL. *MDS clinical diagnostic criteria for Parkinson's disease*. Movement Disorders **30**(12), 1591–1601 (2015).
- [19] G. DEUSCHL, P. BAIN, AND M. BRIN. *Consensus statement of the movement disorder society on tremor*. Movement Disorders **13**(S3), 2–23 (1998).
- [20] A. BERARDELLI, J. ROTHWELL, P. THOMPSON, AND M. HALLETT. *Pathophysiology of bradykinesia in Parkinson's disease*. Brain **124**(11), 2131–2146 (2001).
- [21] M. C. RODRIGUEZ-OROZ, M. JAHANSHAH, P. KRACK, I. LITVAN, R. MACIAS, E. BEZARD, AND J. A. OBESO. *Initial clinical manifestations of Parkinson's disease: features and pathophysiological mechanisms*. The Lancet Neurology **8**(12), 1128–1139 (2009).
- [22] B. R. BLOEM, J. VAN VUGT, AND D. J. BECKLEY. *Postural instability and falls in Parkinson's disease*. Advances in neurology **87**, 209 (2001).
- [23] B. R. BLOEM, J. M. HAUSDORFF, J. E. VISSER, AND N. GILADI. *Falls and freezing of gait in Parkinson's disease: a review of two interconnected, episodic phenomena*. Movement Disorders **19**(8), 871–884 (2004).
- [24] J. E. ALTY AND P. A. KEMPSTER. *A practical guide to the differential diagnosis of tremor*. Postgraduate medical journal pages pgmj–2009 (2011).
- [25] H. LING, L. A. MASSEY, A. J. LEES, P. BROWN, AND B. L. DAY. *Hypokinesia without decrement distinguishes progressive supranuclear palsy from Parkinson's disease*. Brain **135**(4), 1141–1153 (2012).
- [26] M. D. SOCIETY. Mds-pas visiting trainee grant program, (2016).
- [27] D.-B. S. FOR PARKINSON'S DISEASE STUDY GROUP ET AL. *Deep-brain stimulation of the subthalamic nucleus or the pars interna of the globus pallidus in Parkinson's disease*. The New England journal of medicine **345**(13), 956 (2001).
- [28] A. W. WILLIS, M. SCHOOTMAN, N. KUNG, X.-Y. WANG, J. S. PERLMUTTER, AND B. A. RACETTE. *Disparities in deep brain stimulation surgery among insured elders with Parkinson's disease*. Neurology **82**(2), 163–171 (2014).
- [29] A. K. CHAN, R. A. MCGOVERN, L. T. BROWN, J. P. SHEEHY, B. E. ZACHARIA, C. B. MIKELL, S. S. BRUCE, B. FORD, AND G. M. MCKHANN. *Disparities in access to deep brain stimulation surgery for Parkinson's disease: interaction between african american race and medicaid use*. JAMA neurology **71**(3), 291–299 (2014).
- [30] S. A. BRAVO, C. RANGEL-BARAJAS, AND B. F. GARDUÑO. *Pathophysiology of l-dopa induced dyskinesia changes in d1/d3 receptors and their signalling pathway*. A Synopsis of Parkinson's Disease (2014).
- [31] S. A. FACTOR AND W. WEINER. *Parkinson's Disease: Diagnosis & Clinical Management*. Demos Medical Publishing (2007).

-
- [32] J. A. OBESO, C. W. OLANOW, AND J. G. NUTT. *Levodopa motor complications in Parkinson's disease*. Trends in neurosciences **23**, S2–S7 (2000).
- [33] F. STOCCHI, M. TAGLIATI, AND C. W. OLANOW. *Treatment of levodopa-induced motor complications*. Movement Disorders **23**(S3), S599–S612 (2008).
- [34] C. MARRAS, A. LANG, M. KRAHN, G. TOMLINSON, AND G. NAGLIE. *Quality of life in early Parkinson's disease: impact of dyskinesias and motor fluctuations*. Movement disorders **19**(1), 22–28 (2004).
- [35] M. PECHEVIS, C. CLARKE, P. VIEREGGE, B. KHOSHNOOD, C. DESCHASEAUX-VOINET, G. BERDEAUX, AND M. ZIEGLER. *Effects of dyskinesias in Parkinson's disease on quality of life and health-related costs: a prospective european study*. European Journal of Neurology **12**(12), 956–963 (2005).
- [36] A. SCHRAG AND N. QUINN. *Dyskinesias and motor fluctuations in Parkinson's disease*. Brain **123**(11), 2297–2305 (2000).
- [37] A. DAMIANO, M. MCGRATH, M. WILLIAN, C. SNYDER, P. LEWITT, P. REYES, R. RICHTER, AND E. MEANS. *Evaluation of a measurement strategy for Parkinson's disease: assessing patient health-related quality of life*. Quality of Life Research **9**(1), 87–100 (2000).
- [38] W. G. MEISSNER, M. FRASIER, T. GASSER, C. G. GOETZ, A. LOZANO, P. PICCINI, J. A. OBESO, O. RASCOL, A. SCHAPIRA, V. VOON, ET AL. *Priorities in Parkinson's disease research*. Nature reviews Drug discovery **10**(5), 377–393 (2011).
- [39] G. FABBRINI, J. M. BROTCHE, F. GRANDAS, M. NOMOTO, AND C. G. GOETZ. *Levodopa-induced dyskinesias*. Movement disorders **22**(10), 1379–1389 (2007).
- [40] M. D. S. T. F. ON RATING SCALES FOR PARKINSON'S DISEASE ET AL. *The unified Parkinson's disease rating scale (UPDRS): status and recommendations*. Movement disorders: official journal of the Movement Disorder Society **18**(7), 738 (2003).
- [41] C. G. GOETZ, J. G. NUTT, AND G. T. STEBBINS. *The unified dyskinesia rating scale: presentation and clinimetric profile*. Movement Disorders **23**(16), 2398–2403 (2008).
- [42] A. J. RUSH, M. B. FIRST, AND D. BLACKER. *Handbook of psychiatric measures*. American Psychiatric Pub (2008).
- [43] R. A. HAUSER, J. FRIEDLANDER, T. A. ZESIEWICZ, C. H. ADLER, L. C. SEEBERGER, C. F. O'BRIEN, E. S. MOLHO, AND S. A. FACTOR. *A home diary to assess functional status in patients with Parkinson's disease with motor fluctuations and dyskinesia*. Clinical neuropharmacology **23**(2), 75–81 (2000).
- [44] C. G. GOETZ, B. C. TILLEY, S. R. SHAFTMAN, G. T. STEBBINS, S. FAHN, P. MARTINEZ-MARTIN, W. POEWE, C. SAMPAIO, M. B. STERN, R. DODEL, ET AL. *Movement disorder society-sponsored revision of the unified Parkinson's disease rating scale (MDS-UPDRS): Scale presentation and clinimetric testing results*. Movement disorders **23**(15), 2129–2170 (2008).

Ambulatory Monitoring of Levodopa Induced Dyskinesia and PD Motor Symptoms

Wearable sensing technology, specifically sensors concerned with quantification of movement, has been the focus of research efforts to shift clinical assessment of motor dysfunction from the current subjective methods to quantifiable and accurate measures. This chapter introduces wearable sensing technology, showing how technological advances in sensors provided an objective means of monitoring, quantifying and evaluating human movement and other measures.

The focus here is on Inertial Measurement Units (IMUs) in which the different components included are explained, showing the principles behind describing movement through objective measures. Following that, a review of the recent literature is done, showing the application of wearable sensors to objectively and automatically quantify PD motor symptoms and complications as a means of advancing the clinical assessment of the disease.

As this work builds on some of the aspects presented in the mentioned literature and aims to enhance specifically the ability of properly detecting LID in PD patients in a realistic setting, the objectives and contribution of this thesis are presented.

1 Wearable Sensors and Systems

In the past couple of decades, there have been significant advances in the miniaturisation, proliferation, accessibility and sophistication of sensor technology. These advances have fuelled the exploration and implementation of wearable sensors and feedback devices for the mass population with the main objective of improving healthcare. Increasing healthcare costs, incurred by an ageing population and higher rates of survival from acute trauma and disabling diseases in developed countries [1–3], have motivated the scientific community and industry to design and develop wearable systems for health monitoring [4]. Monitoring a patient’s health status remotely and continuously for a long duration without the need for hospitalisation not only provides the opportunity for better management of the patient’s condition, but also reduces the consequent healthcare costs.

Wearable sensors have been applied in a wide range of applications including health related services, entertainment, security and communication fields. When focusing on health related applications

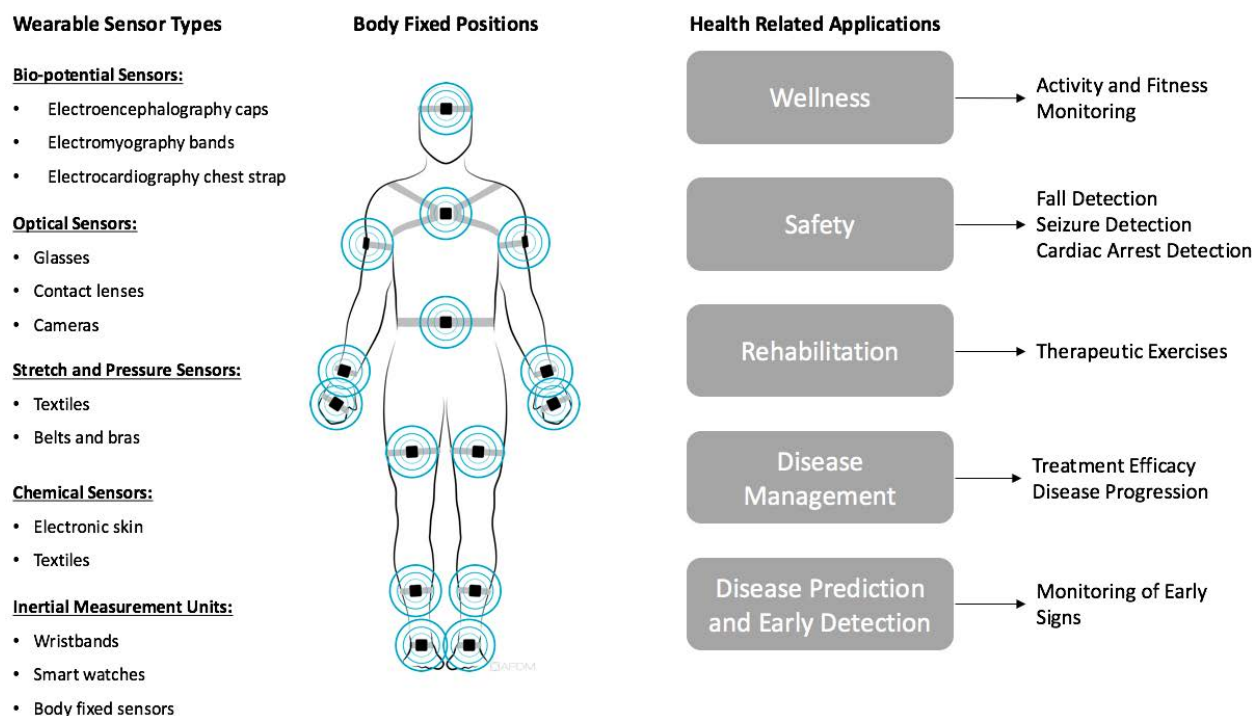


Figure II.1 – Diagram showing the different categories of wearable sensors, common body fixed positions based on sensor type, and a general summary of health related applications [5].

(Figure II.1), wearable sensors can be categorised based on the measured entity into the following subtypes: biopotential sensors, optical sensors, stretch and pressure sensors, chemical sensors, and inertial measurement units. Commercially available devices of the different sensor types have been gradually increasing. For example, existing biopotential sensors include the Emotiv device, which is a wearable EEG system that is designed for brain monitoring and cognitive assessment and has been used in different studies for brain computer interface development, emotion recognition and assessment of auditory events [6–9]. Other examples include the Polar H7 chest strap [10, 11], which is a portable ECG device designed for heart rate monitoring commonly used in fitness domains. Stretch sensors have been used for human body motion sensing [12] and monitoring of chronic diseases [13]. Examples of wearable chemical sensors include measurements of sweat, tears and saliva among several other measures.

Perhaps the most impressive commercialisation of wearable sensors in the past decade is in the area of movement analysis and activity monitoring using IMUs. The rapidly growing trend of self-monitoring and personalised healthcare led to an abundance of devices aimed towards providing the user with simple quantifiable information of activity levels, energy expenditure and sleep patterns. The most popular of which include Fitbit, Jawbone, Misfit, and Withings [14–17]. The highlight of such devices lies in their unobtrusiveness (making it possible for users to wear them on a daily basis), their ease of use and information display, commonly through an application or website, and their ability to transmit

a feeling of control to the user, in which he/she feels able to better manage their health through up-to-date information.

Safety applications have mainly focused on fall detection for the elderly, seizure detection for epileptic patients as well as cardiac arrest for individuals suffering from heart diseases. For example, the studies conducted in [18–20] focused on fall detection for the elderly and people in fall risk groups by means of body worn sensors such as triaxial accelerometers and IMUs. Other studies, such as [21–24], employ miniaturised biopotential sensors and inertial sensors for the detection of seizures in epilepsy patients. The methods explored in these studies aim to provide an objective means of monitoring seizures in epilepsy patients in their daily life instead of over short period specialised EEG assessment performed over several weeks. While studies such as [25–28] have developed wearable systems for real time monitoring of abnormal events such as arrhythmia or arrest in cardiac disease patients. These studies mostly rely on wearable ECG sensors that detect the occurrence of these events and in some cases proceed to alert emergency caregivers. Large emphasis in this area of research has been applied on the early detection and localisation of the victims in hopes for providing assistance rapidly, which in many cases can be a life or death matter.

The incorporation of wearable sensors in rehabilitation and disease management applications has also seen its fair share of growth over the past few decades. In the most part, wearable sensors have been used to facilitate the implementation of home-based rehabilitation therapeutic programs post trauma or surgeries. As an example, the work presented in [29–32] introduces objective means for patient assistance and monitoring in "at-home" therapeutic exercises for patients undergoing rehabilitation. These measures tend to encourage patient compliance and performance of the necessary tasks as well as provide meaningful feedback to the physicians for better assessment of progress. In some cases these applications also provide direct feedback to the patients during the performance of the rehabilitation exercise guiding them through proper gestures to ensure optimal results.

A valuable tool for physicians in disease management is the ability to assess the efficacy of the prescribed treatment plan in a quantitative and objective manner. In many cases, treatment plans require fine tuning based on the patient's responsiveness. However, the lack of information from that perspective during the time between outpatient visits limits the physician's evaluation. As such, efforts have been focused on presenting clinicians with means of quantifying the efficacy of treatment in a wide range of diseases. For example, in [33], a system of wearable sensors is used to assess the efficacy of electroacupuncture for gait disorders in PD patients. Another example is found in [34], where the use of wearable sensors is applied to assess the efficacy of mobility therapy for children with cerebral palsy.

Another area of growing interest is the use of wearable sensors in disease prediction. An example of this is found in [35] where continuous monitoring of ECG, vital signs, and activities using wearable sensors allows for the detection of early symptoms of heart disease. Another example given in [36] presents the assessment of gait and balance impairments by having patients perform certain in-clinic tests while wearing accelerometers and gyroscopes on the shins, thigh and trunk. The obtained objective methods are used to provide early indication of frailty syndrome. Such applications have become a

prominent part of wearable sensor technologies due to the introduced benefits in terms of providing early treatment and reducing the overall associated medical costs.

The Shimmer sensing platforms, on the other hand, are miniature, wearable devices that have been specifically designed for health related applications and research. The Shimmer3 IMUs have been adopted in several applications ranging from gait and fall risk assessment [37–39], sports applications [40], and activity detection and classification [41–43]. The Shimmer sensing platform has also developed wearable ECG and EMG modules that have been validated in several studies [44–48]. For this reason, these sensors were selected for our work. Due to the pivotal role that wearable sensors could play in future healthcare, efforts in research have been multiplied, over the past few years, specifically in detecting and quantifying human movement and measuring movement related disorders.

2 Movement Analysis and Objective Assessment of PD

2.1 Measuring Human Motion Through IMUs

The quantification of human movement is based on key technologies that can be summed up into three parts: the sensors and data collection hardware, the communication hardware and software to transfer the collected data, and finally the processing and analysis methods used to extract meaningful information from the collected data.

The current methods for physical activity monitoring and motion analysis are mostly based on inertial parameters such as acceleration, angular velocity, and in some cases by measuring the magnetic field surrounding the subject. These inertial parameters are well established as suitable measures for quantifying and analysing states of rigid body kinematics [49]. Because of the segmental decomposition of the human body defined in biomechanics, these parameters have shown great relevance in quantifying movement, detecting pathological aspects and movement dysfunction, and assessing performance.

As the understanding of the complexity of simple human movements and gestures grew along with the advances in electronics technology, micro-electro-mechanical systems (MEMS) emerged, allowing for the combination of multiple sensors into miniaturised devices along with processors and data storage capabilities [50]. As a result, major leaps in the field of inertial sensing followed, leading to the development of IMUs [51], which are devices that house a number of sensor components and aim to better quantify different aspects of complex movements [52–54]. The principles of functioning of each of the components of the IMUs are described in the following:

- **Accelerometer:** a device which measures acceleration due to all forces acting on the body, which include the gravitational force as well as any external force applied to the device [55]. The two primary components of acceleration are therefore the inertial and gravitational acceleration, and the total acceleration \mathbf{a}_T measured is expressed as the vector sum of these components:

$$\mathbf{a}_T = \mathbf{a}_I + \mathbf{a}_g \quad (\text{II.1})$$

where \mathbf{a}_I is the inertial component and \mathbf{a}_g is the gravitational component.

Whenever a body is in motion with variable velocity, there exist inertial forces other than gravity acting on it. These forces give rise to inertial acceleration (m/s^2), which is defined as the rate of change of velocity of the body in motion. When a body is completely motionless however, gravity (m/s^2), which is proportional to the body's mass, is the only force acting on the body. In this case, the accelerometer measures a constant acceleration equal in magnitude to the acceleration due to gravity (approximately 9.81 m/s^2).

In the case of a uniaxial accelerometer (Figure II.2), the total acceleration a_T measured along a specific axis can be expressed as:

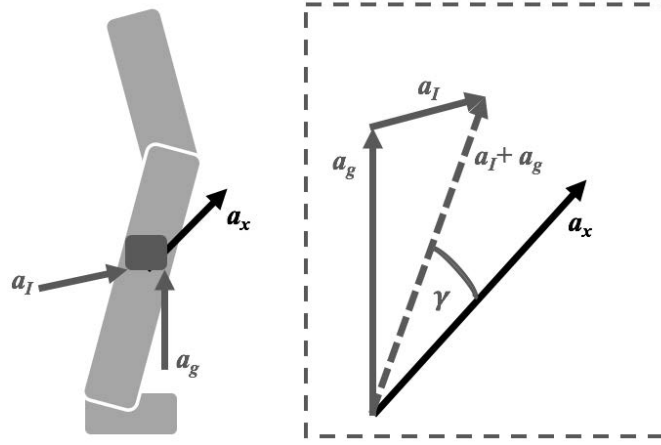


Figure II.2 – Uniaxial accelerometer measurement for a sensor attached to a leg segment.

$$a_T = \|\mathbf{a}_I + \mathbf{a}_g\| \cos(\gamma) \quad (\text{II.2})$$

where $\|\mathbf{a}_I + \mathbf{a}_g\|$ denotes the magnitude of the vector, and γ is the angle between the measurement axis and the total acceleration vector $\mathbf{a}_I + \mathbf{a}_g$. Considering the case of measurement along the x axis for example, the total acceleration can alternatively be expressed as:

$$a_x = \|\mathbf{a}_I\| \cos(\theta_x) + \|\mathbf{a}_g\| \cos(\varphi_x) \quad (\text{II.3})$$

where θ_x and φ_x represent the angle the axis, a_x , makes with the inertial acceleration vector, \mathbf{a}_I , and the gravity vector, \mathbf{a}_g respectively.

Many devices today, including the device used in this study, are equipped with triaxial accelerometers, meaning the acceleration measured has three components, over the mutually orthogonal axes x , y and z axes. Similar to the case of the uniaxial accelerometer, a certain proportion of the inertial and gravitation accelerations are measured by each component, depending on the angles between the axis and the directions of acceleration components. The acceleration vector,

\mathbf{a} , can therefore be expressed as:

$$\mathbf{a} = \begin{bmatrix} a_x \\ a_y \\ a_z \end{bmatrix} = \begin{bmatrix} a_I \cos(\theta_x) + a_g \cos(\varphi_x) \\ a_I \cos(\theta_y) + a_g \cos(\varphi_y) \\ a_I \cos(\theta_z) + a_g \cos(\varphi_z) \end{bmatrix} \quad (\text{II.4})$$

- **Gyroscope:** a device which measures the angular velocity of a body, which is the rate at which the object is rotating, in terms of the speed of rotation and the axis about which it is rotating [56]. A uniaxial gyroscope attached to a rotating plate (Figure II.3) measures the angular velocity, w_x , as:

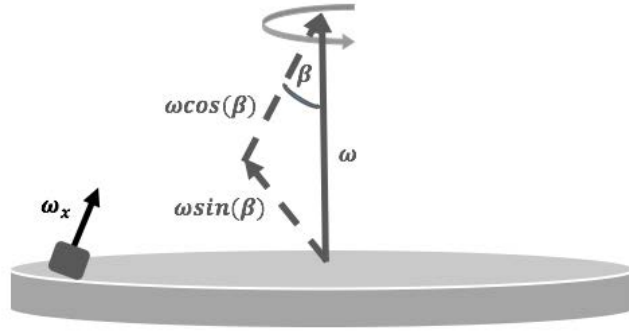


Figure II.3 – Uniaxial gyroscope angular velocity measurement for a sensor attached to a rotating plate.

$$\omega_x = \|\omega\| \cos(\beta) \quad (\text{II.5})$$

where $\|\omega\|$ is the magnitude of the angular velocity vector component along the measuring axis of the gyroscope (in this case x axis), and β is the inclination of the measuring axis with respect to the angular velocity vector ω .

In the case of a triaxial gyroscope, a three dimensional angular velocity vector is obtained from the three orthogonal uniaxial gyroscopes. The measured angular velocity vector, $\omega_{\mathbf{T}}$, then becomes:

$$\omega_{\mathbf{T}} = \begin{bmatrix} \omega_x \\ \omega_y \\ \omega_z \end{bmatrix} = \begin{bmatrix} \omega \cos(\beta_x) \\ \omega \cos(\beta_y) \\ \omega \cos(\beta_z) \end{bmatrix} \quad (\text{II.6})$$

where β_x , β_y , and β_z are the angles between the measurement axes, w_x , w_y and w_z , and the rotation axis, respectively.

- **Magnetometer:** a device that is used to measure the direction and/or strength of the local magnetic field. A uniaxial magnetometer measures the magnetic field vector acting along its measuring axis. The illustration in Figure II.4 shows a uniaxial magnetometer whose measurement

axis is along the x axis, and the measured magnetic field m_x can be expressed as:

$$m_x = ||\mathbf{m}||\cos(\alpha) \quad (\text{II.7})$$

where $||\mathbf{m}||$ is the magnitude of the magnetic field acting on the sensor, and α is the angle between the magnetometer's measurement axis and the magnetic field vector. Similarly to the

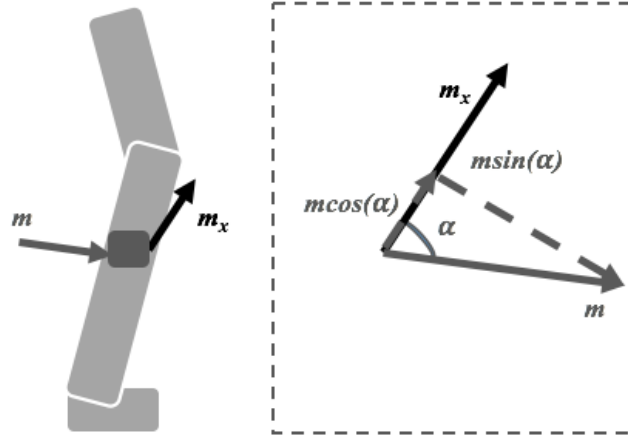


Figure II.4 – Uniaxial magnetometer measurement for a sensor attached to a leg segment.

previous two sensors, the three dimensional magnetic field vector $\mathbf{m_T}$ obtained from a triaxial magnetometer is given by:

$$\mathbf{m_T} = \begin{bmatrix} m_x \\ m_y \\ m_z \end{bmatrix} = \begin{bmatrix} m \cos(\alpha_x) \\ m \cos(\alpha_y) \\ m \cos(\alpha_z) \end{bmatrix} \quad (\text{II.8})$$

where α_x , α_y , and α_z are the angles formed between the measurement axes m_x , m_y , and m_z and the magnetic field vector \mathbf{m} respectively.

The main interest in using IMUs for the measurement of human motion lies in their ability to quantify kinematic parameters of a body with varying levels of difficulty. The complete kinematics of a body in three dimensional space used to describe motion can be obtained using the following variables [57]:

- Linear displacement of centre of mass (x , y , and z);
- Linear velocity of centre of mass (\dot{x} , \dot{y} , and \dot{z});
- Linear acceleration of centre of mass (\ddot{x} , \ddot{y} , and \ddot{z});
- Angular displacement of the body in two planes (θ_{xy} , θ_{yz});
- Angular velocity of the body in two planes (w_{xy} , w_{yz});

- Angular acceleration of the body in two planes (α_{xy} , α_{yz});

The estimation of these parameters gives an overall image of the movement, in terms of speed, orientation and direction, of the body segment to which the IMU is attached.

2.2 Objective Measurement of PD Motor Symptoms and Complications

PD Motor Symptoms

The increasing efforts in the area of objectively quantifying motor symptoms and complications indicates the need for a reliable method of clinical assessment. An ideal evaluation method should provide objective, quantitative and long-term data that relays useful and clear information. A number of previously proposed systems of ambulatory assessment are presented in Table II.1.

Several recent approaches have been explored in detecting and quantifying gait impairments. In [58], gait parameters were accurately estimated and showed high correlation to clinical scales such as the UPDRS. The authors in [59, 60] were able to identify freezing of gait and distinguish it from volitional standing. The approach in [61] identified gait patterns and the authors showed that it was possible to distinguish between different levels of gait impairment. The ability to replace standard gait and TUG tests with an objective system was also validated in [62].

Some studies such as [63] and [64] were concerned with the evaluation of tremor and bradykinesia at the same time. In [63], high sensitivity and specificity values were obtained in tremor detection and calculated parameters related to both tremor and bradykinesia showed high correlation with UPDRS scores. Other studies, on the other hand, focused solely on tremor evaluation. The authors in [65], for example, were able to successfully quantify tremor severity and distinguish between resting and postural tremors.

PD Motor Complications: Levodopa Induced Dyskinesia

Dyskinesia is considered one of the most difficult motor dysfunctions to objectively monitor in PD due to its complexity, random nature and difficulty to distinguish from voluntary activities. Dyskinetic movements are abnormal movements that can be described as smooth tics or chorea and diminished voluntary activities. These movements can range from slight twitching of a limb to the uncontrollable flinging of upper or lower extremities. The types and clinical features of dyskinesia have been detailed in Chapter I, section 3.3.

Recently, attention has been concentrated on detecting and quantifying this phenomenon. Basic findings in this area of research report detection and/or quantification of LID, assessment of its severity, distinguishing from voluntary activities or PD motor symptoms, and correlation between objectively quantified scores and clinical scales. A sample of the published work in this regard is presented in Table II.2.

Table II.1 – Selection of Studies on the Objective Measurement of PD Motor Symptoms.

Ref.	Motor Dysfunction	Device	Placement	Protocol
Salarian 2004 [58]	Gait	uniaxial gyroscopes	left and right thigh, left and right shank	standing up, walking, sitting down
Moore 2007 [59, 60]	Gait	Xsens MT9 IMU	left shank	walking
Salarian 2007 [63]	Tremor and Bradyskinesia	ASUR	both forearms	17 activities of daily living
Barth 2011 [61]	Gait	Shimmer	lateral heel of shoe	standardised gait tests: 10-meter walk, heel-toe tapping, circling
Mera 2012 [64]	Tremor and Bradyskinesia	Kinesia	finger	tremor and bradykinesia motor tasks based on UPDRS III motor examination
Rigas 2012 [65]	Tremor	accelerometers	right and left wrist, right and left leg, chest and waist	postural activities
Mariani 2013 [62]	Gait	Physilog module	On-shoe fixation	standard 3-m TUG and gait tests

The authors in [66] reported that overall mean acceleration correlated well with mean clinical ratings of the performed tasks in their study and showed that dyskinesias increase the power spectrum density of accelerometer signals in the frequency band between 1 and 3 Hz. While in [67], the authors obtained high correlation between objectively quantified LID and m-AIMs scores. On the other hand, [68] showed that it is possible to distinguish LID from voluntary movements and assess its severity by using the frequency and amplitude of the signals. While in the work presented in [69], the authors were able to distinguish between dyskinetic and non-dyskinetic patients. In a different approach, the authors in [70] reported high efficiency in distinguishing LID from other PD motor symptoms by analysing the signal energy within 2-5 and 5-10 Hz frequency bands and entropy of the frequency spectrum. More recently, detection of dyskinesia in [71] was done with sensitivity and specificity higher than 90% and severity assessment was accomplished. Certain studies also combine the evaluation of dyskinesia with presence of other motor symptoms. For example, in [72] high sensitivity and specificity values were reported in detecting both tremor and dyskinesia. While in [73], severity assessment and time spent at different levels of dyskinesia as well as bradykinesia were successfully achieved.

With the abundance and versatility of new technologies, and the complex algorithms on which they rely, recent studies have provided a wide variety of measures to show that the ability to objectively capture motor symptoms and complications of PD with high accuracy and reproducibility is feasible. With the absence of validated biomarkers of the disease or its progression, these measures can serve to enhance disease management and therapies, thereby providing better quality of life for the patients.

Table II.2 – Selection of Studies on the Objective Measurement of Dyskinesia.

Ref.	Motor Dysfunction	Device	Placement	Protocol
Manson 2000 [66]	Dyskinesia	triaxial accelerometer	shoulder	activities from Goetz Scale and other dyskinesia-inducing tasks
Hoff 2001 [67]	Dyskinesia	uniaxial accelerometers	upper leg, upper arm, and wrist of most affected side and trunk	seven 1-minute tasks including tasks from UDysRS
Keijsers 2003 [68]	Dyskinesia	ADXL-202 accelerometers	both upper arms, both upper legs, wrist of most dyskinetic side and trunk	functional daily life activities
Chelaru 2010 [69]	Dyskinesia	Innovative Sports Training	posterior of the head, thorax (T1), sacrum, superior spine of the scapula, dorsal hand and lateral shank	standing with arms stretched horizontally
Cole 2010 [72]	Dyskinesia and Tremor	accelerometers and sEMG	wrist extensor of dominant arm	free voluntary movement
Tsipouras 2012 [70]	Dyskinesia	accelerometers and gyroscopes	right and left wrist, right and left leg, chest and waist	protocol of daily life activities
Griffiths 2012 [73]	Dyskinesia and Bradykinesia	Parkinson's Kinetigraph PKG	wrist	free movement
Perez-Lopez 2016 [71]	Dyskinesia	accelerometer	waist	activities of daily living

3 Objectives of the Thesis

The prevalence of motor symptoms and complications in PD patients has been shown to be highly dependent on external factors, such as setting (wide or narrow pathways), white-coat effect, and complexity of performed activity. However, rarely do studies assessing these motor symptoms consider the external factors affecting the patient's condition, which could have substantial influence on the results, specifically in short-duration acquisitions.

The ability to capture movement data and employ it to optimise treatment strategies relies on the understanding of behaviours that occur over long periods of time. In the absence of continuous visual observation, providing context to the measured quantities is essential in identifying the incidents occurring. For example, a measured slowness of movement could be attributed to bradykinesia, or it could be attributed to fatigue following certain physical effort. A measured incident could be identified as random voluntary action, however when put into context, for example when the patient is in a sedentary state, is more likely to be dystonia.

While several different approaches have been investigated and applied for the objective monitoring

of PD patients' motor and non-motor developments, rarely has physical activity been assessed. This aspect of the patient's life encompasses a large part of the general understanding of disease progression and effectiveness of therapeutic plans.

For the purpose of this work, in order to objectively quantify and evaluate the severity of LID episodes in long-term observations, we are interested in following the pattern of activities and dyskinesia prevalence throughout a typical day in the life of a PD patient. Therefore, an activity classification step is introduced and assessed to determine whether classifying patient's activities could enhance the detection of LID.

The contribution of this thesis is achieved through a number of objectives which can be summarised as follows:

- The development and implementation of an automated system for recording movements of PD patients. In this sense, the system composed of six Shimmer3 IMUs, each containing two triaxial accelerometers, a triaxial gyroscope and a triaxial magnetometer, is a promising approach.
- The proposition of an automated and reliable method for the detection of LID in PD patients. During this process, several strategies were proposed in order to evaluate the effect of activity separation on the detection of dyskinesia. As such, dyskinesia detection for PD patients' data is evaluated without separation of activities, for manually separated activities, and for automatically separated activities.
- In relation to the previous objective, the development an accurate activity classifier based on the data collected using the monitoring system is required. As such, the data collected from healthy individuals is used to design and validate the performance of the activity classifier. This classifier is also tested using the data collected from the PD patients to determine its capability of recognising the activities performed by PD patients despite the presence of motor dysfunction.
- The development of an optimal reduced system with a minimum number of incorporated modules. During this process, the performance obtained using each IMU will be assessed and a combination of the most relevant IMUs with respect to the detection of dyskinesia is chosen. The purpose here is to reach a compromise between the number of modules in the system and the accuracy of dyskinesia detection.
- The application of a novel method for activity classification and dyskinesia detection based on complex network analysis, taking into account the relationships between the modules. The developed system composed of the six IMUs forms a natural network structure and the correlation between the different IMUs is thought to reveal information about the relationship between different body segments with respect to the activities performed of the presence of dyskinesia.
- The evaluation of the proposed system and method in an unsupervised, at-home patient acquisition. The aim here is to assess the performance of the system in a home environment without supervision

as would be the case in the patient's normal daily life. This would be done by collecting movement data from a patient over a certain period of time, and then performing LID detection by introducing the recording data as a validation set.

- The development of a platform that incorporates the methods and analysis approaches performed during the course of this work. This platform serves to integrate the different analysis methods pursued in a simple interface that allows the user to vary the conditions and evaluate the performance for newly collected data.

It is important to put into perspective the scope of this work in terms of the research carried out today in the objective monitoring of PD motor symptoms and complications. A comprehensive understanding of the motor dysfunction associated with PD requires the incorporation of the entire spectrum of motor symptoms and complications, with consideration of inter and intra-subject clinical variability. So far, such a system has yet to be developed, and although several motor aspects of PD have been successfully quantified, clinical assessment has yet to adopt any of these systems.

The work presented in this thesis is concerned with the detection of LID, which has proved to be a difficult phenomenon to quantify due to its randomness and large variability over the course of a patient's disease progression as well as among different patients. This aspect of the disease relates to therapeutic management and ensuring that the patient receives the best treatment results with Levodopa therapy. The measurement of LID is justified by the need to enhance our understanding of the complexities of the interactions of Levodopa in the brain and to prolong the period of beneficial therapy. The use of quantitative measures delivered through reliable and objectives methods carries the potential of improving the decision-making process in treatment and permit a better regulation of the need and dose of the drug.

The designed system offers a number advantages that are presented in the next section. However, we acknowledge that the work implemented also presents certain limitations. We attempted throughout this work to overcome these limitations through processing techniques.

Bibliography

- [1] P. A. MUENNIG AND S. A. GLIED. *What changes in survival rates tell us about us health care*. Health Affairs pages 10–1377 (2010).
- [2] S. P. GULLEY, E. K. RASCH, AND L. CHAN. *If we build it, who will come?: Working-age adults with chronic health care needs and the medical home*. Medical care **49**(2), 149 (2011).
- [3] S. P. GULLEY, E. K. RASCH, AND L. CHAN. *Ongoing coverage for ongoing care: access, utilization, and out-of-pocket spending among uninsured working-aged adults with chronic health care needs*. American journal of public health **101**(2), 368–375 (2011).
- [4] A. PANTELOPOULOS AND N. G. BOURBAKIS. *A survey on wearable sensor-based systems for health monitoring and prognosis*. Systems, Man, and Cybernetics, Part C: Applications and Reviews, IEEE Transactions on **40**(1), 1–12 (2010).
- [5] S. PATEL, H. PARK, P. BONATO, L. CHAN, AND M. RODGERS. *A review of wearable sensors and systems with application in rehabilitation*. Journal of neuroengineering and rehabilitation **9**(1), 1 (2012).
- [6] Y. LIU, X. JIANG, T. CAO, F. WAN, P. U. MAK, P.-I. MAK, AND M. I. VAI. *Implementation of ssvep based bci with emotiv epoc*. In *Virtual Environments Human-Computer Interfaces and Measurement Systems (VECIMS), 2012 IEEE International Conference on*, pages 34–37. IEEE (2012).
- [7] N. VALA AND K. TRIVEDI. *Brain computer interface: Data acquisition using non-invasive emotiv epoc neuroheadset*. International Journal of Software & Hardware Research in Engineering, ISSN pages 2347–4890 (2014).
- [8] N. A. BADCOCK, P. MOUSIKOU, Y. MAHAJAN, P. DE LISSA, J. THIE, AND G. MCARTHUR. *Validation of the emotiv epoc® eeg gaming system for measuring research quality auditory erps*. PeerJ **1**, e38 (2013).
- [9] T. D. PHAM AND D. TRAN. *Emotion recognition using the emotiv epoc device*. In *Neural Information Processing*, pages 394–399. Springer (2012).
- [10] M. MATEU-MATEUS, F. GUEDE-FERNÁNDEZ, AND M. A. GARCÍA-GONZÁLEZ. *RR time series comparison obtained by h7 polar sensors or by photoplethysmography using smartphones: breathing and devices influences*. In 6th European Conference of the International Federation for Medical and Biological Engineering, pages 264–267. Springer (2015).
- [11] C. SUCHY, L. MASSEN, Ø. ROGNMO, E. M. VAN CRAENENBROECK, P. BECKERS, E. KRAIGHER-KRAINER, A. LINKE, V. ADAMS, U. WISLØFF, B. PIESKE, ET AL. *Optimising exercise training in prevention and treatment of diastolic heart failure (optimex-clin): rationale and design of a prospective, randomised, controlled trial*. European journal of preventive cardiology **21**(2 suppl), 18–25 (2014).
- [12] B. O'BRIEN, T. GISBY, AND I. A. ANDERSON. *Stretch sensors for human body motion*. In *SPIE Smart Structures and Materials+ Nondestructive Evaluation and Health Monitoring*, pages 905618–905618. International Society for Optics and Photonics (2014).

BIBLIOGRAPHY

- [13] C. O'QUIGLEY, M. SABOURIN, S. COYLE, J. CONNOLLY, J. CONDALL, K. CURRAN, B. CORCORAN, AND D. DIAMOND. Characteristics of a piezo-resistive fabric stretch sensor glove for home-monitoring of rheumatoid arthritis. In *Wearable and Implantable Body Sensor Networks Workshops (BSN Workshops), 2014 11th International Conference on*, pages 23–26. IEEE (2014).
- [14] I. FITBIT. Fitbit devices. <http://www.fitbit.com/fr/devices>, (2016).
- [15] I. JAWBONE. Jawbone. <https://jawbone.com>, (2016).
- [16] I. MISFIT. Misfit. <http://misfit.com/?locale>, (2016).
- [17] W. SA. Withings. <http://www.withings.com/eu/en/products/activite-steel>, (2016).
- [18] J. CHEN, K. KWONG, D. CHANG, J. LUK, AND R. BAJCSY. Wearable sensors for reliable fall detection. In *Engineering in Medicine and Biology Society*, pages 3551–3554 (2005).
- [19] T. ZHANG, J. WANG, L. XU, AND P. LIU. Fall detection by wearable sensor and one-class SVM algorithm. In *Intelligent computing in signal processing and pattern recognition*, pages 858–863. Springer (2006).
- [20] A. T. ÖZDEMİR AND B. BARSHAN. *Detecting falls with wearable sensors using machine learning techniques*. *Sensors* **14**(6), 10691–10708 (2014).
- [21] M.-Z. POH, T. LODDENKEMPER, C. REINSBERGER, N. C. SWENSON, S. GOYAL, M. C. SABTALA, J. R. MADSEN, AND R. W. PICARD. *Convulsive seizure detection using a wrist-worn electrodermal activity and accelerometry biosensor*. *Epilepsia* **53**(5), e93–e97 (2012).
- [22] S. PATEL, C. MANCINELLI, A. DALTON, B. PATRITTI, T. PANG, S. SCHACHTER, AND P. BONATO. Detecting epileptic seizures using wearable sensors. In *2009 IEEE 35th Annual Northeast Bioengineering Conference*, pages 1–2. IEEE (2009).
- [23] A. DALTON, S. PATEL, A. R. CHOWDHURY, M. WELSH, T. PANG, S. SCHACHTER, G. ÓLAIGHIN, AND P. BONATO. *Development of a body sensor network to detect motor patterns of epileptic seizures*. *IEEE Transactions on Biomedical Engineering* **59**(11), 3204–3211 (2012).
- [24] F. MASSÉ, M. V. BUSSEL, A. SERTEYN, J. ARENDS, AND J. PENDERS. *Miniaturized wireless ECG monitor for real-time detection of epileptic seizures*. *ACM Transactions on Embedded Computing Systems (TECS)* **12**(4), 102 (2013).
- [25] R. FENSLI, E. GUNNARSON, AND O. HEJLESEN. A wireless ECG system for continuous event recording and communication to a clinical alarm station. , **1**, pages 2208–2211. IEEE (2004).
- [26] V. GAY AND P. LEIJDEKKERS. *A health monitoring system using smart phones and wearable sensors*. *International journal of ARM* **8**(2), 29–35 (2007).
- [27] J. J. ORESKO, Z. JIN, J. CHENG, S. HUANG, Y. SUN, H. DUSCHL, AND A. C. CHENG. *A wearable smartphone-based platform for real-time cardiovascular disease detection via electrocardiogram processing*. *IEEE Transactions on Information Technology in Biomedicine* **14**(3), 734–740 (2010).
- [28] K. J. KAPPIARUKUDIL AND M. V. RAMESH. Real-time monitoring and detection of "heart attack" using wireless sensor networks. In *Sensor technologies and applications (SENSORCOMM), 2010 fourth international conference on*, pages 632–636. IEEE (2010).
- [29] S. ANANTHANARAYAN, M. SHEH, A. CHIEN, H. PROFITA, AND K. SIEK. Pt viz: towards a wearable device for visualizing knee rehabilitation exercises. In *Proceedings of the SIGCHI Conference on Human Factors in Computing Systems*, pages 1247–1250. ACM (2013).

-
- [30] K. HUANG, P. J. SPARTO, S. KIESLER, A. SMAILAGIC, J. MANKOFF, AND D. SIEWIOREK. A technology probe of wearable in-home computer-assisted physical therapy. In *Proceedings of the SIGCHI Conference on Human Factors in Computing Systems*, pages 2541–2550. ACM (2014).
 - [31] K.-H. CHEN, P.-C. CHEN, K.-C. LIU, AND C.-T. CHAN. *Wearable sensor-based rehabilitation exercise assessment for knee osteoarthritis*. *Sensors* **15**(2), 4193–4211 (2015).
 - [32] B. HUANG, O. M. GIGGINS, T. KECHADI, AND B. CAULFIELD. The limb movement analysis of rehabilitation exercises using wearable inertial sensors. In *38th Annual International Conference of the IEEE Engineering in Medicine and Biology Society, Florida, United States of America, 16-20 August 2016*. IEEE (2016).
 - [33] H. LEI, N. TOOSIZADEH, M. SCHWENK, S. SHERMAN, S. KARP, E. STERNBERG, AND B. NAJAFI. *A pilot clinical trial to objectively assess the efficacy of electroacupuncture on gait in patients with Parkinson’s disease using body worn sensors*. *PloS one* **11**(5), e0155613 (2016).
 - [34] W. D. SMITH AND A. BAGLEY. A miniature, wearable activity/fall monitor to assess the efficacy of mobility therapy for children with cerebral palsy during everyday living. In *2010 Annual International Conference of the IEEE Engineering in Medicine and Biology*, pages 5030–5033. IEEE (2010).
 - [35] A. FORKAN, I. KHALIL, AND Z. TARI. Context-aware cardiac monitoring for early detection of heart diseases. In *Computing in Cardiology 2013*, pages 277–280. IEEE (2013).
 - [36] R. THIEDE, N. TOOSIZADEH, J. L. MILLS, M. ZAKY, J. MOHLER, AND B. NAJAFI. *Gait and balance assessments as early indicators of frailty in patients with known peripheral artery disease*. *Clinical Biomechanics* **32**, 1–7 (2016).
 - [37] S. ABBATE, M. AVVENUTI, F. BONATESTA, G. COLA, P. CORSINI, AND A. VECCHIO. *A smartphone-based fall detection system*. *Pervasive and Mobile Computing* **8**(6), 883–899 (2012).
 - [38] G. COLA, M. AVVENUTI, A. VECCHIO, G.-Z. YANG, AND B. LO. An unsupervised approach for gait-based authentication. In *Wearable and Implantable Body Sensor Networks (BSN), 2015 IEEE 12th International Conference on*, pages 1–6. IEEE (2015).
 - [39] E. P. DOHENY, C. WALSH, T. FORAN, B. R. GREENE, C. W. FAN, C. CUNNINGHAM, AND R. A. KENNY. *Falls classification using tri-axial accelerometers during the five-times-sit-to-stand test*. *Gait & posture* **38**(4), 1021–1025 (2013).
 - [40] P. I. AKÇETIN, S. Ç. ERGEN, AND T. M. SEZGIN. HMM based inertial sensor system for coaching of rowing activity. In *Signal Processing and Communications Applications Conference (SIU), 2012 20th*, pages 1–4. IEEE (2012).
 - [41] D. BISWAS, A. CRANNY, N. GUPTA, K. MAHARATNA, J. ACHNER, J. KLEMKE, M. JÖBGES, AND S. ORTMANN. *Recognizing upper limb movements with wrist worn inertial sensors using k-means clustering classification*. *Human movement science* **40**, 59–76 (2015).
 - [42] E. FORTUNE, M. TIERNEY, C. N. SCANAILL, A. BOURKE, N. KENNEDY, AND J. NELSON. Activity level classification algorithm using shimmer wearable sensors for individuals with rheumatoid arthritis. In *Engineering in Medicine and Biology Society, EMBC, 2011 Annual International Conference of the IEEE*, pages 3059–3062. IEEE (2011).
 - [43] S. I. LEE, M. Y. OZSECEN, L. DELLA TOFFOLA, J.-F. DANEALT, A. PUIATTI, S. PATEL, AND P. BONATO. Activity detection in uncontrolled free-living conditions using a single accelerometer. In *Wearable and Implantable Body Sensor Networks (BSN), 2015 IEEE 12th International Conference on*, pages 1–6. IEEE (2015).

BIBLIOGRAPHY

- [44] N. U. AHAMED, K. SUNDARAJ, R. B. AHMAD, M. RAHMAN, AND M. A. ISLAM. *Analysis of right arm biceps brachii muscle activity with varying the electrode placement on three male age groups during isometric contractions using a wireless EMG sensor*. *Procedia Engineering* **41**, 61–67 (2012).
- [45] V. BALASUBRAMANIAN AND A. STRANIERI. A scalable cloud platform for active healthcare monitoring applications. In *e-Learning, e-Management and e-Services (IC3e), 2014 IEEE Conference on*, pages 93–98. IEEE (2014).
- [46] S. GRADL, P. KUGLER, C. LOHMULLER, AND B. ESKOFIER. Real-time ECG monitoring and arrhythmia detection using android-based mobile devices. In *Engineering in Medicine and Biology Society (EMBC), 2012 Annual International Conference of the IEEE*, pages 2452–2455. IEEE (2012).
- [47] A. IBRAHIM, V. GANNAPATHY, L. CHONG, AND I. ISA. Analysis of electromyography (EMG) signal for human arm muscle: A review. In *Advanced Computer and Communication Engineering Technology*, pages 567–575. Springer (2016).
- [48] N. H. KAMARUDIN, S. A. AHMAD, M. K. HASSAN, R. M. YUSOFF, AND S. Z. DAWAL. Muscle contraction analysis during lifting task. In *Biomedical Engineering and Sciences (IECBES), 2014 IEEE Conference on*, pages 452–457. IEEE (2014).
- [49] H. J. LUNGE. *Inertial sensing of human movement*. Twente University Press (2002).
- [50] R. GHODSSI AND P. LIN. , **1**. Springer Science & Business Media (2011).
- [51] O. J. WOODMAN. *An introduction to inertial navigation*. University of Cambridge, Computer Laboratory, Tech. Rep. UCAMCL-TR-696 **14**, 15 (2007).
- [52] H. J. LUNGE AND P. H. VELTINK. *Measuring orientation of human body segments using miniature gyroscopes and accelerometers*. *Medical and Biological Engineering and computing* **43**(2), 273–282 (2005).
- [53] A. BULLING, U. BLANKE, AND B. SCHIELE. *A tutorial on human activity recognition using body-worn inertial sensors*. *ACM Computing Surveys (CSUR)* **46**(3), 33 (2014).
- [54] S. LAMBRECHT AND A. J. DEL AMA. Human movement analysis with inertial sensors. In *Emerging Therapies in Neurorehabilitation*, pages 305–328. Springer (2014).
- [55] J. DOSCHER AND M. EVANGELIST. *Accelerometer design and applications*. *Analog Devices* **3** (1998).
- [56] S. K. RANGE AND J. MULLINS. *Brief history of gyroscopes*.
- [57] D. A. WINTER. *Biomechanics and motor control of human movement*. John Wiley & Sons (2009).
- [58] A. SALARIAN, H. RUSSMANN, F. J. VINGERHOETS, C. DEHOLLAIN, Y. BLANC, P. R. BURKHARD, AND K. AMINIAN. *Gait assessment in Parkinson’s disease: toward an ambulatory system for long-term monitoring*. *Biomedical Engineering, IEEE Transactions on* **51**(8), 1434–1443 (2004).
- [59] S. T. MOORE, H. G. MACDOUGALL, J.-M. GRACIES, H. S. COHEN, AND W. G. ONDO. *Long-term monitoring of gait in Parkinson’s disease*. *Gait & posture* **26**(2), 200–207 (2007).
- [60] S. T. MOORE, H. G. MACDOUGALL, AND W. G. ONDO. *Ambulatory monitoring of freezing of gait in Parkinson’s disease*. *Journal of neuroscience methods* **167**(2), 340–348 (2008).
- [61] J. BARTH, J. KLUCKEN, P. KUGLER, T. KAMMERER, R. STEIDL, J. WINKLER, J. HORNEGGER, AND B. ESKOFIER. Biometric and mobile gait analysis for early diagnosis and therapy monitoring in Parkinson’s disease. In *Engineering in Medicine and Biology Society, EMBC, 2011 Annual International Conference of the IEEE*, pages 868–871. IEEE (2011).

-
- [62] B. MARIANI, M. C. JIMÉNEZ, F. J. VINGERHOETS, AND K. AMINIAN. *On-shoe wearable sensors for gait and turning assessment of patients with Parkinson's disease*. Biomedical Engineering, IEEE Transactions on **60**(1), 155–158 (2013).
 - [63] A. SALARIAN, H. RUSSMANN, C. WIDER, P. R. BURKHARD, F. J. VINGERHOETS, AND K. AMINIAN. *Quantification of tremor and bradykinesia in Parkinson's disease using a novel ambulatory monitoring system*. Biomedical Engineering, IEEE Transactions on **54**(2), 313–322 (2007).
 - [64] T. O. MERA, D. A. HELDMAN, A. J. ESPAY, M. PAYNE, AND J. P. GIUFFRIDA. *Feasibility of home-based automated Parkinson's disease motor assessment*. Journal of neuroscience methods **203**(1), 152–156 (2012).
 - [65] G. RIGAS, A. T. TZALLAS, M. G. TSIPOURAS, P. BOUGIA, E. E. TRIPOLITI, D. BAGA, D. I. FOTIADIS, S. G. TSOULI, AND S. KONITSIOTIS. *Assessment of tremor activity in the Parkinson's disease using a set of wearable sensors*. Information Technology in Biomedicine, IEEE Transactions on **16**(3), 478–487 (2012).
 - [66] A. MANSON, P. BROWN, J. O'SULLIVAN, P. ASSELMAN, D. BUCKWELL, AND A. LEES. *An ambulatory dyskinesia monitor*. Journal of Neurology, Neurosurgery & Psychiatry **68**(2), 196–201 (2000).
 - [67] J. HOFF, E. WAGEMANS, J. VAN HILTEN, ET AL. *Accelerometric assessment of levodopa-induced dyskinesias in Parkinson's disease*. Movement disorders **16**(1), 58–61 (2001).
 - [68] N. L. KEIJERS, M. W. HORSTINK, AND S. C. GIELEN. *Automatic assessment of levodopa-induced dyskinesias in daily life by neural networks*. Movement disorders **18**(1), 70–80 (2003).
 - [69] M. I. CHELARU, C. DUVAL, AND M. JOG. *Levodopa-induced dyskinesias detection based on the complexity of involuntary movements*. Journal of neuroscience methods **186**(1), 81–89 (2010).
 - [70] M. G. TSIPOURAS, A. T. TZALLAS, G. RIGAS, S. TSOULI, D. I. FOTIADIS, AND S. KONITSIOTIS. *An automated methodology for levodopa-induced dyskinesia: assessment based on gyroscope and accelerometer signals*. artificial intelligence in Medicine **55**(2), 127–135 (2012).
 - [71] C. PÉREZ-LÓPEZ, A. SAMÀ, D. RODRÍGUEZ-MARTÍN, J. M. MORENO-ARÓSTEGUI, J. CABESTANY, A. BAYES, B. MESTRE, S. ALCAINE, P. QUISPE, G. Ó. LAIGHIN, ET AL. *Dopaminergic-induced dyskinesia assessment based on a single belt-worn accelerometer*. Artificial Intelligence in Medicine (2016).
 - [72] B. T. COLE, S. H. ROY, C. J. DE LUCA, AND S. H. NAWAB. *Dynamic neural network detection of tremor and dyskinesia from wearable sensor data*. In *Engineering in Medicine and Biology Society (EMBC), 2010 Annual International Conference of the IEEE*, pages 6062–6065. IEEE (2010).
 - [73] R. I. GRIFFITHS, K. KOTSCHET, S. ARFON, Z. M. XU, W. JOHNSON, J. DRAGO, A. EVANS, P. KEMPTER, S. RAGHAV, AND M. K. HORNE. *Automated assessment of bradykinesia and dyskinesia in Parkinson's disease*. Journal of Parkinson's disease **2**(1), 47–55 (2012).
 - [74] M. VAN NIMWEGEN, A. D. SPEELMAN, E. J. HOFMAN-VAN ROSSUM, S. OVEREEM, D. J. DEEG, G. F. BORM, M. H. VAN DER HORST, B. R. BLOEM, AND M. MUNNEKE. *Physical inactivity in Parkinson's disease*. Journal of neurology **258**(12), 2214–2221 (2011).
 - [75] A. D. SPEELMAN, B. P. VAN DE WARRENBURG, M. VAN NIMWEGEN, G. M. PETZINGER, M. MUNNEKE, AND B. R. BLOEM. *How might physical activity benefit patients with Parkinson's disease?* Nature Reviews Neurology **7**(9), 528–534 (2011).
 - [76] S. CHAPUIS, L. OUCHCHANE, O. METZ, L. GERBAUD, AND F. DURIF. *Impact of the motor complications of Parkinson's disease on the quality of life*. Movement disorders **20**(2), 224–230 (2005).
 - [77] V. A. GOODWIN, S. H. RICHARDS, R. S. TAYLOR, A. H. TAYLOR, AND J. L. CAMPBELL. *The effectiveness of exercise interventions for people with Parkinson's disease: A systematic review and meta-analysis*. Movement disorders **23**(5), 631–640 (2008).

Part II

Automated, Objective Quantification of Levodopa Induced Dyskinesia

Materials and Measurement Protocol

The previous chapters allowed us to identify the requirements of an automated assessment method, and as such defined the choice of the monitoring system that we intend to use. In this chapter, the architecture of the chosen sensing modules is detailed to provide a clear understanding of the acquired measures. We describe the design and composition of the pilot monitoring system. The pilot system is initially set up to record the widest possible movement patterns. The protocol of activities set up for the participants to follow and the data acquisition process are also described. This chapter also highlights the advantages of the designed system, as well as providing a discussion pertaining to the limitations faced during this work.

1 Activity Monitoring and Recognition using IMUs

An inertial Measurement Unit (IMU) is an electronic device that houses a number of different sensors, usually collecting linear acceleration, angular velocity, and in certain cases, the magnetic field around the body to which it is attached. These devices have been frequently used for ambulatory monitoring of human movement due to their practicality, low cost, and reliability in measurement without obstructing the free movement of the subject [1–3]. IMUs are characterised by their Degrees of Freedom (DoF), which define the sensor configuration present in the device.

Perhaps the most investigated aspect of the use of IMUs in monitoring movement over the past two decades is the field of activity monitoring and recognition, with applications mostly in healthcare and fitness. The ability to provide accurate and opportune information on the physical activities and behaviours of certain individuals is highly interesting in certain areas of healthcare. For example, patients suffering from physical disabilities or recovering from trauma might be required to follow strict regiments during their rehabilitation stages at home. Feedback from these sensors could offer major insight inside the patient’s performance and progress, as well as aid in restructuring the rehabilitation program in light of the information obtained [4].

Another area which has been extensively researched includes monitoring activities of the elderly and individuals with disease and/or movement dysfunction, who are prone to falls and show a high risk of injury. Real-time detection of falls and/or injuries is primitive to provide rapid and efficient response

that could make a significant difference in life threatening situations [5, 6]. Furthermore, monitoring activities and providing descriptive measures of certain parameters, such as gait or posture analysis, gives physicians and nurses the ability to better assess a patient's condition. A better understanding of the progression and/or deterioration of physical activities could play a major role in early diagnosis, allowing for more efficient treatment and consequently lower healthcare costs [7, 8].

Activity trackers used in the sports and fitness domain have had the most commercial success in recent years, with statistics showing that in 2013, 15 million people were already using activity and fitness trackers and the number of users is expected to increase to almost 100 million in 2018 [9]. These devices are becoming increasingly popular in personal healthcare, providing people with direct information about their daily routine or fitness through clear and easy to use interfaces (such as mobile phone Apps or websites). The information gathered by these devices is relayed to the user in real-time and offers the possibility of automating the monitoring and recording of daily activities and fitness. As such, users might feel motivated to exercise more, increase their daily activity rate, or even adjust their dietary regiment in order to achieve fitness goals [10].

Generally, research in the domain of activity recognition, regardless of the application considered, follows the scheme in Figure III.1. While several advances have been made in this domain, certain design issues have been addressed in recent years. Some of these issues include choice of sensors, optimal sensor positions, data collection protocols, as well as attribute selection [11]. However, the large



Figure III.1 – General scheme of development of an activity recognition system.

scope of sensors, methods and applications considered, has made it very difficult to properly identify optimal conditions for human activity recognition. That is not to say that activity recognition has not been achieved and validated in several works. In fact, many studies have reported high accuracies in recognising different activities, under different acquisition protocols, and using different sensors. Table III.1 gives a brief overview of some of the literature published in the past few years, showing sensor and sensor placement, protocol of acquisition, extracted features, and performance of the activity classification method.

Many of the already published literature has been reviewed [21, 22] and it has been shown clear that the results displayed in these studies are highly dependant on the variable sensing modules, protocols and processing techniques. As a result, the choices made in this study, depended on previous literature that namely focused on detection of motor symptoms of PD, activity recognition for patients with motor disorder, and gathering sufficient data in order to understand the affect of these motor symptoms on performance of daily life activities.

Table III.1 – Review of Recent Literature on Activity Recognition.

Ref.	Sensor	Placement	Protocol	Classifier	Accuracy
Maurer 2006 [12]	ACC	wrist, belt, necklace, trouser pocket, shirt pocket, bag	sitting, standing, walking, ascending & descending stairs, running	DT	72.6-87.2%
Ermes 2008 [13]	ACC	Hip, Wrist	supervised indoor & outdoor daily activities including sports, free unsupervised period	Hybrid (DT& ANN)	89%
Altun 2010 [14]	IMU: ACC, GYRO, MAG	Wrists, Knees, Trunk	19 activities including ADL, sports & exercise	BDM	99.2%
Zhang 2013 [15]	IMU: ACC, GYRO	Hip	walking, ascending & descending stairs, jumping, running, standing, sitting	SR	96.1%
Mannini 2013 [16]	ACC	Wrist/Ankle	guided sequence of 26 laboratory-based activities and simulated daily activities grouped into 4 target classes	SVM	84.7-95.0%
Ahmadi 2014 [17]	IMU	Shanks, Thighs	series of actions of an outdoor sports training session	DWT-based algorithm	98.3%
Biswas 2015 [18]	IMU: ACC, GYRO	Arm	arm movements	k-means	83-88%
Lee 2015 [19]	IMU	Knee	daily activities and sports related activities	RF	90%
Ayachi 2016 [20]	Motion Capture Suit of 17 IMUs: ACC, GYRO, MAG	17 positions	10 ADL	DWT-based algorithm	95.55%

2 Ambulatory Monitoring System

2.1 Shimmer3 Inertial Measurement Units

In this thesis, we propose the use of six Shimmer3 IMUs [23] with integrated 10 DoF for measurement. Each of these units is equipped with a low noise triaxial accelerometer, a wide range triaxial accelerometer, a triaxial gyroscope, a digital triaxial magnetometer, an altimeter, and a temperature sensor (Table III.2). For the purposes of this study, which concentrates on inertial sensing, only the data collected from the two accelerometers, gyroscope and magnetometer of each IMU is considered.

The Shimmer3 IMUs (Figure III.2) are specifically designed for wearable sensing applications and are frequently used in human health monitoring studies, sports science studies, and intelligent

Table III.2 – Technical Specifications of the Shimmer3 Modules.

Sensor	Microcontroller	Range	Sensitivity	Operating Current	RMS Noise*
Low Noise ACC	Kionix KXRB5-2042	$\pm 2g$	$600 \pm 18 \text{ mV/g}$	$500 \mu A$	$5.09 \times 10^{-3} \text{ m/s}^2$
Wide Range ACC	STMicro LSM303DLHC	$\pm 2g, \pm 4g, \pm 8g, \pm 16g$	$1000 \text{ LSB/g at } \pm 2g$	$110 \mu A$	$27.5 \times 10^{-3} \text{ m/s}^2$
GYRO	Invensense MPU9150	$\pm 250, \pm 500, \pm 1000, \pm 2000 \text{ dps}$	$131 \text{ LSB/dps at } \pm 250$	3.5 mA	0.0481 dps
MAG	STMicro LSM303DLHC	$\pm 1.3, \pm 1.9, \pm 2.5, \pm 4.0, \pm 4.7, \pm 5.6, \pm 8.1 \text{ Ga}$	$1100 \text{ LSB/g at } \pm 1.3$	$110 \mu A$	$0.0081 \text{ normalised local flux}$

applications studies [18, 24–26]. These IMUs were found to be very practical for monitoring PD patients during daily activities as they fulfil the following criteria:

- Size and weight of the modules is small and placement of sensors is done through elastic straps, without any wiring or connection between modules, ensuring that the system does not obstruct the normal movements of the patients.
- Battery life can last up to twelve hours making the system suitable for long term monitoring.
- The modules are discreet and unobtrusive, with simple ON-OFF switch and LED indicators, ensuring ease of use in an unsupervised environment and acceptability among patients.

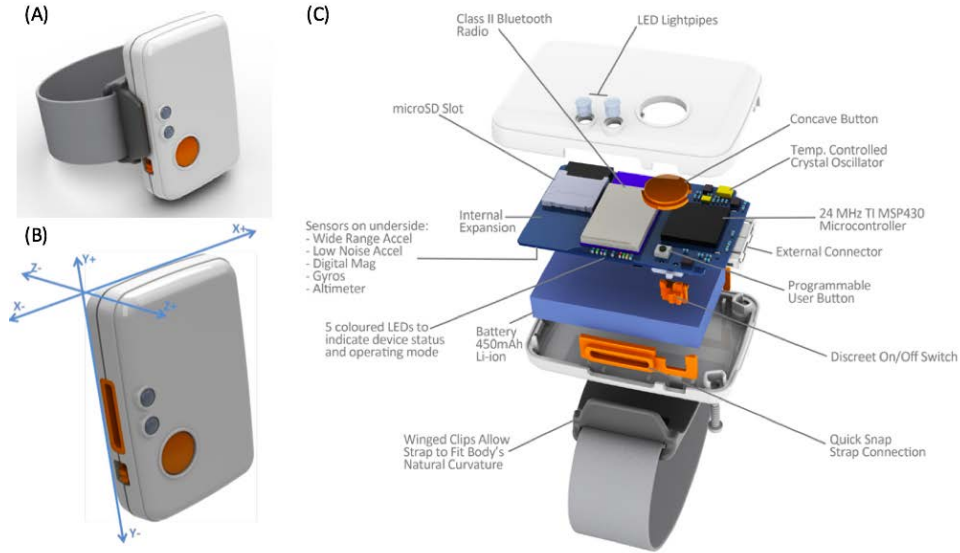


Figure III.2 – Shimmer3 IMU: (A) enclosed module, (B) default axis position, (C) exploded view showing individual components.

2.2 System Architecture

The individual components of each Shimmer3 IMU are shown in Figure III.2 (C). The Shimmer3 platform is factory programmed with *LogAndStream* firmware (Figure III.3 (A)). This offers the option

of direct Bluetooth streaming to a nearby station or data logging onto a microSD card located in a socket inside the mainboard.

Programming the Shimmer IMUs is done through the Shimmer Dock (Figure III.3 (B)), which is a multipurpose device that connects to a PC via USB cable. The Dock is connected to the Shimmer mainboard and provides the following main functions:

- Programming the Shimmer
- MicroSD card access
- Charging the Shimmer

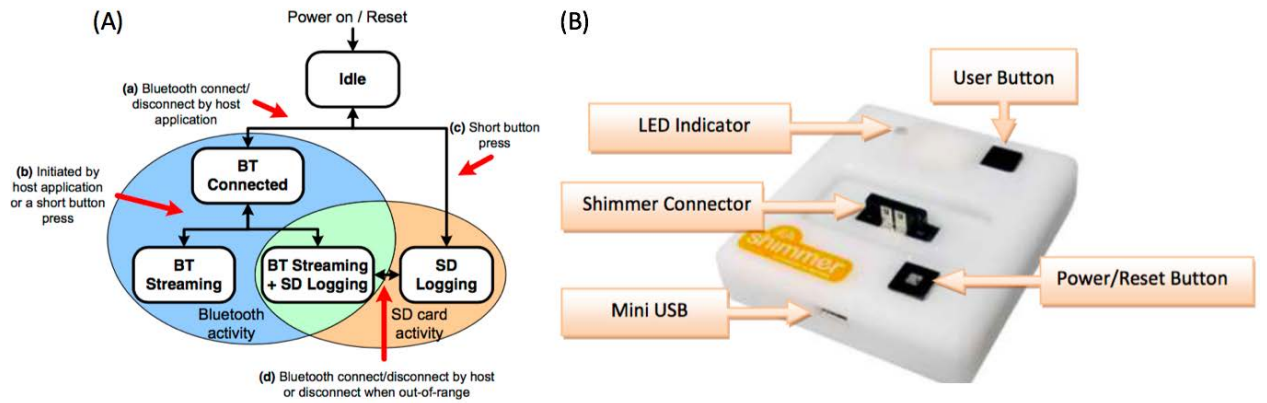


Figure III.3 – (A): Simplified schema of the Shimmer3 *LogAndStream* operational hierarchy. (B): Shimmer Dock - enclosure view.

The Shimmer3 platform is also accompanied by an integrated software solution called Consensys, for managing the IMUs. The Consensys software allows for firmware programming, configuration, synchronisation, and data management of the Shimmer data captured over Bluetooth and/or to the Shimmer SD card. The general scheme for configuration and data logging is presented in Figure III.4.

3 Acquisition Protocol, Database and Measurement Technique

3.1 Laboratory Setting

The acquisition protocol was set up based on a series of simple daily life activities. The activities were chosen to mirror realistic conditions in the patients daily life and to ensure simple repeatable measurements considering the patients' varying motor states. During the acquisition sessions, patients were asked to take their medication as originally prescribed. Measurements were repeated twice during the same day, before and after the intake of Levodopa. Both healthy subjects and patients performed

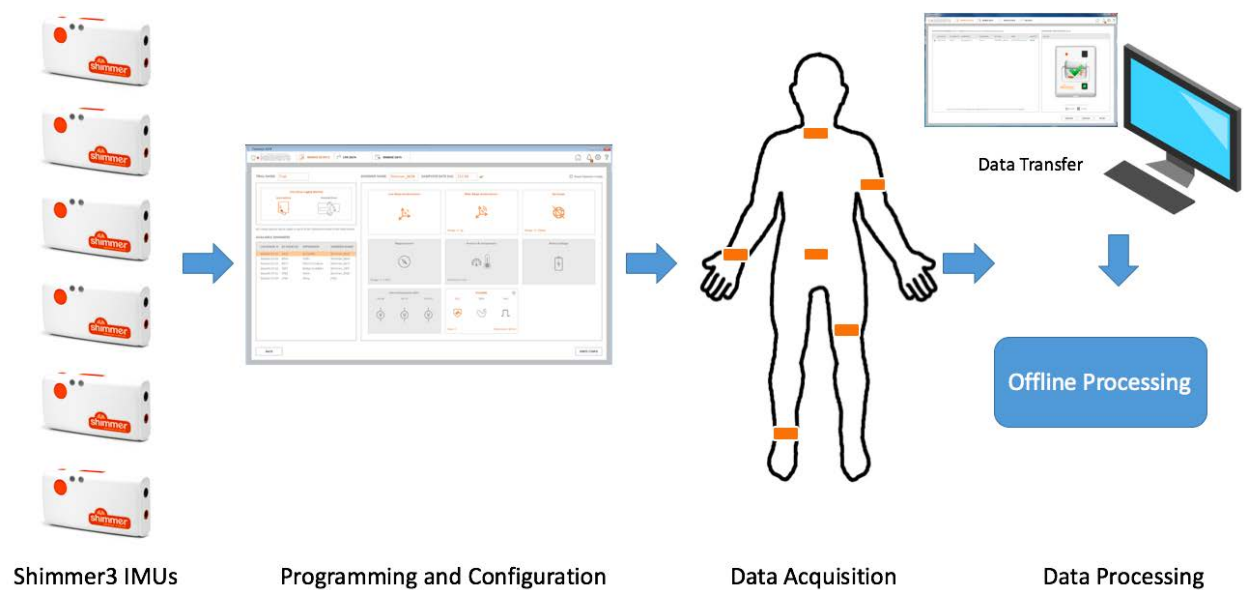


Figure III.4 – General scheme of programming, configuration, and data logging for the system of acquisition.



Figure III.5 – Room layout in the laboratory where patients and healthy individuals performed the protocol of activities.

the same protocol of activities at two similar laboratory settings. Fig. III.5 shows a layout of the setting where the sequence of activities took place.

The activities were timed to approximately two minutes each, except in cases when the patient was unable to continue the activity and chose to move on to the next. The sequence of activities performed by both the healthy individuals and the patients is presented in Table III.3.

The healthy individuals performed the protocol without any difficulty and in the order instructed. However, PD patients had slightly more difficulty in completing the protocol or certain activities depending on their motor condition. For example, patient M01 was only able to perform the activity of lying down for a few seconds at a time when suffering from LID. Patient J02, on the other hand, experienced fatigue and would run out of breath when performing the walking activity or ascending the stairs while in the OFF state, and would occasionally stop for short breaks. Patient P03 performed the protocol without any issues, however the degree of LID experienced is significantly lower than that of the other two patients.

Table III.3 – Protocol of Simple Daily Life Activities.

	Activity	Minimum Time
1	Lying down	120 s
2	Sitting on the edge of the bed	120 s
3	Standing up beside the bed	120 s
4	Walking towards desk chair	10 s
5	Sitting still on the desk chair	120 s
6	Writing a paragraph	120 s
7	Reading a newspaper out loud	60 s
8	Eating and drinking	120 s
9	Walking in a hallway	120 s
10	Descending stairs	14 s
11	Ascending stairs	14 s
12	Walking towards desk chair	15 s
13	Sitting still on the desk chair	120 s
14	Walking towards the bed	10 s
15	Sitting on the edge of the bed	120 s
16	Lying down	120 s

3.2 Sensor Placement

Placement locations of wearable sensors have varied in literature based on sensor type and application (see [27] for review). For this application, the positions were chosen based on body segments that could possibly yield the most information for the event classification. The sensing modules were physically attached to the individual's body using elastic straps at the following positions: dominant ankle and wrist, non-dominant thigh and arm, hip and neck (Figure III.6).

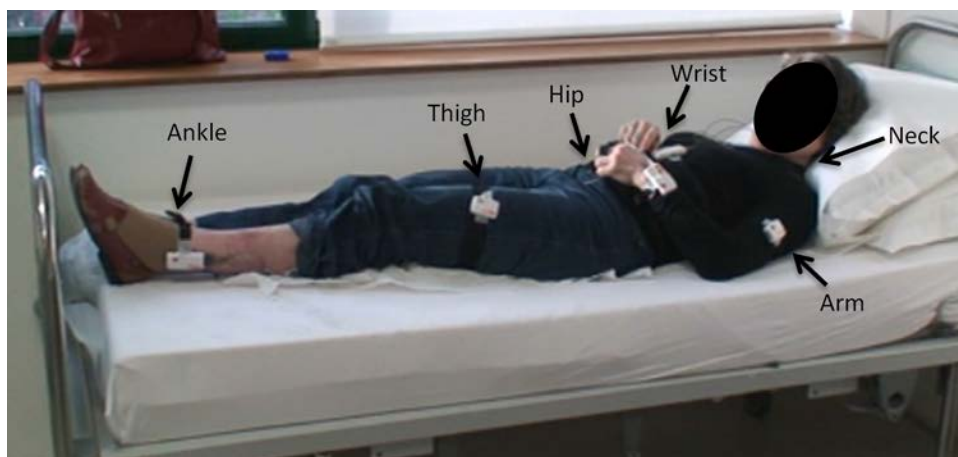


Figure III.6 – Placement of the sensing modules on the subject's body.

3.3 Presentation of the Database

Two different subject groups participated in this study: a control group and a patient group. The control group consisted of nine healthy subjects (four females and five males) aged 25-50. These subjects did not present any major or neurological diseases, motor dysfunction or disabilities that would affect the outcome of the study. The purpose of incorporating healthy individuals in this study relates to the activity classification phase, which is detailed in Chapter IV.

The patient group consisted of three PD patients (one male and two females). The patients had earlier diagnosis of idiopathic PD and had been following a Levodopa treatment plan along with a combination of other anti-parkinsonian medication (detailed in Table III.4). All patients had been displaying varying intensities of LID prior to this study, and none had had DBS. The patients had not previously experienced rest tremor but did suffer from other PD motor symptoms such as akinesia and bradykinesia.

Table III.4 – Parkinson's Disease Patients

Patient	Age	Diagnosis	Current Medication	Levodopa	Dyskinesia
M01	65	15 years	Sinemet, Modopar, Deroxat, Sifrol, Azilec	8 years	since 1 year, mostly on the left side
J02	68	22 years	Sinemet, Modopar, Xatral Al-fuzosin, Inexium, Seropram, Lexomil, AlteisColmetec, For-lax, Azilec, Patch	22 years	since diagnosis, severe dyskinesia caused heart fatigue and recent hospitalisation
P03	56	14 years	Stalevo, Modopar, Apokinson, Azilec, Patch	14 years	since 2-3 years, dyskinesia decreased after changing from Sinemet to Stalevo

3.4 Data Acquisition

Twelve different signals were collected from each Shimmer IMU, corresponding to the triaxial low noise accelerometer, triaxial wide range accelerometer, triaxial gyroscope and triaxial magnetometer. Therefore, a total of seventy-two signals were analysed for all module positions. Movement data was recorded with a sampling frequency of 512 Hz directly onto a 2 Gbyte built-in memory card and no connections between the modules were present. This enabled the individuals to perform the activities freely without feeling like the modules presented any obstacle.

In Figure III.7, an example of the collected signals from the ankle module of a healthy individual is shown for the different activities performed. The signals are collected from the triaxial low noise accelerometer, gyroscope, wide range accelerometer and magnetometer (top-down order) for the activities of walking, standing, lying and sitting (left-right order). A clear difference can be observed in characteristics of the signals collected by the same sensor for different activities. For example, the signals collected by the wide range accelerometer show periodic characteristics in the case of walking, as opposed to the static nature of the same signals in the case of lying down. In another example, the signals collected by the low noise accelerometer in the cases of lying and sitting both show a static nature. However, there is a large difference in signal magnitude for the three axes.

Figures III.8 and III.9, however, show an example of the signals collected from the ankle module of a PD patient in absence and in presence of LID, respectively. In both figures, similar differences can be observed between the signals collected from the same sensors during the performance of the different activities. On the other hand, if we compare the signals collected from the four sensors during the activity of sitting, in the non-dyskinetic case (Figure III.8) with those collected during the same activity in the dyskinetic state (Figure III.9), a large difference can be observed. In the non-dyskinetic case, the collected signals are somewhat static, which corresponds to the fact that the patient is in fact in a still position. However, in the dyskinetic state, the signals collected show certain random fluctuations, which can be attributed to the spastic and involuntary movements that the patient is experiencing during this motor state.

All protocol sessions were video-taped, and the exact start and end times of each activity were annotated based on the collected video-recordings in order to label the data. Dyskinetic periods were also identified from the video recordings.

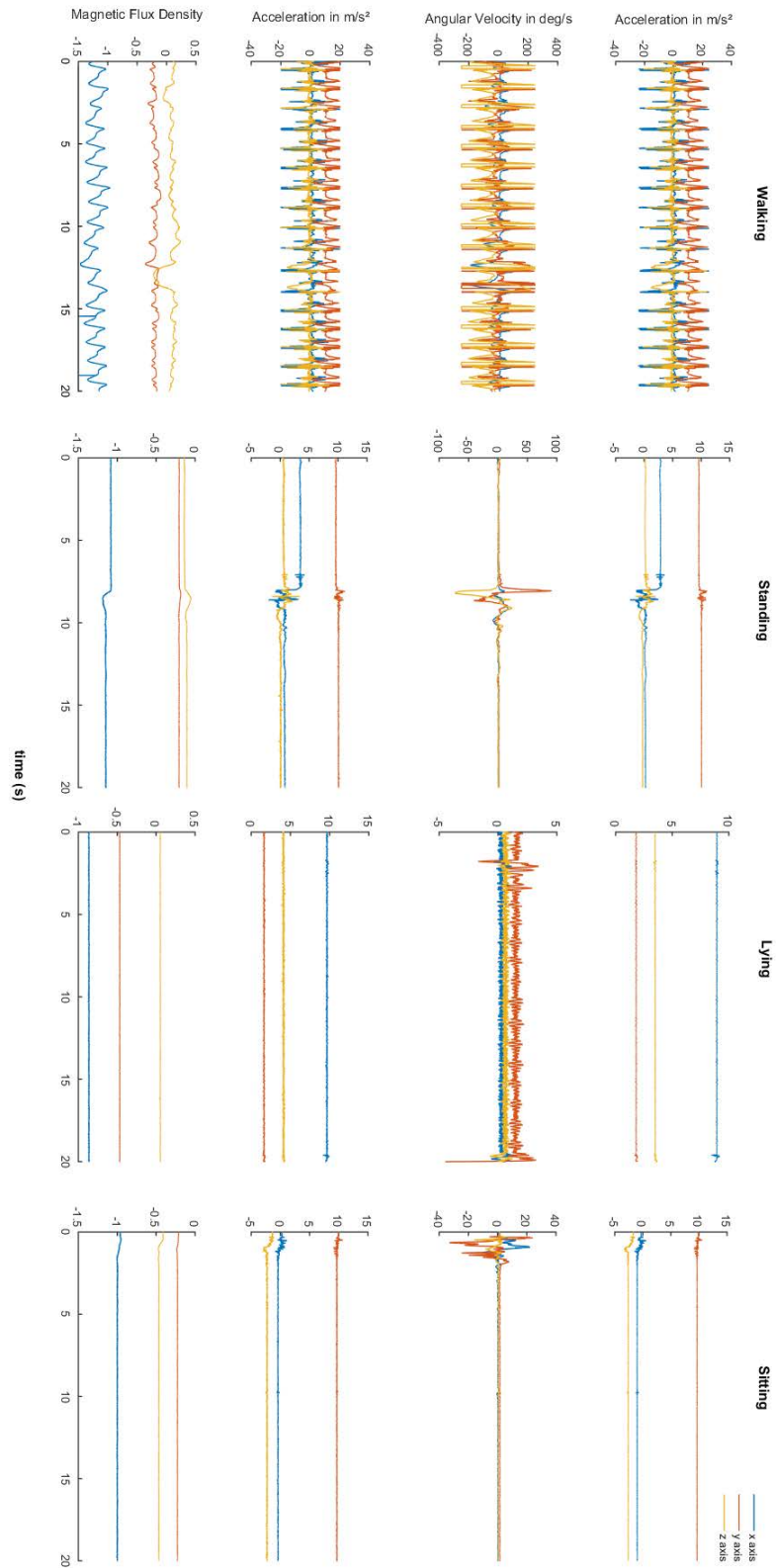


Figure III.7 – Signals collected from the Ankle module of a healthy individual.

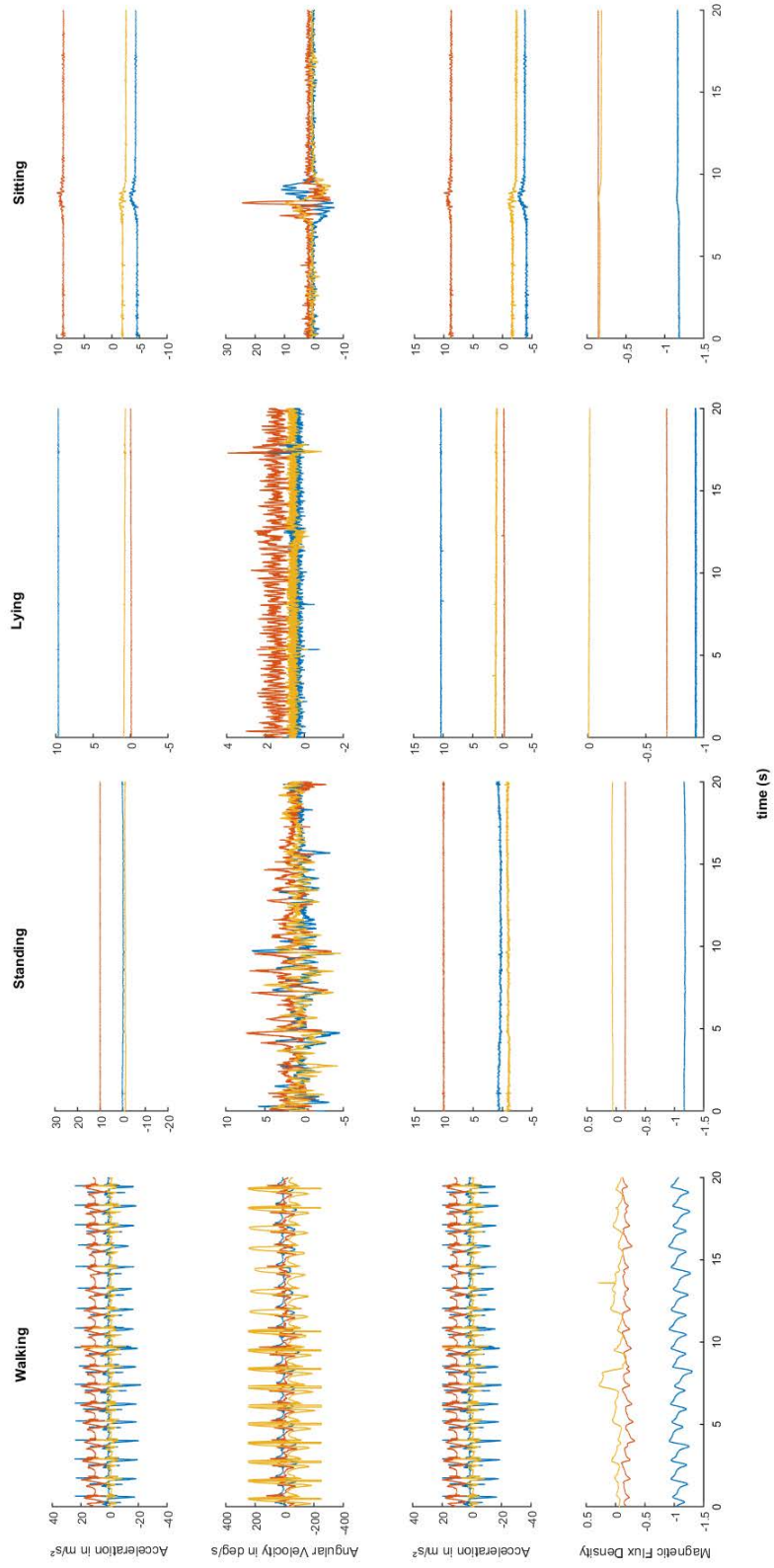


Figure III.8 – Signals collected from the Ankle module of a PD patient in absence of LID.

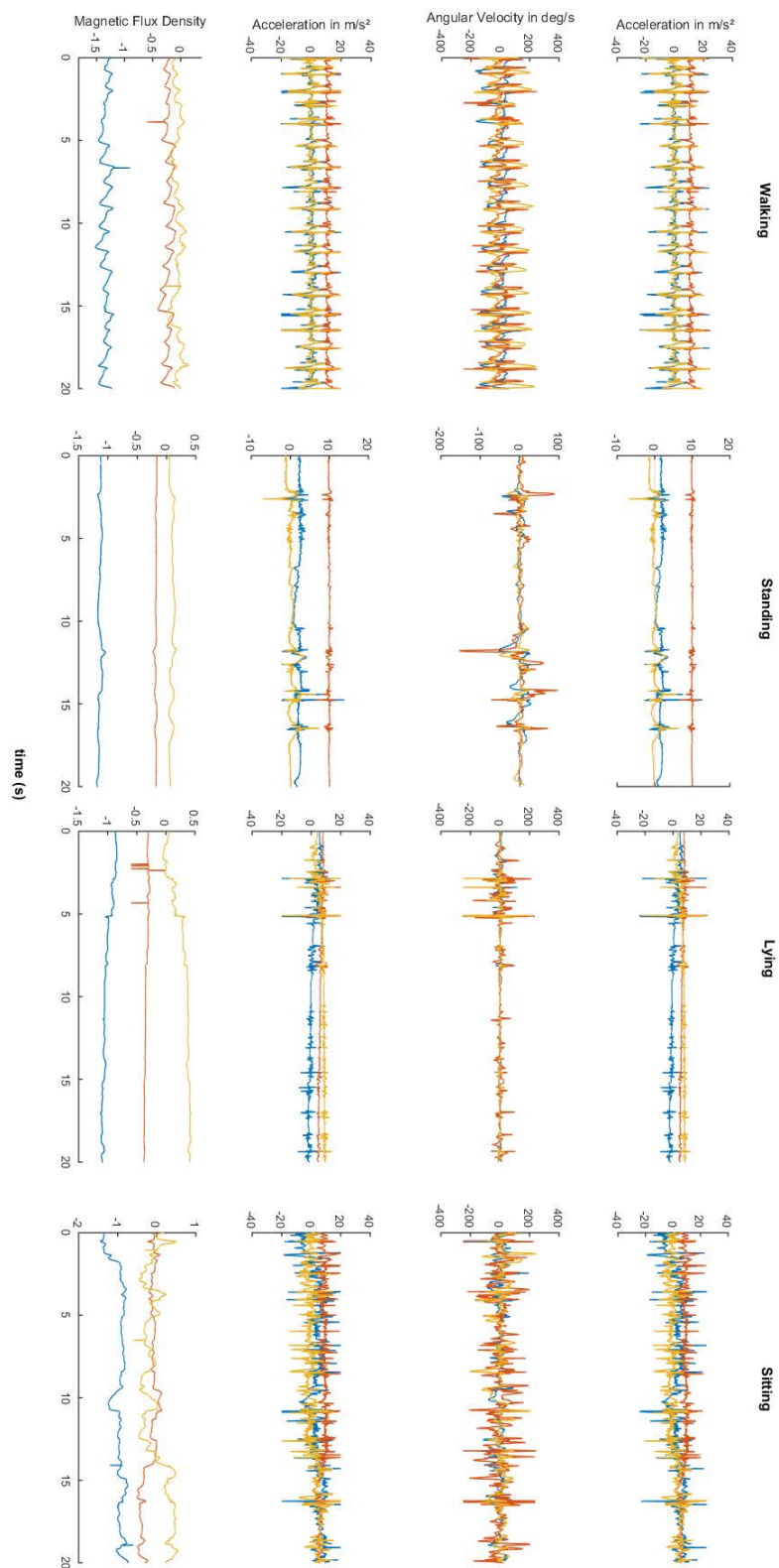


Figure III.9 – Signals collected from the Ankle module of a PD patient in presence LID.

4 Conclusion

In this chapter, we presented the designed ambulatory monitoring system, the protocol of data acquisition and the database consisting of movement data collected from healthy individuals and PD patients. The system has several advantages, presented in the following:

One of the major issues facing the transition of wearable devices into clinical practice is the incompatibility between different systems and the incoherence of results reported by devices developed by the same manufacturers. The Shimmer sensing devices, however, are designed specifically for effective capturing, transmission, processing and displaying of body sensed data in real time. These devices provide equipment, supporting devices and possibility of incorporating external sensors; all of which ensures higher compatibility and allows for the development of a complete monitoring system. These devices have already been used for gait analysis [28, 29], dyskinesia, bradykinesia and tremor evaluation in PD [30–32].

The relatively low cost of the constructed system makes it possible to initiate large scale studies and open-source the collected datasets in order to advance the incorporation of the different aspects of the disease, validate the mathematical algorithms used to govern the data processing, and ensure the reliability of the obtained results.

On the other hand, we acknowledge the presence of certain limitations, presented in the following:

It is worth noting that the small number of patients available for this work provides certain challenges in interpreting the obtained results. However, several processing techniques were utilised in order to ensure the robustness of the results as much as possible, such as applying a bootstrap method.

The patients included in this study portrayed specific and similar PD symptoms. None of the patients experienced rest tremor during the time of the study, and they displayed somewhat similar gaits. The patients themselves reported experiencing different degrees of freezing of gate (FoG) and other PD symptoms such as bradykinesia and akinesia. However, all of the patients experienced mild to severe LID recently. As this was the main concern of our study, the patients therefore made for well suited candidates to investigate this phenomenon. The presence of other PD motor symptoms, on the other hand, such as tremor, could interfere with the detection of LID. The absence of these symptoms in the patients involved in this study made it impossible for us to investigate this influence. However, it encourages the prospect of incorporating other previously applied methods in order to quantify and distinguish between PD motor symptoms and LID.

Bibliography

- [1] M. J. MATHIE, A. C. COSTER, N. H. LOVELL, AND B. G. CELLER. *Accelerometry: providing an integrated, practical method for long-term, ambulatory monitoring of human movement*. *Physiological measurement* **25**(2), R1 (2004).
- [2] H. J. LUINGE AND P. H. VELTINK. *Measuring orientation of human body segments using miniature gyroscopes and accelerometers*. *Medical and Biological Engineering and computing* **43**(2), 273–282 (2005).
- [3] S. PATEL, H. PARK, P. BONATO, L. CHAN, AND M. RODGERS. *A review of wearable sensors and systems with application in rehabilitation*. *Journal of neuroengineering and rehabilitation* **9**(1), 1 (2012).
- [4] F. HORAK, L. KING, AND M. MANCINI. *Role of body-worn movement monitor technology for balance and gait rehabilitation*. *Physical therapy* **95**(3), 461–470 (2015).
- [5] M. MUBASHIR, L. SHAO, AND L. SEED. *A survey on fall detection: Principles and approaches*. *Neurocomputing* **100**, 144–152 (2013).
- [6] T. SHANY, S. J. REDMOND, M. R. NARAYANAN, AND N. H. LOVELL. *Sensors-based wearable systems for monitoring of human movement and falls*. *Sensors Journal, IEEE* **12**(3), 658–670 (2012).
- [7] B. ZHANG, S. JIANG, D. WEI, M. MARSCHOLLEK, AND W. ZHANG. *State of the art in gait analysis using wearable sensors for healthcare applications*. In *Computer and Information Science (ICIS), 2012 IEEE/ACIS 11th International Conference on*, pages 213–218. IEEE (2012).
- [8] P. RASHIDI AND A. MIHAILIDIS. *A survey on ambient-assisted living tools for older adults*. *Biomedical and Health Informatics, IEEE Journal of* **17**(3), 579–590 (2013).
- [9] STATISTA. *Health & fitness tracker global unit sales forecast 2014-2015, by region*. <http://www.statista.com>, (2016).
- [10] K. KAEWKANNATE AND S. KIM. *A comparison of wearable fitness devices*. *BMC public health* **16**(1), 1 (2016).
- [11] J. K. AGGARWAL AND M. S. RYOO. *Human activity analysis: A review*. *ACM Computing Surveys (CSUR)* **43**(3), 16 (2011).
- [12] U. MAURER, A. SMAILAGIC, D. P. SIEWIOREK, AND M. DEISHER. *Activity recognition and monitoring using multiple sensors on different body positions*. In *Wearable and Implantable Body Sensor Networks, 2006. BSN 2006. International Workshop on*, pages 4–pp. IEEE (2006).
- [13] M. ERMES, J. PARKKA, J. MANTYJARVI, AND I. KORHONEN. *Detection of daily activities and sports with wearable sensors in controlled and uncontrolled conditions*. *Information Technology in Biomedicine, IEEE Transactions on* **12**(1), 20–26 (2008).
- [14] K. ALTUN, B. BARSHAN, AND O. TUNÇEL. *Comparative study on classifying human activities with miniature inertial and magnetic sensors*. *Pattern Recognition* **43**(10), 3605–3620 (2010).

BIBLIOGRAPHY

- [15] M. ZHANG AND A. A. SAWCHUK. *Human daily activity recognition with sparse representation using wearable sensors*. Biomedical and Health Informatics, IEEE Journal of **17**(3), 553–560 (2013).
- [16] A. MANNINI, S. S. INTILLE, M. ROSENBERGER, A. M. SABATINI, AND W. HASKELL. *Activity recognition using a single accelerometer placed at the wrist or ankle*. Medicine and science in sports and exercise **45**(11), 2193 (2013).
- [17] A. AHMADI, E. MITCHELL, F. DESTELLE, M. GOWING, N. E. O’CONNOR, C. RICHTER, AND K. MORAN. Automatic activity classification and movement assessment during a sports training session using wearable inertial sensors. In *Wearable and Implantable Body Sensor Networks (BSN), 2014 11th International Conference on*, pages 98–103. IEEE (2014).
- [18] D. BISWAS, A. CRANNY, N. GUPTA, K. MAHARATNA, J. ACHNER, J. KLEMKE, M. JÖBGES, AND S. ORTMANN. *Recognizing upper limb movements with wrist worn inertial sensors using k-means clustering classification*. Human movement science **40**, 59–76 (2015).
- [19] S. I. LEE, M. Y. OZSECEN, L. DELLA TOFFOLA, J.-F. DANEAU, A. PUIATTI, S. PATEL, AND P. BONATO. Activity detection in uncontrolled free-living conditions using a single accelerometer. In *Wearable and Implantable Body Sensor Networks (BSN), 2015 IEEE 12th International Conference on*, pages 1–6. IEEE (2015).
- [20] F. S. AYACHI, H. P. NGUYEN, C. LAVIGNE-PELLETIER, E. GOUBAULT, P. BOISSY, AND C. DUVAL. *Wavelet-based algorithm for auto-detection of daily living activities of older adults captured by multiple inertial measurement units (imus)*. Physiological measurement **37**(3), 442 (2016).
- [21] O. D. LARA AND M. A. LABRADOR. *A survey on human activity recognition using wearable sensors*. IEEE Communications Surveys & Tutorials **15**(3), 1192–1209 (2013).
- [22] S. C. MUKHOPADHYAY. *Wearable sensors for human activity monitoring: A review*. IEEE Sensors Journal **15**(3), 1321–1330 (2015).
- [23] A. BURNS, B. R. GREENE, M. J. MCGRATH, T. J. O’SHEA, B. KURIS, S. M. AYER, F. STROIESCU, AND V. CIONCA. *Shimmer—a wireless sensor platform for noninvasive biomedical research*. Sensors Journal, IEEE **10**(9), 1527–1534 (2010).
- [24] E. MITCHELL, A. AHMADI, N. E. O’CONNOR, C. RICHTER, E. FARRELL, J. KAVANAGH, AND K. MORAN. Automatically detecting asymmetric running using time and frequency domain features. In *Wearable and Implantable Body Sensor Networks (BSN), 2015 IEEE 12th International Conference on*, pages 1–6. IEEE (2015).
- [25] S. GRADL, H. LEUTHEUSER, P. KUGLER, T. BIERMANN, S. KREIL, J. KORNHUBER, M. BERGNER, AND B. ESKOFIER. Somnography using unobtrusive motion sensors and android-based mobile phones. In *Engineering in Medicine and Biology Society (EMBC), 2013 35th Annual International Conference of the IEEE*, pages 1182–1185. IEEE (2013).
- [26] G. COLA, M. AVVENUTI, A. VECCHIO, G.-Z. YANG, AND B. LO. *An on-node processing approach for anomaly detection in gait*. Sensors Journal, IEEE **15**(11), 6640–6649 (2015).
- [27] R. KHUSAINOV, D. AZZI, I. E. ACHUMBA, AND S. D. BERSCH. *Real-time human ambulation, activity, and physiological monitoring: taxonomy of issues, techniques, applications, challenges and limitations*. Sensors **13**(10), 12852–12902 (2013).
- [28] J. KLUCKEN, J. BARTH, P. KUGLER, J. SCHLACHETZKI, T. HENZE, F. MARXREITER, Z. KOHL, R. STEIDL, J. HORNEGGER, B. ESKOFIER, ET AL. *Unbiased and mobile gait analysis detects motor impairment in Parkinson’s disease*. PloS one **8**(2), e56956 (2013).

- [29] F. PARISI, G. FERRARI, V. CIMOLIN, M. GIUBERTI, C. AZZARO, G. ALBANI, L. CONTIN, AND A. MAURO. On the correlation between UPDRS scoring in the leg agility, sit-to-stand, and gait tasks for parkinsonians. In *2015 IEEE 12th International Conference on Wearable and Implantable Body Sensor Networks (BSN)*, pages 1–6. IEEE (2015).
- [30] S. PATEL, K. LORINCZ, R. HUGHES, N. HUGGINS, J. H. GROWDON, M. WELSH, AND P. BONATO. Analysis of feature space for monitoring persons with Parkinson’s disease with application to a wireless wearable sensor system. In *2007 29th Annual International Conference of the IEEE Engineering in Medicine and Biology Society*, pages 6290–6293. IEEE (2007).
- [31] S. PATEL, K. LORINCZ, R. HUGHES, N. HUGGINS, J. GROWDON, D. STANDAERT, M. AKAY, J. DY, M. WELSH, AND P. BONATO. *Monitoring motor fluctuations in patients with Parkinson’s disease using wearable sensors*. IEEE transactions on information technology in biomedicine **13**(6), 864–873 (2009).
- [32] B.-R. CHEN, S. PATEL, T. BUCKLEY, R. REDNIC, D. J. MCCLURE, L. SHIH, D. TARSY, M. WELSH, AND P. BONATO. *A web-based system for home monitoring of patients with Parkinson’s disease using wearable sensors*. IEEE transactions on Biomedical Engineering **58**(3), 831–836 (2011).

Pattern Recognition for Activity Classification and Dyskinesia Detection

This chapter presents the data processing methods applied for the classification of activities and the detection of dyskinesia based on a pattern recognition approach. First, we define the features extracted from the data collected from healthy individuals and PD patients. Then, the activity classification step is discussed, explaining the choice and design of the selected activity classifier. Following that, the different approaches pursued for the assessment of dyskinesia detection, with and without the classification of activities, are presented. Finally, the results obtained for the activity classification and dyskinesia detection approaches are introduced along with a discussion of the obtained performances in each approach.

Since the objectives of this work also include designing a monitoring system with a minimal number of sensing modules in order to promote patient compliance and comfort, and minimise obstruction of daily activities, two analysis methods aiming towards the reduction the total number of modules are performed. The results of these analysis methods are presented and discussed, showing the possibility of achieving a compromise between the total number of modules in the system and the accuracy of dyskinesia detection.

The conclusion presents a summary of the processing methods applied and the obtained results. These results are discussed highlighting how the designed system and the developed algorithm present a reliable and objective method for the detection of dyskinesia.

1 Data Processing Methods

Offline processing was performed on the data collected from the patients and the healthy subjects. Considering the hypothesis that activity recognition could influence the accuracy of dyskinesia detection, we will present the work done in two parts. The first part (Figure IV.1) is concerned with activity classification and is based on the healthy subjects dataset. This part is necessary in order to properly evaluate the performance of the activity classifier in the case where no motor dysfunction is present. The second part is concerned with activity classification and dyskinesia detection (Figure IV.2) and is based on the PD patients dataset. The processing methods will be detailed in the following sections.

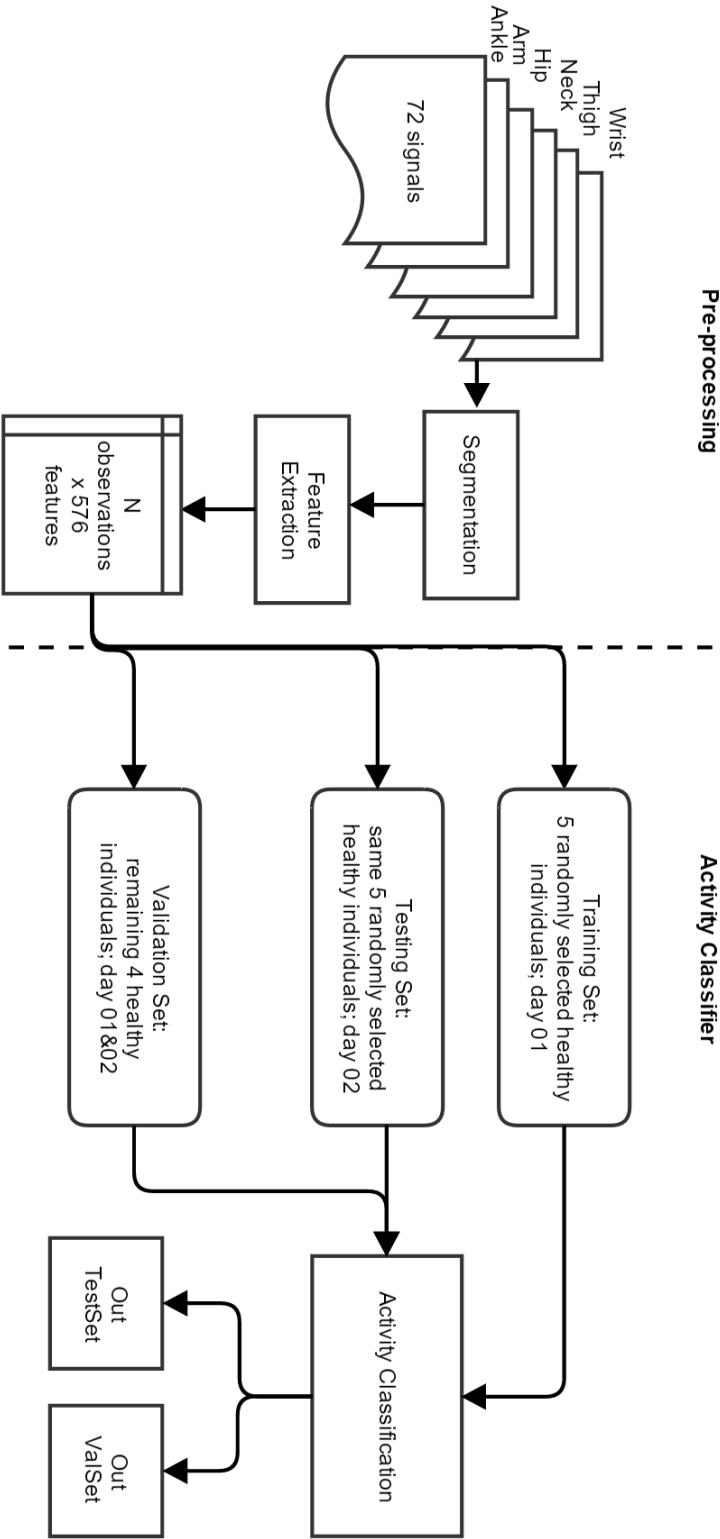


Figure IV.1 – Schema of the preprocessing and activity classification procedures performed on the data collected from the healthy individuals.

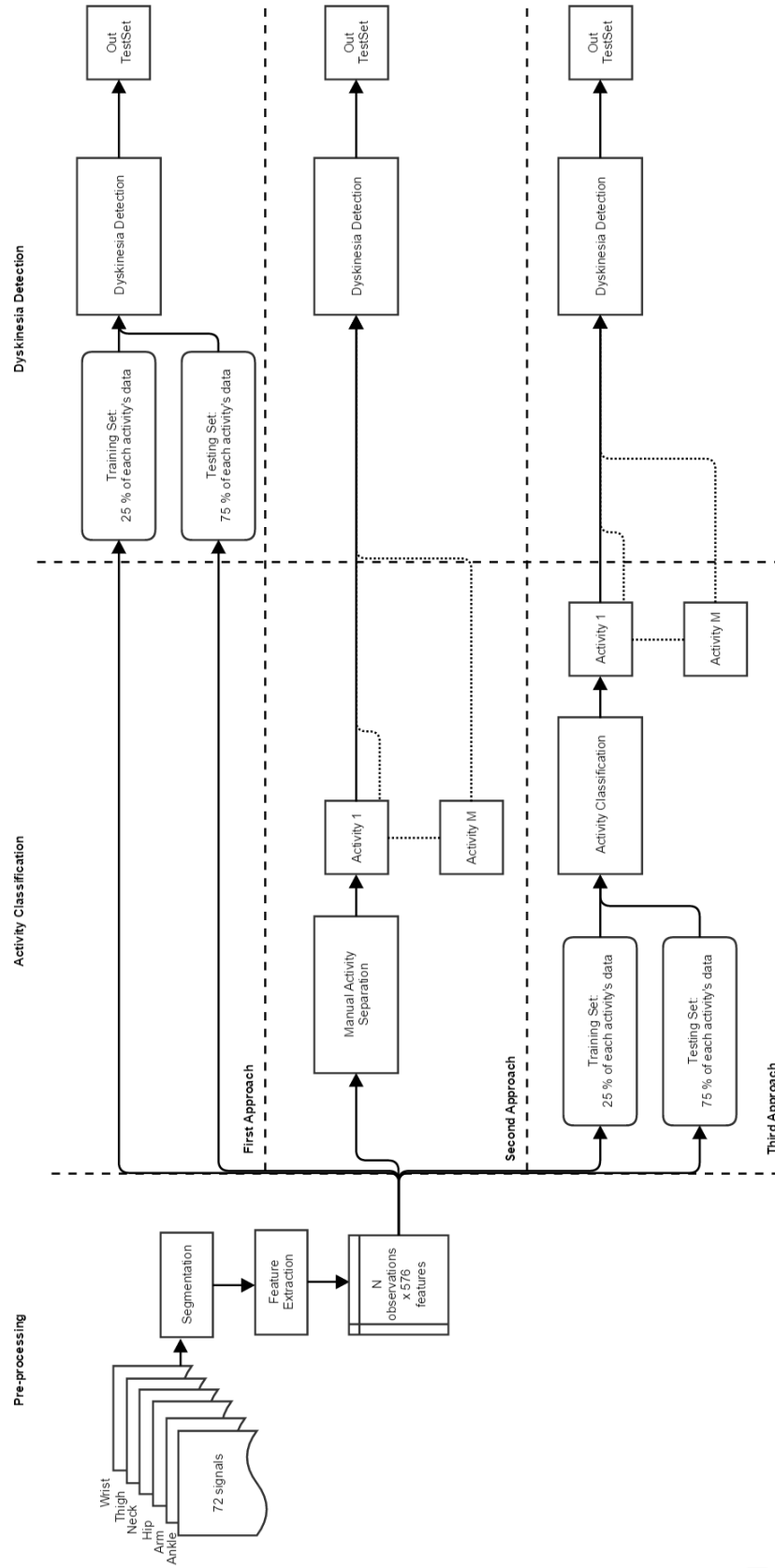


Figure IV.2 – The algorithms applied on the data collected from the PD patients. First Approach: dyskinesia detection without activity classification. Second Approach: dyskinesia detection for manually separated activities. Third Approach: dyskinesia detection for automatically classified activities.

1.1 Preprocessing

Each activity's raw signal data was first extracted from the total acquired data based on that activity's annotated start and end times. The data corresponding to each raw signal was segmented into $\Delta t = 7$ second time windows with a 50% overlap based on the proposed method in [1].

Then, for each time window, features in both the time and frequency domain were extracted. Each collected signal was centred before the calculation of the following features:

- Mean (μ) and standard deviation (σ) of the signal data over the specified time window.
- Mobility (M_x), defined as the ratio of the standard deviation of the first derivative of $x(t)$ with respect to time to the standard deviation of $x(t)$ itself [2]:

$$M_x = \sqrt{\frac{a_2}{a_0}} \quad (\text{IV.1})$$

where

$$a_0 = \sigma_x^2 \quad (\text{IV.2})$$

and

$$a_2 = E \left[\left(\frac{dx(t)}{dt} \right)^2 \right] \quad (\text{IV.3})$$

- Complexity (C_x), defined as the ratio of the mobility of $x'(t)$, the first derivative of $x(t)$, to the mobility of $x(t)$ [2]:

$$C_x = \sqrt{\frac{a_4/a_2}{a_0}} \quad (\text{IV.4})$$

where

$$a_4 = E \left[\left(\frac{d^2x(t)}{dt^2} \right)^2 \right] \quad (\text{IV.5})$$

- Peak cross correlation ($CORR$) between the three orthogonal axes of each sensor present in a single sensing module. The maximum value of cross correlation between the sensor axes gives an indication of the time lag/leads between the signals corresponding to each axis:

$$CORR = \max_{\tau} (R_{x_1x_2}(\tau)) = \max_{\tau} \left(\frac{E\{x_1(t+\tau)x_2^*(t)\}}{\sigma_{x_1}\sigma_{x_2}} \right) \quad (\text{IV.6})$$

where x_1 and x_2 represent a pair of orthogonal axes.

- Energy was calculated as the sum of squared discrete Fourier Transform component magnitudes for each time window [1]:

$$Energy = \int |X(f)|^2 df \quad (IV.7)$$

where

$$X(f) = \int_{-\infty}^{\infty} x(t)e^{-j2\pi ft} dt \quad (IV.8)$$

is the Fourier Transform of the signal over the entire time axis.

- In order to obtain the mean and median frequencies, denoted as MNF and MDF respectively, the power spectral density of each window was first estimated using the Burg method, which fits an autoregressive model to the signal by minimising the forward and backward prediction errors. The mean frequency is defined as the average of the obtained power spectrum, while the median frequency is defined as the value dividing the power spectrum into two equal areas [3]. The order of the autoregressive model was selected after an exhaustive search on the entire database using the Akaike information criterion.

The total number of features obtained for each IMU was therefore 96 (8 features x 12 signals per module). The entire data set used for classification consisted of the features obtained from the 6 IMUs and therefore had a total of 576 features (96 features per module x 6 modules).

1.2 Activity Classification

Presentation of the Classifiers

As an initial step, we choose to introduce a priori knowledge to the activity classification phase of the study by comparing the performance of the following classifiers:

- **k-Nearest Neighbour** [4]: an instance-based learning algorithm, where classification is done by identifying the class of the nearest neighbours to an instance. Classification is based directly on the training examples, and the class of the nearest neighbours is determined based on majority voting or distance-weighted voting.

This classifier is commonly based on the Euclidean distance between a test sample and the specified training samples. Given an input sample x_i with N feature vectors, such that:

$$x_i = x_{i1}, x_{i2}, \dots, x_{iN} \quad (IV.9)$$

and K is the total number of input samples, $i = 1, \dots, K$, the Euclidean distance between x_i and

a test sample x_l , where $l = 1, \dots, N$ is defined as:

$$d(x_i, x_l) = \sqrt{(x_{i1} - x_{l1})^2 + (x_{i2} - x_{l2})^2 + \dots + (x_{iN} - x_{lN})^2} \quad (\text{IV.10})$$

Assuming w is the true class of the training sample x_i , and \hat{w} is the predicted class of the test sample, x_l , then the predicted class \hat{w} of the test sample is set equal to the true class w of its nearest neighbour, where m_i is a nearest neighbour to x_l , if:

$$d(m_i, x_l) = \min_j d\{(m_j, x_l)\} \quad (\text{IV.11})$$

with

$$j = 1, \dots, N \quad (\text{IV.12})$$

For k nearest neighbours, the predicted class of test sample is set equal to the most frequent true class among k nearest training samples.

- **Naive Bayes** [5]: a specialised form of the Bayesian Network, providing a simple approach to representing, using and learning probabilistic knowledge for supervised induction tasks. This classifier assumes conditional independence between predictive attributes and given classes, and posits that no hidden attributes influence the prediction process.

Given a class variable y and a dependant feature vector $x = \{x_1, \dots, x_N\}$, Bayes' theorem states the following:

$$P(y \mid x_1, \dots, x_N) = \frac{P(y)P(x_1, \dots, x_N \mid y)}{P(x_1, \dots, x_N)} \quad (\text{IV.13})$$

Using the naive independence assumption that:

$$P(x_i \mid y, x_1, \dots, x_{i-1}, x_{i+1}, \dots, x_N) = P(x_i \mid y) \quad (\text{IV.14})$$

The relationship can be simplified, for all i :

$$P(y \mid x_1, \dots, x_N) = \frac{P(y) \prod_{i=1}^N P(x_i \mid y)}{P(x_1, \dots, x_N)} \quad (\text{IV.15})$$

Since $P(x_1, \dots, x_N)$ is constant, the classification rule becomes:

$$\begin{aligned}
 P(y \mid x_1, \dots, x_N) &\propto P(y) \prod_{i=1}^N P(x_i \mid y) \\
 &\Downarrow \\
 \hat{y} &= \arg \max_y P(y) \prod_{i=1}^N P(x_i \mid y)
 \end{aligned} \tag{IV.16}$$

The maximum a posteriori estimation is then used to estimate $P(y)$ and $P(x_i \mid y)$, where $P(y)$ is dependant on the frequency of class y in the training set.

Although this type of classification might appear over-simplified, it seems to work quite well in real world problems. It also offers the advantage of performing extremely fast computations compared to more sophisticated methods.

- **Decision Tree** [6]: a predictive model approach based on the mapping of observations to a target value. Decision trees are flow-chart-like representations of non-leaf (internal) nodes and leaf (terminal) nodes. The internal nodes represent conjunctions of the feature set based on certain splitting criterion that lead to a class label, or the leaf nodes. The learning process or the construction of the tree stems from labelled training observations. This process begins with the original feature set as a source set and is split into smaller subsets based on the feature set values. The splitting is then repeated at each internal node on each derived subset and stops when the subset at a node belongs to the same class.

Given an input set of variables $X = \{x_1, \dots, x_N\}$ with $Y = \{y_1, \dots, y_N\}$ target values, a variable is chosen at each step that best splits the set of observations. The default metrics used for measuring the best variable is determined through Gini's Diversity Index (*gdi*), which is a measure of node impurity. The *gdi* measures how often a randomly chosen observation from the set would be incorrectly classified if it was randomly classified according to the distribution of the labels in the set, and can be computed as:

$$gdi = 1 - \sum_{i=1}^N p^2(i) \tag{IV.17}$$

where the sum is over the classes i of the node, and $p(i)$ is the observed fraction of classes with class i that reach the node. A *pure* node is defined as a node with only one class, and therefore has a $gdi = 0$, otherwise the gdi is positive.

- **Random Forests** [6]: a combination of tree predictors. Classification is based on the majority vote of a collection of decision trees, where each tree depends on the value of an independently sampled random vector with the same distribution for all trees. Decision tree classification

operates by mapping observations about an instance to conclusions about this instance's target variable. Trees that have a finite number of target values are called classification trees, where the leaves represent class labels and branches represent conjunctions of features that lead to those labels. However, one disadvantage of decision trees is their trend to learn highly irregular patterns, and having low bias and high variance causes them to over fit to the training data.

Random forests on the other hand aim to reduce the variance by averaging multiple decision trees trained on different parts of the same training set. The training algorithm for this classifier applies bootstrap aggregating [7] to tree learners.

In the bagging algorithm for trees, and given a training set $X = \{x_1, \dots, x_N\}$ with $Y = \{y_1, \dots, y_N\}$ target values, a random sample with replacement is selected from the training set, or in other words bagging repeatedly, and trees are fitted to these samples. After training, new samples are assigned target variables by taking the majority vote of the decision trees. Random forests differ from this algorithm in one aspect only, where at each candidate split in the learning process, a random subset of the features is selected.

Activity classification for healthy individuals dataset

When considering the data collected from the healthy subjects (HS), the activity classification algorithm seen in Figure IV.1 was performed. The healthy individuals' activity data was separated into a training set (TrainSet), a testing set and a validation set. Five randomly chosen healthy individuals served as the training and testing sets, where the training set consisted of data collected on the first day, and the testing set (TestSet) consisted of data collected on the second day. These datasets were used to design the activity classifier. The validation set (ValSet), consisted of the remaining healthy individuals' data that were not included in the training and testing sets. The dimensions of each dataset are shown in Table IV.1.

Table IV.1 – Healthy Subjects Data Split.

Data	Subjects	Size
Training Set (TrainSet)	5 randomly chosen subjects Day01	1188 instances x 576 features
Testing Set (TestSet)	5 randomly chosen subjects Day02	1202 instances x 576 features
Validation Set (ValSet)	4 remaining subjects Day01&Day02	2062 instances x 576 features
Total	9 subjects	4452 instances x 576 features

Table IV.2 shows the number of observations obtained per type of activity for the data collected from healthy individuals. The activities of sedentary sitting, writing, reading, and eating performed during the protocol were later combined into one class, labelled as "sitting". As such, the number of observations of this class is significantly higher than the three other classes (Table IV.3).

Table IV.2 – Number of Instances per Activity for Healthy Subjects: Case of Seven Classes.

Activity	Training Set	Testing Set	Validation Set
Walking	145	153	246
Standing	139	142	224
Lying	295	290	469
Sedentary Sitting	307	290	493
Writing	138	130	242
Reading	60	70	135
Eating	104	127	253
Total	1188	1202	2062

Table IV.3 – Number of Instances per Activity for Healthy Subjects: Case of Four Classes.

Activity	Training Set	Testing Set	Validation Set
Walking	145	153	246
Standing	139	142	224
Lying	295	290	469
Sitting	609	617	1123
Total	1188	1202	2062

Activity classification for PD patients dataset

As for the data collected from the PD patients, the activity classification phase of Figure IV.2 (Top view) was applied. In this case, the patients performed the activity protocol in an irregular manner depending on their motor state during the particular acquisition session. During certain sessions, the patients were not able to perform a given activity, while during others they were perfectly able to comply to the protocol. This made it impossible for us to separate the data into a day01-day02 training-testing split. Therefore, the dataset was separated into a training set of 25%, and a testing set which consisted of the remaining 75% of the activity data (Table IV.4).

Table IV.4 – Patient Data Split.

Data	Subjects	Size
Training Set (25%)	3 patients Day01&Day02	530 instances x 576 features
Testing Set (75%)	3 patients Day01&Day02	1591 instances x 576 features
Total	3 patients	2121 instances x 576 features

A bootstrap validation method [8] with $r = 100$ iterations was used to ensure robustness of the obtained results.

1.3 Dyskinesia Detection

Similar to the activity classification phase, a comparison between the previously listed classifiers was done for the detection of dyskinesic instances. In this case, dyskinesia detection (DD) was performed for the entire dataset of the three patients collected over the acquisition sessions without the separation of activities. The same bootstrap validation method used in the activity classification phase was also

Table IV.5 – Number of Instances per Motor State.

Motor State	Dyskinesia	No Dyskinesia
Training Set (25%)	167	363
Testing Set (75%)	463	1128
Total	630	1491

applied here.

On the other hand, in order to evaluate the effect of activity classification on the detection of dyskinetic instances, three different classification approaches were performed (Figure IV.2):

- *First Approach (App1)*: Detection of dyskinetic instances without separating activity data. In this case, the dyskinesia detector was used to detect whether a certain instance is dyskinetic or non-dyskinetic from the entire dataset collected from the patients (Figure IV.2 Top).
- *Second Approach (App2)*: Detection of dyskinetic instances for manually separated and annotated activity datasets. In other words, the different activity datasets were manually separated and dyskinesia detection was performed on each particular dataset (Figure IV.2 Middle).
- *Third Approach (App3)*: Application of our developed algorithm which consists of first classifying the performed activities, then detecting the presence of dyskinesia based on the identified activity class (Figure IV.2 Bottom).

The three different approaches here serve to investigate the entire motor state of PD patients. This includes exploring the ability to classify PD patients' activities with presence of motor impairments as well as dyskinesia. One of the major difficulties of detecting dyskinesia lies in its complexity and difficulty of distinguishing it from voluntary movements, and achieving this requires information about the specific movement features. Many studies have focused on frequency and amplitude of accelerometric signals in order to distinguish LID from voluntary movement [9–11], however it has been proven that there is a large overlap in frequency between the two [12, 13]. This suggests that frequency components alone are not sufficient to separate dyskinesia from different voluntary movements. However, if we consider features corresponding to a single type of voluntary movement, then it might be simpler to identify the movement patterns belonging to dyskinesia.

2 Results

In this section, we present the results of the performed analyses, starting with the measures used to evaluate the performance. For the activity classification phase, we present the obtained performance of the activity classifier for the healthy subjects and PD patients. Then for the dyskinesia detection phase, we present the performance of the dyskinesia detector for each of the suggested approaches. Finally, we test two different strategies for the reduction of the total number of modules included in the system.

2.1 Performance Measures

Evaluating the accuracy and performance of the classifiers tested both in the activity classification and dyskinesia detection cases was done through calculating standard measures of performance, which are the sensitivity, specificity and accuracy [14], such that (Table IV.6):

- **True Positive (TP):** classified as positive, while true condition is positive.
- **False Negative (TN):** classified as negative, while true condition is positive.
- **False Positive (FP):** classified as positive, while true condition is negative.
- **True Negative (TN):** classified as negative, while true class is negative.

Table IV.6 – Performance Measures for Classifier Performance Evaluation (* indicates the predicted class).

	Condition Positive	Condition Negative
Condition Positive*	TP	FP
Condition Negative*	FN	TN

- **Sensitivity (Se):** otherwise known as the True Positive Rate, and is defined as the proportion of positives that are correctly classified.

$$Se = \frac{TP}{TP + FN} \quad (IV.18)$$

- **Specificity (Sp):** otherwise known as True Negative Rate, and is defined as the proportion of negatives that are correctly classified.

$$Sp = \frac{TN}{TN + FP} \quad (IV.19)$$

- **Accuracy (Acc):** defined as the proportion of correctly classified conditions (both positive and negative) with respect to the total number.

$$Acc = \frac{TP + TN}{TP + FP + FN + TN} \quad (IV.20)$$

In the case of activity classification the TP condition is defined as the current activity class. While in the case of dyskinesia detection, the TP condition is defined as the condition in which dyskinesia is present.

2.2 Activity Classification

In a first attempt, a study was performed in order to evaluate the performance of the different types of classifiers in correctly identifying the activities performed by the healthy individuals [15, 16]. In this

study, the performed activities were divided into the following seven classes: {Walking, Standing, Lying, Sitting, Writing, Reading, and Eating}. However, the results obtained showed that the separation of the activities performed while sitting down introduced unnecessary misclassifications (Figure IV.3 left). These activities were therefore grouped into one category labeled "sitting". In this case, the comparison of the different types of classifiers revealed that the RF classification method yielded the highest performance (Figure IV.3 right), with an overall accuracy of 98.5% for the healthy individuals' TestSet. As a result, this type of classifier was adopted for the activity classification phase for both

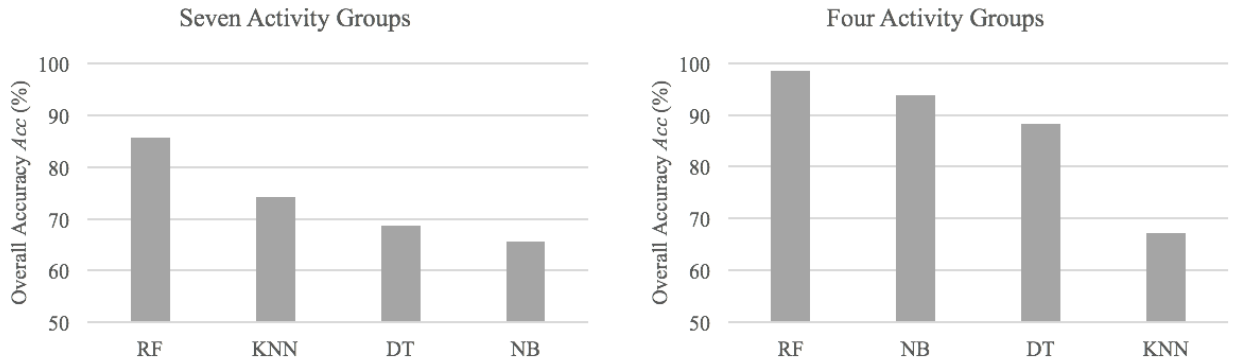


Figure IV.3 – Performance of the classifiers for seven or four groups of activities showing the classification accuracy of the healthy subjects' TestSet (RF: Random Forest, KNN: K Nearest Neighbour, DT: Decision Tree, NB: Naive Bayes).

healthy individuals and patients data. From this point on, the results presented concerning the activity classification phase of the algorithms are performed using the RF classifier.

An example of the performance measures for the classification of instances in the HS TestSet is given in Tables IV.7 and IV.8, where Table IV.7 represents the contingency matrix obtained for one iteration of the HS TestSet classification, and Table IV.8 shows the computed measures for this iteration.

Se and Sp values were computed for each class of activity, while an overall accuracy Acc was evaluated with respect to the number of observations per type of activity for the datasets corresponding to the healthy individuals (Figure IV.4 (A)), and to the PD patients (Figure IV.4 (B)). It is observed that the overall accuracy of activity classification in the case of PD patients ($Acc = 93.6\%$) is slightly lower than that of the HS (TestSet $Acc = 98.5\%$, ValSet $Acc = 95.6\%$). This decrease can be attributed to the presence of motor dysfunction such as dyskinesia which makes distinguishing between activities more difficult. However, the obtained results are still considered to be satisfactory.

Table IV.7 – An Example of the Contingency Table Obtained for the Healthy Subjects TestSet.

Activity	Walking	Standing	Lying	Sitting
Walking*	153	0	0	2
Standing*	0	138	0	4
Lying*	0	0	296	2
Sitting*	1	2	2	618

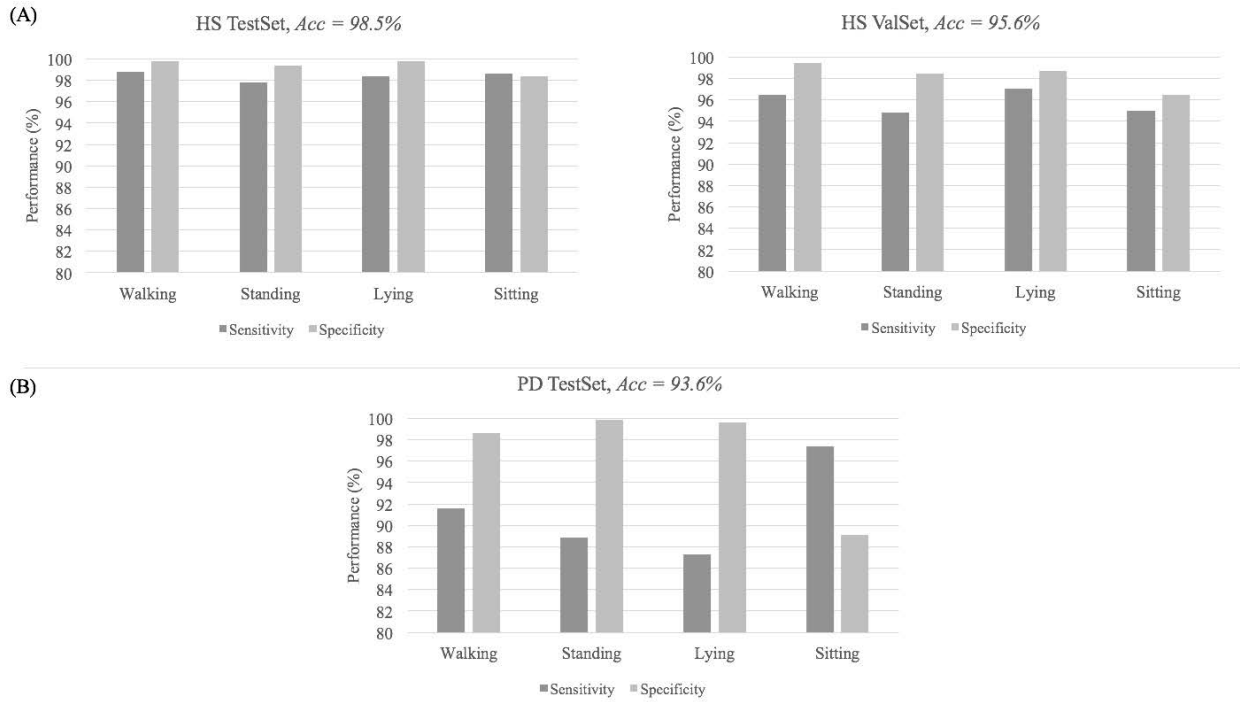


Figure IV.4 – Activity classification results in terms of Se and Sp for the healthy subjects' TestSet and Valset (A), and the PD patients' TestSet (B). The overall accuracy Acc is displayed in the titles.

Table IV.8 – Performance Measures Obtained for the Healthy Subjects TestSet.

Activity	Walking	Standing	Lying	Sitting
TP	153	138	296	618
FP	2	4	2	5
FN	1	2	2	8
TN	1062	1074	918	587
Sensitivity	99.1	99.4	99.8	99.8
Specificity	100	100	100	100
Accuracy	99.7			

2.3 Dyskinesia Detection

The data collected from the PD patients was analysed under three different approaches as previously explained. In this section, the results obtained for each analysis approach are presented and compared. As an initial measure of analysis, a comparison was also performed between the different types of classifiers in order to select the appropriate classification method for detecting dyskinesia. This evaluation of the classifiers' performance was done on the entire dataset collected from the PD patients without separation of activities, as described in *App1*. Each instance is classified as either D or \bar{D} , to indicate the presence or absence of dyskinesia, respectively. The results presented in Figure IV.5 also revealed that the RF classifier exceeded in performance the other classification methods, with an overall accuracy of 94.3%. Therefore it was again adopted as the classification method for the

dyskinesia detection phase of the algorithm. The results displayed from this point on with respect to dyskinesia detection are done with the RF classifier.

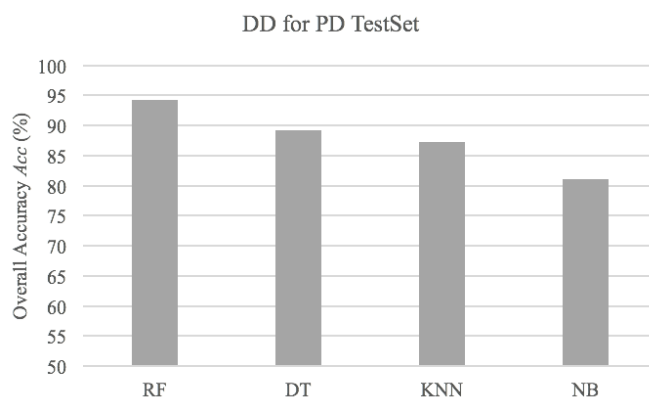


Figure IV.5 – Overall accuracy of the classifiers in detecting dyskinesia for the PD patients’ dataset as described in *App1* (RF: Random Forest, KNN: K Nearest Neighbour, DT: Decision Tree, NB: Naive Bayes).

An example of the performance measures for the detection of dyskinetic instances in the PD patients’ TestSet is given in Tables IV.9, where the contingency matrix obtained for one iteration of dyskinesia detection of the PD patients’ TestSet and its corresponding performance measures are presented.

Table IV.9 – An Example of the Contingency Table Obtained for the PD Patients TestSet Without Separation of Activities.

Motor State	Dyskinesia	No Dyskinesia
Dyskinesia*	402	33
No Dyskinesia*	61	1095
Sensitivity	87.5	
Specificity	97.3	
Accuracy	94.2	

First Approach: Dyskinesia Detection without Separation of Activities

As described in the previous section, in *App1*, dyskinesia detection was performed on the entire dataset collected from PD patients that included the four groups of activities. In this case, each instance is directly labeled as either D or \bar{D} .

In this approach, the purpose is to determine how well the classifier can detect dyskinetic instances experienced by the patient in a general movement context based on the information from the extracted features. The postural state of the patient is not taken into account and the information relative to the patient’s behaviour is withheld from the classification process. Using this approach, we obtained Se and Sp of 87.2% and 97.3% and an Acc of 94.3% (Table IV.12).

Second Approach: Dyskinesia Detection for Manually Separated Activities

The second approach, described in *App2*, applies DD on separate activity datasets. The purpose of this process is to compare the performance of the DD process obtained for datasets relating to single types of activities or postural behaviours with that obtained when the postural state is not considered.

The activity datasets were manually separated based on the start and end times of each activity taken from the session's video recordings. *Se*, *Sp* and *Acc* values were calculated for each separate activity dataset (Table IV.10). For comparison purposes, the overall values were computed with respect to the size of each dataset. In this case, *Se* increased significantly reaching 91.9% with an equally high *Sp* at 97.4%, and as a result the *Acc* increased to 95.7% (Table IV.12).

Table IV.10 – Dyskinesia Detection Results for *App2* Computed for Each Activity Dataset.

Activity	Sensitivity (%)	Specificity (%)	Accuracy (%)
Walking	91.2	99.0	94.3
Standing	83.1	97.9	95.7
Lying	94.4	97.8	94.8
Sitting	92.3	96.8	94.8

Third Approach: Dyskinesia Detection for Automatically Separated Activities

The third approach, described in *App3*, tests the activity classifier developed earlier along with the process of dyskinesia detection. In this case, the activity datasets are separated by the activity classifier, in which instances are labeled as one of the four activity groups: *Walking**, *Standing**, *Lying**, or *Sitting**, where "*" indicates predicted activity datasets. Following that, the instances belonging to each activity group are passed to the DD process, in which they are labeled as *D* or \bar{D} to indicate presence or absence of dyskinesia respectively.

Similarly, the performance of the DD process in this case was also evaluated for each predicted activity dataset (Table IV.11) by computing the *Se*, *Sp* and *Acc* values, as well as the overall values with respect to the size of each dataset for comparison purposes.

Table IV.11 – Dyskinesia Detection Results for *App3* Computed for Each Predicted Activity Dataset.

Activity	Sensitivity (%)	Specificity (%)	Accuracy (%)
<i>Walking*</i>	88.6	97.8	94.0
<i>Standing*</i>	74.11	98.1	93.6
<i>Lying*</i>	92.7	97.4	97.4
<i>Sitting*</i>	90.7	95.2	94.0

As can be observed, the *Se* and *Sp* values (Table IV.11) slightly decreased in comparison to *App2* (Table IV.10). The overall *Se* and *Sp* reached 89.7% and 96.4%, and the overall *Acc* of DD dropped to 94.8% (Table IV.12). This slight decrease in performance was expected due to the error of classification resulting from the activity classification phase. The robustness of the activity classifier, however, proved to be reliable and thus the DD process was only slightly affected. In comparison to *App1*, however,

the obtained performance in this case is superior. Although the overall *Acc* only slightly increased, a significant increase in the *Se* of DD can be observed.

Table IV.12 – Dyskinesia Detection Results for the 3 Approaches.

Dyskinesia Detection	Sensitivity (%)	Specificity (%)	Accuracy (%)
<i>App1</i>	87.2	97.3	94.3
<i>App2</i>	91.9	97.4	95.7
<i>App3</i>	89.7	96.4	94.8

2.4 Towards a Simplified System: Reduction of Number of Modules

An important factor in the development of this device lies in user acceptability and the ability to incorporate it in a patient's life without producing complications or hindering the patient from performing activities. In this respect, two methods aiming towards the reduction of the total number of modules used in the system were applied.

Reduction by Feature Selection

A preliminary study was conducted for the reduction of the total number of modules included in the system, based on a feature selection approach. This approach was pursued in the early stages of the study and consisted of the data collected from two PD patients only (patients M01&J02). The results are detailed in Appendix A, and a brief summary of this approach is described here.

Feature selection is the process of detecting the relevant features and discarding the irrelevant ones. This process allows the identification of a subset of features that best distinguishes between the given classes [17]. In order to identify the features that best correlate with the activity classes and those that best correlate with the motor states, we performed the analysis separately on the data collected from HS and PD patients. In the first analysis, labeled "Experiment I", we use the data collected from the nine HS to determine the features most relevant to the different activity classes. In the second analysis, labeled "Experiment II", we use the data collected from PD patients to identify the features most relevant to the dyskinesia class.

In both experiments, we begin by using the correlation-based feature subset evaluation method (Cfs) to extract a subset of features that are highly correlated with the class while having low intercorrelation [18]. This method is generally used to identify a subset of features that have high global predictive power. In most cases, Cfs selects a good "core" subset of features that enhance or provide comparable performance of classification algorithms while at the same time reducing the number of features used in learning. Other feature selection methods were also applied on the same dataset for comparison while only retaining an equal number of features to the subset selected by the Cfs method. The applied methods included Chi-squared [19], Gain Ratio [20], Information Gain [21], OneR [22], and ReliefF [23] feature selection methods.

In Experiment I, concerning the data collected from the HS, the correlation was evaluated with respect to the seven activity classes {Walking, Standing, Lying, Sitting, Writing, Reading, and Eating} using the Cfs evaluation method. This resulted in the selection of a subset of 50 features from the original feature set. The remaining feature selection methods were also applied on the HS dataset while retaining only the top 50 selected features, for comparison purposes. While the highest ranked features in most of the feature selection methods corresponded to the Ankle, Hip and Thigh modules, the variance in the selected features did not reveal a clear set of modules that can be considered of higher importance when considering the activity classification phase. Activity classification was repeated using the different feature subsets selected by the applied methods and by gradually decreasing the number of features considered. The highest overall accuracy was obtained at 88.0% by applying the Information Gain method with a subset of the first five highest ranked features.

In Experiment II, concerning the data collected from PD patients, a similar approach was applied starting with the evaluation of the correlation with respect to the motor state class {Dyskinetic or Non-Dyskinetic} using the Cfs evaluation method. In this case, a subset of 100 features considered as highly correlated to the presence or absence of dyskinesia is chosen from the original feature set. The feature selection methods listed before are also applied on the dataset of the PD patients while retaining the same number of features as in the Cfs-selected subset. The features present in the selected subsets by the different feature selection methods corresponded to all module positions, hence making it impossible to determine a reduced number of modules that could be considered of higher relevance with respect to dyskinesia detection. The highest overall accuracy of dyskinesia detection was obtained at 84.5% by applying the Information Gain method with a subset of the first fifty highest ranked features.

While feature selection methods often offer a means for reducing the size of the dataset and the computational complexity, the conducted analysis shows that these methods are not quite appropriate for our application. The objective here is to reduce the total number of modules in the system, and the inconsistency of feature rankings by the compared feature selection methods made it difficult to define which modules provided the most relevant information, in both the activity classification and dyskinesia detection cases. As a result, this approach is abandoned and an evaluation based on single modules is pursued.

Reduction by Single Module Assessment

In this method, dyskinesia detection was firstly done using single modules. In order to assess the importance of each module, the detection was performed for the entire dataset without separation of activities (*App1*), on each activity's manually separated dataset (*App2*), and for automatically separated activities (*App3*). The *Se*, *Sp* and *Acc* of DD using each module are presented in Figure IV.6.

Based on the obtained accuracies, it was evident that the importance of each module position

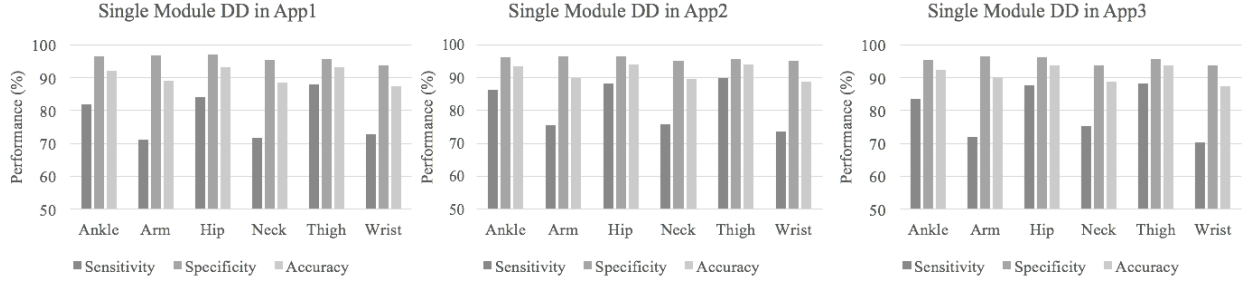


Figure IV.6 – Overall performance of single module dyskinesia detection arranged by decreasing order of accuracy.

varies depending on the performed activity and location of dyskinesia for each patient. However, in the three approaches, the Thigh, Hip and Ankle modules present the highest performance in detecting dyskinetic instances. Therefore, all possible combinations of these three modules were tested for dyskinesia detection in order to enhance the overall performance and simplify the system of acquisition. Tables IV.13 and IV.14 show the results obtained using the different combinations in *App1* and *App2* respectively.

Table IV.13 – Overall Performance of DD Using Combinations of the Top Three Modules for *App1*.

Modules	Sensitivity (%)	Specificity (%)	Accuracy (%)
Ankle, Hip, Thigh	91.8	96.7	95.2
Ankle, Hip	89.8	96.7	94.7
Ankle, Thigh	90.4	96.4	94.7
Hip, Thigh	91.7	96.4	94.9
All Modules	87.2	97.3	94.3

Table IV.14 – Overall Performance of DD Using Combinations of the Top Three Modules for *App2*.

Modules	Sensitivity (%)	Specificity (%)	Accuracy (%)
Ankle, Hip, Thigh	88.1	97.1	94.4
Ankle, Hip	85.2	97.0	93.5
Ankle, Thigh	86.5	96.5	93.5
Hip, Thigh	89.4	97.2	94.9
All Modules	91.9	97.4	95.7

Using a combination of the Ankle, Hip and Thigh modules yielded the second best accuracies when considering the entire dataset without separation of activities (*App1*) and the best accuracies in detecting dyskinesia when considering manually separated activity datasets (*App2*). Therefore, we tested our developed algorithm (*App3*) using the data collected from the ankle, hip and thigh modules only. Figure IV.7 shows the results for the activity classification phase and the dyskinesia detection phase using the Ankle, Hip and Thigh modules only versus the obtained results when considering the six modules.

The performance obtained when using only the Ankle, Hip and Thigh modules is slightly enhanced in comparison to that when using all the modules. In the activity classification phase of the algorithm, the sensitivity, specificity and overall accuracy when using all modules was $Se = 93.9\%$, $Sp = 93.4\%$

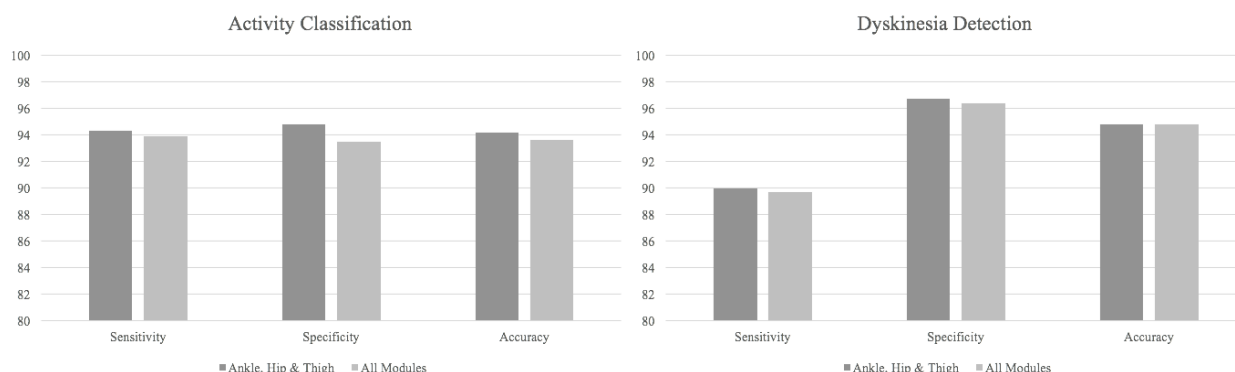


Figure IV.7 – Overall performance of the three best performing modules, Ankle, Hip and Thigh, in both AC and DD phases versus the performance obtained when using all the modules when applying *App3*.

and $Acc = 93.6\%$. However, by considering only the Ankle, Hip and Thigh modules, these values increased to $Se = 94.3\%$, $Sp = 94.8\%$ and $Acc = 94.2\%$. The same can be observed during the dyskinesia detection phase, where the sensitivity and specificity values increased from $Se = 89.7\%$, $Sp = 96.4\%$, when using all modules, to $Se = 90.0\%$ and $Sp = 96.7\%$. The overall accuracy, on the other hand, remained the same at $Acc = 94.8\%$. This is due to the fact that the overall performance presented here is computed with respect to the size of each predicted activity dataset and the variations of the Se , Sp values of each activity dataset in the two cases produced the same overall Acc .

2.5 Conclusion

The transition from subjective clinical scales towards objective and automated assessment of PD motor symptoms and complications is a process that requires the integration of the several aspects of the disease that are treated separately in literature. While symptoms such as tremor and bradykinesia have been successfully quantified (see [27] for review), the incorporation of dyskinesias and activity assessment seems to lag. Recent studies have been incorporating an activity classifier into ambulatory monitoring systems of PD patients. In [28], emphasis was put on classification of PD patients activities without exploring motor symptoms of PD. While it was shown that accurate classification of PD patients activities could be done, characteristics of motor symptoms and fluctuations were excluded using filtering and processing methods. In [29] on the other hand, only static activities were considered and a few basic aspects of PD motor symptoms were evaluated. A more detailed analysis is presented in [30], where parameters relevant to each motor symptom are calculated based on the output of the activity classifier. However, dyskinesia is not considered in this case which leaves out the motor symptom that can most significantly affect the patients activity performance. More recently, the work in [31], focused on the ability to detect choreaic dyskinesia. Using only one sensing module placed at the waist, sensitivity of dyskinesia detection varied from above 90% to 39% depending on the severity and location of the dyskinesia, with specificity values remaining above 90% in both cases. These results

show that there is room for enhancement if a more global system is considered, enabling the detection of mild as well as severe dyskinesias.

The objective of this chapter was to design an ambulatory monitoring system that is able to detect the occurrence of dyskinesia in PD patients. As detailed in this section, several approaches were tested in order to determine whether dyskinesia detection accuracy is affected if the data considered is specific to one type of activity.

An activity classifier was therefore designed and validated using data collected from healthy individuals. The classification accuracy for the test set (TestSet) was obtained at 98,5% and that of the validation dataset (ValSet) was 95,6%. This proves that the classifier is suitable to identify activities of healthy individuals, without the need for a priori information.

A comparison was then performed where dyskinetic instances are detected in the entire protocol data collected from the patients without separation of activities (*App1*), in manually separated activity sets (*App2*), and in automatically separated activity sets using the previously designed activity classifier (*App3*). The activity classifier was re-trained and tested using the data collected from PD patients before moving on to dyskinesia detection due to the differences in activity patterns between healthy individuals and PD patients [24].

In this study, we have proven that the designed ambulatory monitoring system is capable of classifying PD patients' activities with an overall accuracy of 93,6% and detect dyskinetic instances with an overall accuracy of 94,8% using our developed algorithm. We were also able to successfully reduce the number of modules present in the monitoring system to three modules placed at the Ankle, Hip and Thigh positions of the patient's body. The activity classification performance in this case increased reaching an accuracy of 94,2%, while dyskinesia detection remained the same at 94,8%.

The obtained results for our automated algorithm show that an activity classification step offers slight enhancement in the detection of dyskinesia. However, despite the presence of motor dysfunction, classifying the activities performed by PD patients can be done with certain accuracy. During the patient sessions, it was clearly noted that the patients had no problem performing certain activities, such as walking and standing, in both dyskinetic and non-dyskinetic states. Other activities, such as lying down and sitting, however, were extremely difficult to perform during the presence of dyskinesia. Tracking the presence and frequency of dyskinesia in certain types of activities could therefore offer important insight into the patient's motor condition, disease progression and the response to the current therapeutic plan. These different aspects of PD motor state assessment should eventually be combined in order to truly have an all-inclusive ambulatory monitoring system able to evaluate the disease's progression. In addition, monitoring activities can be essential relative to understanding the quality of life of PD patients. Improving clinical management of PD patients requires taking into account ecological variables, such as performance of activities of daily living, as well as the objective measures that contribute to understanding disease progression and the success of the therapeutic plan [25]. The progression of PD will gradually have a negative effect on the patient, hindering his/her ability to perform simple daily life activities. These limitations are considered more burdensome to

patients than the motor impairments of the disease itself [26]. Therefore, providing measures of activity performance along with motor dysfunction could help with transitioning towards more personalised and tailored treatment plans.

While the obtained results are promising, further tests are required in order to properly validate the system's performance. The main issue in this study is considered to be the small number of patients. Therefore, the next steps include testing on a larger number of PD patients at different stages of disease progression and displaying various intensities of dyskinesia, as well as performing long-duration acquisitions that could establish the system's performance in more realistic settings. Nevertheless, the results presented here show that the developed system can be used to monitor a PD patient's activities throughout the day, enabling the assessment of the patient's QL for instance. The preliminary results also show that the parameters corresponding to the Ankle, Hip and Thigh modules offer satisfactory classification performance and a system composed of these three modules only might have higher acceptability from patients. However, during this primary analysis, the relationship between the different modules had not been taken into consideration. The objective of the next chapter is therefore to explore the relationships between the modules and test whether exploiting them could have an effect on the classification performance.

Bibliography

- [1] LING BAO AND STEPHEN S INTILLE. *Activity recognition from user-annotated acceleration data*. Pervasive computing pages 1–17 (2004).
- [2] BO HJORTH. *EEG analysis based on time domain properties*. Electroencephalography and clinical neurophysiology **29**(3), 306–310 (1970).
- [3] S THONGPANJA, A PHINYOMARK, P PHUKPATTARANONT, AND C LIMSAKUL. *Mean and median frequency of EMG signal to determine muscle force based on time-dependent power spectrum*. Elektronika ir Elektrotechnika **19**(3), 51–56 (2013).
- [4] LEIF E PETERSON. *K-nearest neighbor*. Scholarpedia **4**(2), 1883 (2009).
- [5] K MING LEUNG. *Naive bayesian classifier*. Polytechnic University Department of Computer Science/Finance and Risk Engineering (2007).
- [6] LEO BREIMAN. *Random forests*. Machine learning **45**(1), 5–32 (2001).
- [7] LEO BREIMAN. *Bagging predictors*. Machine learning **24**(2), 123–140 (1996).
- [8] RON KOHAVI ET AL. A study of cross-validation and bootstrap for accuracy estimation and model selection. Ijcai **14**, pages 1137–1145 (1995).
- [9] PIERRE R BURKHARD, HEIDI SHALE, J WILLIAM LANGSTON, AND JAMES W TETRUD. *Quantification of dyskinesia in Parkinson’s disease: validation of a novel instrumental method*. Movement disorders **14**(5), 754–763 (1999).
- [10] JI HOFF, EAH WAGEMANS, JJ VAN HILTEN, ET AL. *Accelerometric assessment of levodopa-induced dyskinesias in Parkinson’s disease*. Movement disorders **16**(1), 58–61 (2001).
- [11] AJ MANSON, P BROWN, JD O’SULLIVAN, P ASSELMAN, D BUCKWELL, AND AJ LEES. *An ambulatory dyskinesia monitor*. Journal of Neurology, Neurosurgery & Psychiatry **68**(2), 196–201 (2000).
- [12] NLW KEIJSERS, MWIM HORSTINK, JJ VAN HILTEN, JI HOFF, AND CCAM GIELEN. *Detection and assessment of the severity of levodopa-induced dyskinesia in patients with Parkinson’s disease by neural networks*. Movement disorders **15**(6), 1104–1111 (2000).
- [13] NOËL LW KEIJSERS, MARTIN WIM HORSTINK, AND STAN CAM GIELEN. *Automatic assessment of levodopa-induced dyskinesias in daily life by neural networks*. Movement disorders **18**(1), 70–80 (2003).
- [14] ALIREZA BARATLOO, MOSTAFA HOSSEINI, AHMED NEGIDA, AND GEHAD EL ASHAL. *Part 1: simple definition and calculation of accuracy, sensitivity and specificity*. EMERGENCY-An Academic Emergency Medicine Journal **3**(2), 48–49 (2015).
- [15] NAHED JALLOUL, FABIENNE PORÉE, GEOFFREY VIARDOT, PHILIPPE L’HOSTIS, AND GUY CARRAULT. *Activity recognition using multiple inertial measurement units*. IRBM **37**(3), 180–186 (2016).

BIBLIOGRAPHY

- [16] NAHED JALLOUL, FABIENNE PORÉE, GEOFFREY VIARDOT, PHILIPPE L'HOSTIS, AND GUY CARRAULT. Detection of levodopa induced dyskinesia in Parkinson's disease patients based on activity classification. In *2015 37th Annual International Conference of the IEEE Engineering in Medicine and Biology Society (EMBC)*, pages 5134–5137. IEEE (2015).
- [17] ISABELLE GUYON AND ANDRÉ ELISSEEFF. *An introduction to variable and feature selection*. Journal of machine learning research **3**(Mar), 1157–1182 (2003).
- [18] MARK A HALL. *Correlation-based feature selection for machine learning*. Thèse de Doctorat, The University of Waikato (1999).
- [19] CHI SQUARE STATISTIC. *Chi-square tests*.
- [20] R PRAVEENA PRIYADARSINI, ML VALARMATHI, AND S SIVAKUMARI. *Gain ratio based feature selection method for privacy preservation*. ICTACT Journal on soft computing **1**(04), 20011 (2011).
- [21] DANNY ROOBAERT, GRIGORIS KARAKOULAS, AND NITESH V CHAWLA. Information gain, correlation and support vector machines. In *Feature Extraction*, pages 463–470. Springer (2006).
- [22] ROBERT C HOLTE. *Very simple classification rules perform well on most commonly used datasets*. Machine learning **11**(1), 63–90 (1993).
- [23] KENJI KIRA AND LARRY A RENDELL. The feature selection problem: Traditional methods and a new algorithm. , **2**, pages 129–134 (1992).
- [24] DIANE J COOK, MAUREEN SCHMITTER-EDGEcombe, AND PRAFULLA DAWADI. *Analyzing activity behavior and movement in a naturalistic environment using smart home techniques*. Biomedical and Health Informatics, IEEE Journal of **19**(6), 1882–1892 (2015).
- [25] ALBERTO J ESPAY, PAOLO BONATO, FATTA B NAHAB, WALTER MAETZLER, JOHN M DEAN, JOCHEN KLUCKEN, BJOERN M ESKOFIER, ARISTIDE MEROLA, FAY HORAK, ANTHONY E LANG, ET AL. *Technology in Parkinson's disease: Challenges and opportunities*. Movement Disorders (2016).
- [26] G-M HARIZ AND LARS FORSGREN. *Activities of daily living and quality of life in persons with newly diagnosed Parkinson's disease according to subtype of disease, and in comparison to healthy controls*. Acta Neurologica Scandinavica **123**(1), 20–27 (2011).
- [27] WALTER MAETZLER, JOSEFA DOMINGOS, KARIN SRULIJES, JOAQUIM J FERREIRA, AND BASTIAAN R BLOEM. *Quantitative wearable sensors for objective assessment of Parkinson's disease*. Movement Disorders **28**(12), 1628–1637 (2013).
- [28] ARASH SALARIAN, HEIKE RUSSMANN, FRANÇOIS JG VINGERHOETS, PIERRE R BURKHARD, AND KAMIAR AMINIAN. *Ambulatory monitoring of physical activities in patients with Parkinson's disease*. Biomedical Engineering, IEEE Transactions on **54**(12), 2296–2299 (2007).
- [29] ROB JW DUNNEWOLD, JORRIT I HOFF, HANS CJ VAN PELT, PAULINE Q FREDRIKZE, ERIK AH WAGEMANS, AND BOB JJ VAN HILTEN. *Ambulatory quantitative assessment of body position, bradykinesia, and hypokinesia in Parkinson's disease*. Journal of Clinical Neurophysiology **15**(3), 235–242 (1998).
- [30] DAPHNE GM ZWARTJES, TJITSKE HEIDA, JEROEN PP VAN VUGT, JAN AG GEELLEN, AND PETER H VELTINK. *Ambulatory monitoring of activities and motor symptoms in Parkinson's disease*. Biomedical Engineering, IEEE Transactions on **57**(11), 2778–2786 (2010).
- [31] CARLOS PÉREZ-LÓPEZ, ALBERT SAMÀ, DANIEL RODRÍGUEZ-MARTÍN, JUAN MANUEL MORENO-ARÓSTEGUI, JOAN CABESTANY, ANGELS BAYES, BERTA MESTRE, SHEILA ALCÁINE, PAOLA QUISPE, GERIOD Ó LAIGHIN, ET AL. *Dopaminergic-induced dyskinesia assessment based on a single belt-worn accelerometer*. Artificial Intelligence in Medicine (2016).

Complex Network Analysis for Activity Classification and Dyskinesia Detection

Complex network analysis is a new multidisciplinary approach combining graph theory and statistical measures that represent datasets derived from the real world. These datasets normally comprise networks with anatomical or functional connections. This type of analysis aims to characterise networks with a limited number of simple yet meaningful measures. Based on this simple principle, and the structure of our system composed of a set of IMUs that naturally presented a network of sensors, exploring this method of analysis seemed interesting for our application.

This chapter introduces the basic principles of graph theory, certain terminology and definitions, as well as the concepts associated with complex network analysis. Following that, we present the application of this method of analysis on the data collected, starting with the construction of the networks, the data processing approach based on the correlation between the different IMUs, the computation of network measures and finally the classification process.

The results obtained using this analysis method are then presented and discussed with respect to those obtained using the pattern recognition based method of Chapter IV. To our knowledge, this is the first time a network based analysis has been applied to a network composed of wearable sensors for the classification of activities and the detection of LID.

1 Graph Theory: Definitions and Methodology

Graph theory is a branch of discrete mathematics that has applications in a wide range of areas such as computing, social, and natural science. It was first applied in 1736 by the Swiss mathematician Leonhard Euler in order to find a solution to the Königsberg bridge problem, which consisted of finding a round trip that traversed each of the bridges of Königsberg exactly once [1]. By representing the problem as a graph, Königsberg showed that this conjecture was impossible. Since then, graph theory has seen many developments that allowed for a noticeable expansion in the areas of application [2].

The concepts of graph theory are considered simple and applicable to a wide variety of problems. As such, some basic terminology will be defined in this section to be used in the following chapter.

1.1 Definitions

A graph is a representation which is composed by a set of vertices (or nodes) and edges (or links) between these vertices. Any mathematical object consisting of points and connections between them can be considered a graph. Assuming that $V = \{v_1, v_2, \dots, v_i\}$ is a set of vertices, and $E = \{e_1, e_2, \dots, e_j\}$ is a set of edges formed by pairs of vertices, then the graph $G = (V, E)$ is a conceptual representation; an example of which is given in Figure V.1. In this case, the set of vertices V is composed of $V = \{v_1, v_2, v_3, v_4, v_5\}$,

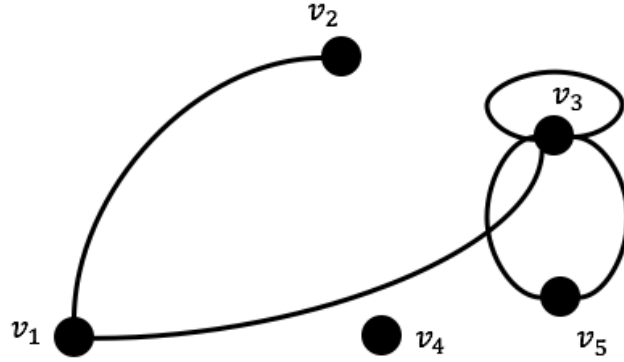


Figure V.1 – Example of a graph, formed by vertices and edges [3].

while the set of edges E is composed of $E = \{(v_1, v_2), (v_1, v_3), (v_3, v_3), (v_3, v_5), (v_5, v_3)\}$. The set of edges E can also be expressed as $E = \{e_1, e_2, e_3, e_4, e_5\}$, where $e_1 = (v_1, v_2)$, $e_2 = (v_1, v_3)$, and so on.

For any graph G , assume that u and v are two vertices. Certain terminology is commonly used when describing graphs, and is briefly introduced below:

- The two vertices u and v are considered to be *end* vertices of the edge $e = (u, v)$, and edges having the same end vertices are considered to be *parallel*.
- An edge formed by the same vertex, $e = (v, v)$, is known as a *loop*.
- A graph with no *parallel* edges or *loops* is said to be a *simple* graph, while a graph with no edges is said to be an *empty* graph, and a graph with no vertices is said to be a *null* graph.
- *Adjacent* edges are those who share a common *end* vertex, while *adjacent* vertices are those connected by an edge.

In the example shown in Figure V.1, the terminology therefore applies as:

- v_3 and v_5 are vertices of $e_5 = (v_5, v_3)$.
- $e_4 = (v_3, v_5)$ and $e_5 = (v_5, v_3)$ are *parallel*, while $e_3 = (v_3, v_3)$ is a *loop*.
- This graph is not considered to be *simple*.

- $e_1 = (v_1, v_2)$ and $e_2 = (v_1, v_3)$ are *adjacent*, and v_1 and v_2 are *adjacent*.

The previous terminology lists only a few simple concepts of graphs that are relevant to the analysis performed in this chapter. The field of graph theory is based on many complex theorems that are detailed in several references such as [4–6].

1.2 Directed Graphs and Weighted Graphs

A directed graph is defined as a graph constructed by vertices that are connected by directed edges. Given a directed graph $G = (V, E)$, where V is the set of vertices and E is the set of edges, the difference between this graph and a usual graph is that the elements of E are now ordered pairs. Figure V.2 shows an example of a directed graph, where E is now expressed as:

$$E = \{e_1, e_2, e_3, e_4, e_5\} = \{(v_1, v_2), (v_1, v_3), (v_3, v_3), (v_3, v_5), (v_5, v_3)\} \quad (\text{V.1})$$

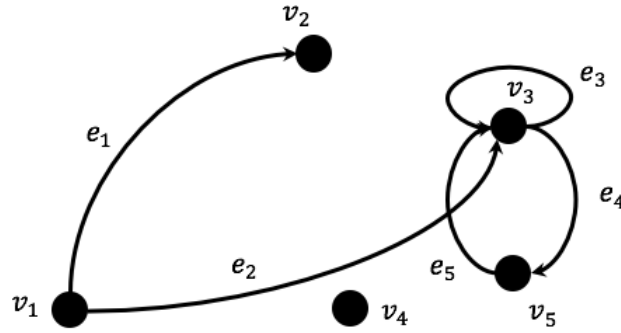


Figure V.2 – Example of a directed graph, formed by vertices and directed edges [3].

A weighted, or edge-weighted, graph is a pair (G, w) , where $G = (V, E)$ is a graph and $w : E \rightarrow \mathbb{R}$ is the corresponding weight function. In many applications, the edges of a graph are associated with a weight value, which is otherwise known as the "cost". Both directed and undirected graphs can have weighted edges, which can represent for example the measure of a length or the cost of moving from one point to another.

2 Complex Network Analysis

2.1 Definitions

Complex networks analysis is an approach that combines graph theory and statistical measures [7]. This type of analysis is concerned with real-life networks, which are usually characterized by an irregular and complex structure that continuously evolves with time [8]. The reason behind its growing popularity is that any discrete structure that results from the relationships between elements of real-life networks

can be represented by a series of graphs. This is followed by topological characterisation of the obtained graphs, which is the process of representing each graph by a set of informative measures [9]. One application of complex networks analysis is the use of these measures to identify different classes of a structure. The interest of applying this approach lies in its ability to define structural and functional properties of a network with dynamical units through simple measures that characterise the topology of the network.

Complex networks are networks whose structure is irregular, complex and dynamically evolving with time. These networks offer a more accurate representation of real world problems. In graph theory, a network is composed of a set of vertices, which will be referred to as nodes from this point on, and edges, which will be referred to as links from this point on, between them. In the following sections, basic network characteristics and measures will be introduced.

2.2 Network Measures: Mapping from a Complex Network to a Feature Vector

The topology of a network can be described by a wide variety of measures that reveal structural and functional characteristics about the network. It is worth noting that the suitability of different measure is reliant on the application at hand, so we are not able to deem certain measures to be more appropriate than others.

Real networks, or networks derived from real data, are characterised by certain structural features, that are not explained by uniformly random connectivity. In many cases, these networks are dynamic, undergoing continuous topological changes as well. Network measures therefore provide a valorisation method of the network's natural structure and its dynamic topological changes.

While the main purpose of these measures includes providing a topological characterisation of the network, many applications have used them to identify different categories of structures, enabling the classification of different structures.

Network measures originally included simple quantitative techniques of the network's structure, but have been evolving significantly. The advances in machine learning techniques as well as big data processing capabilities have led to the incorporation of new measures with higher complexity to derive specific information from the structure. In the most part, these measures can be categorised as distance-based measurements, clustering coefficients, degree correlations, entropies, centrality, subgraphs, spectral analysis, community-based measurements, hierarchical measurements and fractal dimensions. These measures are explained in detail and reviewed in several publications such as [7, 10–15]. In the following sections, only the measures used in the performed analysis will be introduced.

Through the calculation of network measures, informative and quantitative features of the network can be characterised, analysed and related to the network's respective dynamics. Different measures allow for different investigations of the network, that include representation, characterisation, classification and modelling.

Any suitable set of network measures used to describe a complex network structure forms a feature

vector, μ , which is a representation of the original structure. A mapping from a complex network structure into a feature vector $\mu = [\mu_1, \mu_2, \dots, \mu_M]$, where M is the number of computed network measures, is shown in Figure V.3.

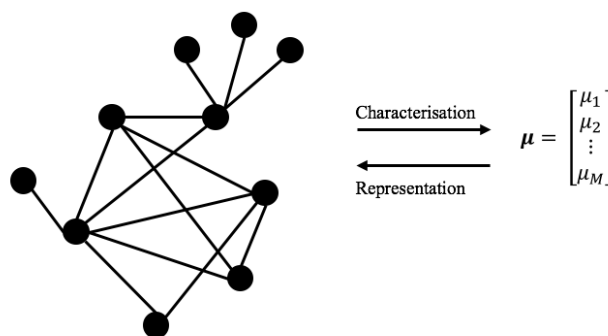


Figure V.3 – Mapping from a complex network to a feature vector, which is used to obtain a characterisation of the network through a set of measures. If the mapping is invertible, then it is considered a complete representation of the original structure [9].

The choice of measurements to obtain the most meaningful and informative characterisation of a network is highly dependant on the application. There is an unlimited number of topological measurements that are often correlated depending on the application at hand, hence introducing repetition and noise into the characterisation. Different approaches, such statistical testing and de-correlation methods, have been proposed to deal with this issue.

For our application, we extract a number of network measures. The objective is to determine the set of network measures directly related to the constructed networks. This process is explained in detail in the following sections.

3 Methods

In this section, we present the construction of a structural connectivity network based on the correlation between the set of IMUs positioned at different parts of the body. The set of IMUs comprises the nodes of the constructed network, and each node represents the movement data collected from the body part at which the IMU is placed. The correlation between the different body parts acts as the links between the nodes, representing the relationship between pairs of nodes while the individual performs various movements.

The performed analysis, detailed in this section, is based on the connectivity matrices obtained using the data collected from healthy individuals and PD patients. Firstly, the construction of the networks relating to the healthy individuals and PD patients are explained. Following that, network representation is performed by means of circular graphs and the selected network measures are computed. A statistical significance test is performed on the computed measures in order to determine the optimal

set of measures relating to each constructed network. Finally the retained measures are used for the classification of activities, in the case of healthy individuals, and dyskinesia detection, in the case of PD patients.

3.1 Network Construction

Two separate datasets were considered for the construction of the complex networks in the case of HS and PD patients. With the objective of simplifying the constructed networks, processing was limited to a single type of sensor for all IMUs (for example, only the low noise accelerometer). In order to determine the sensor data that provided the most relative information in the case of activity classification and in the case of dyskinesia detection, a number of tests were conducted. During these tests, we compared the classification performance obtained for each network while varying the considered sensor in the IMUs.

In the case of HS, it became evident that the data collected from the low noise accelerometer of each IMU was most relevant to the classification of activities. Similarly, testing the performance of the different sensors located in the IMUs showed that for dyskinesia detection, in the case of PD patients, the gyroscope proved to be most relevant. Two specific networks were constructed to respond to our objectives of activity classification and dyskinesia detection:

- **Activity Classification Network:** a network constructed based on the data collected from the low noise accelerometer of each IMU positioned on the nine HS. Each low noise accelerometer provides acceleration measures in three channels (x , y , and z). Each channel of the low noise accelerometers is taken to be a node, and therefore the constructed network is composed of $N_1 = 18$ nodes (3 channels x 6 IMUs).
- **Dyskinesia Detection Network:** a network constructed based on the data collected from the gyroscope of each IMU positioned on the three PD patients. Each gyroscope provides angular velocity measures in three channels (x , y , and z). Similarly to the above, each channel of the gyroscopes is taken to be a node, and therefore the constructed network is composed of $N_2 = 18$ nodes (3 channels x 6 IMUs).

3.2 Data Processing

The processing steps included in the analysis of the constructed networks is shown in Figure V.4, and will be detailed in this section.

For the Activity Classification Network, the analysis is based on the data collected from the HS, and specifically from the three-channel low noise accelerometer in each IMU. While for the Dyskinesia Detection Network, the analysis is based on the data collected from the PD patients, and specifically from the three-channel gyroscope in each IMU. The following steps of processing are identical in both networks and will therefore be introduced only once.

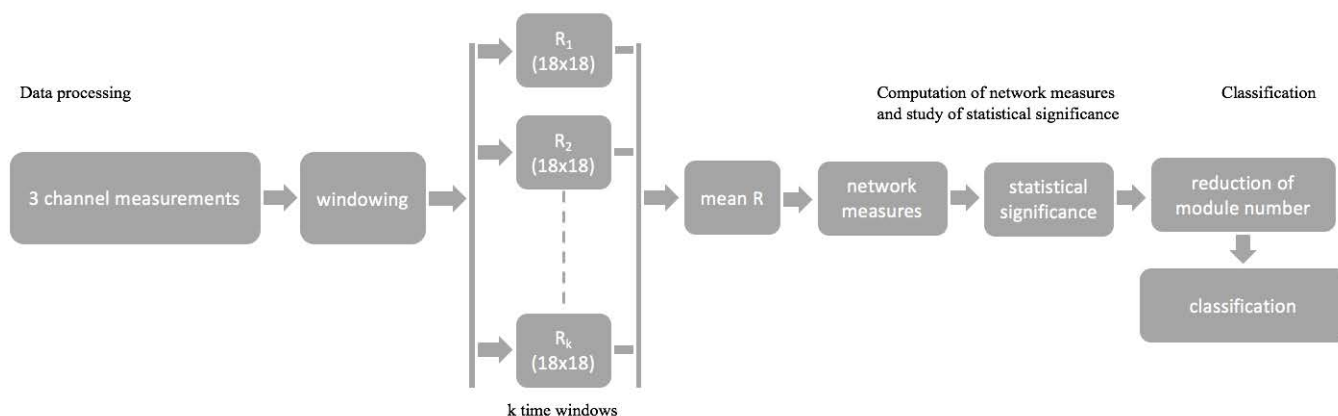


Figure V.4 – Flow chart representing the steps carried out in order to classify the activities performed by HS in the case of Activity Classification Network, or to detect presence of LID in PD patients in the case of Dyskinesia Detection Network.

Firstly, the raw data extracted from the three-channel sensor of each IMU is segmented into $\Delta t = 7$ second time windows with 50% overlap, as described in section 1.1, chapter IV. The linear pairwise correlation is then calculated between each pair of nodes, and acts as the weight function of the network, where the link between each pair of nodes is represented by the correlation coefficient:

$$R_{XY} = \text{corr}(\mathbf{X}, \mathbf{Y}) = \frac{\text{cov}(\mathbf{X}, \mathbf{Y})}{\sigma_X \sigma_Y} = \frac{E[(\mathbf{X} - \mu_X)(\mathbf{Y} - \mu_Y)]}{\sigma_X \sigma_Y} \quad (\text{V.2})$$

where \mathbf{X} and \mathbf{Y} represent vectors of raw data collected from any pair of nodes, and μ_X , μ_Y , and σ_X , σ_Y represent the means and standard deviations of those nodes respectively. No time lag was introduced, compared to the precious chapter, since experiments showed that it was often close to zero.

For each subject, k correlation matrices are therefore computed per category, where k is equal to the number of time windows obtained per category. An example of this matrix is shown in Figure V.5, where each column represents a node, and the elements of the matrix are the correlation coefficients obtained between each pair of nodes.

The correlation coefficient between any node and itself is equal to 1, hence the diagonal of the matrix is always equal to 1. The triangular areas shown in the figure signify that the upper and lower triangular areas of the matrix are equal. Hence, the calculated weight matrix is undirected, since there is no difference between the link $(Node1, Node2)$ and $(Node2, Node1)$.

In the Activity Classification Network, we define four categories corresponding to the classes of activities performed by the HS. On the other hand, in the Dyskinesia Detection Network, we define two categories corresponding to the presence or absence of dyskinesia.

In order to obtain a more coherent and informative count of the correlation between the different nodes in each category, the connectivity matrix is computed as the average correlation matrix obtained over the total number of correlation matrices per category. In other words, for the duration of a single

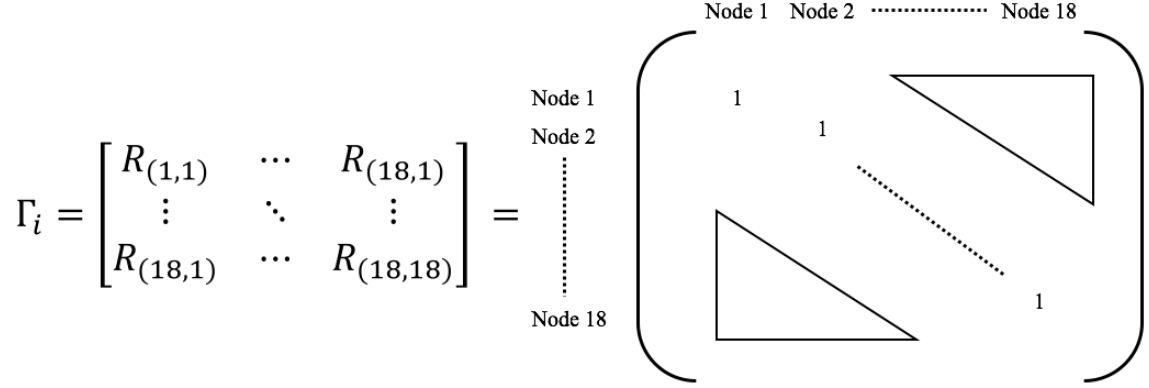


Figure V.5 – An example of the correlation matrix calculated for a segment of $\Delta t = 7$ seconds between the nodes.

activity which is approximately 2 minutes (in the case of HS), we obtain an average of 32 correlation matrices corresponding to the segmented time windows. However, each of these correlation matrices describes a small portion of the activity performed and therefore provides only a small aspect of the true correlation between the IMUs during the performance of the activity. Therefore, in order to properly assess the correlation between the IMUs over the entire duration of the activity, the mean correlation matrix is computed and serves as the connectivity matrix for the network representation and computation of measures.

3.3 Network representation and computation of measures

Network Representation

After obtaining the weight matrix, or the connectivity matrix, for each subject's data, the following step consists of representing the obtained networks and observing the topological features and differences between different classes, both in the Activity Classification Network as well as the Dyskinesia Detection Network. The graphical representation of the network is done using a circular graph [16]. This type of graph is a visualisation of the network where the nodes are placed on the circumference of a unit circle, and the links between nodes are represented by curved lines.

In this visualisation, link weights are represented by the thickness of the drawn lines. The nodes are ordered as seen in Figure V.6, and it should be noted that node order has no effect on the computation of network measures. However, it can be important for network visualisation in certain cases.

Nodes are labeled based on IMU position and sensor channel. In the case of the Activity Classification Network, the node "*AnkleX*" represents the ankle module's low noise accelerometer *X* channel, and node "*ArmZ*" represents the arm module's low noise accelerometer *Z* channel, and so on. In the case of the Dyskinesia Detection Network on the other hand, the node "*AnkleX*" represents the ankle module's gyroscope *X* channel, and the node "*ArmZ*" represents the arm module's gyroscope *Z* channel, and so

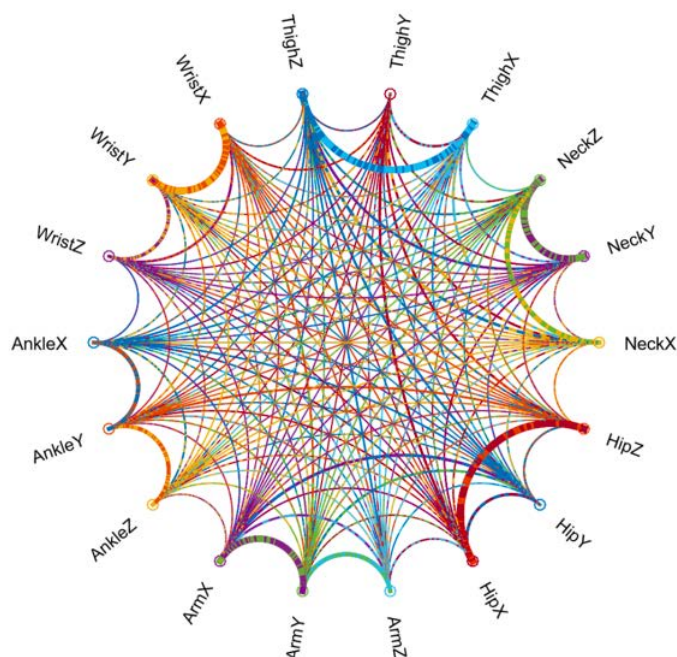


Figure V.6 – Example of the complex network representation using a circular graph showing the nodes (module position and channel), the links (correlation between the channels) and the weights (correlation coefficients represented by link thickness).

on.

For the Activity Classification Network, visualisation provides an interesting method of observing the difference in correlation between different body segments for different activity classes. In Figure V.7, an example of the visualisation of two networks belonging to the same subject while performing the activity of standing (A) and walking (B) is presented. Differences between the two networks are difficult to discern visually but can be observed, specifically between the Neck, Hip and Arm modules.

In the case of the Dyskinesia Detection Network, an example of the visualisation obtained from a single PD patient is shown in Figure V.8. In visualisation (A), the patient is performing the activity of Lying in the absence of LID, while in (B) there is presence of LID. Some differences between these two networks can be observed in the Arm, Hip, Neck and Thigh IMUs.

Network Measures

In order to quantify the topological differences between the different classes in both the Activity Classification and the Dyskinesia Detection Networks, the computation of network measures is required. These measures are computed for each individual network element, which are the nodes and links. This leads to the quantification of the connectivity profiles associated with these elements, and reflects how these elements are embedded in the network.

However, network measures of all individual elements comprise a distribution which provides a more

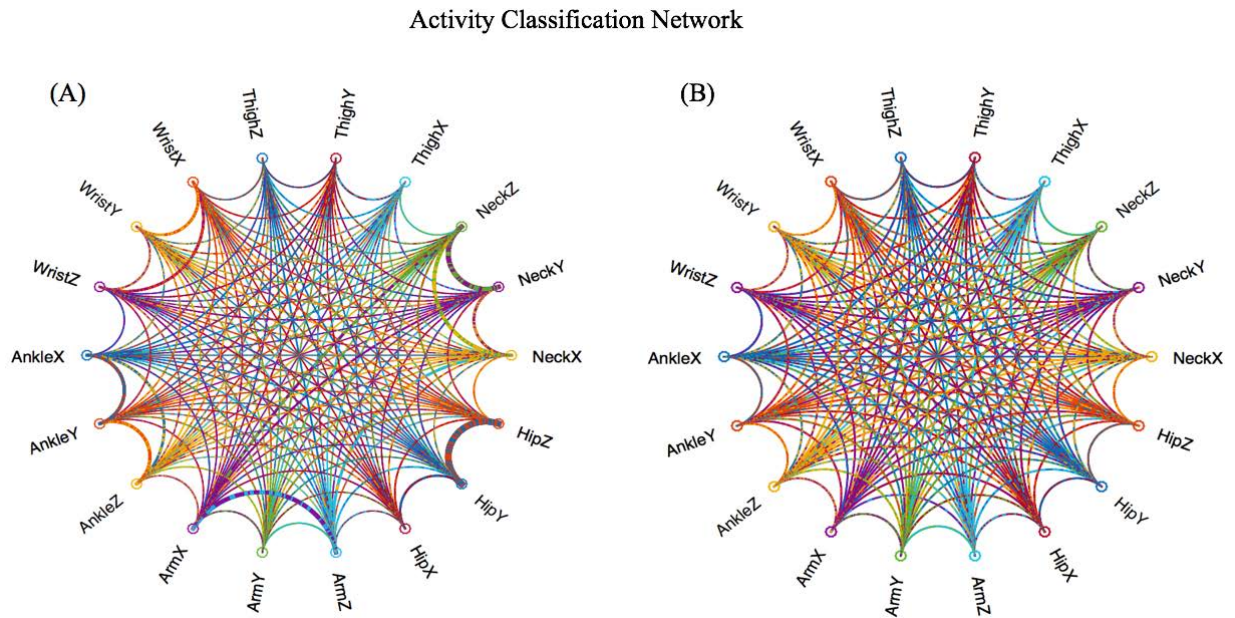


Figure V.7 – Example of the circular graph visualisation for the Activity Classification Network taken from the same individual while performing the activities of standing (A), and walking (B).

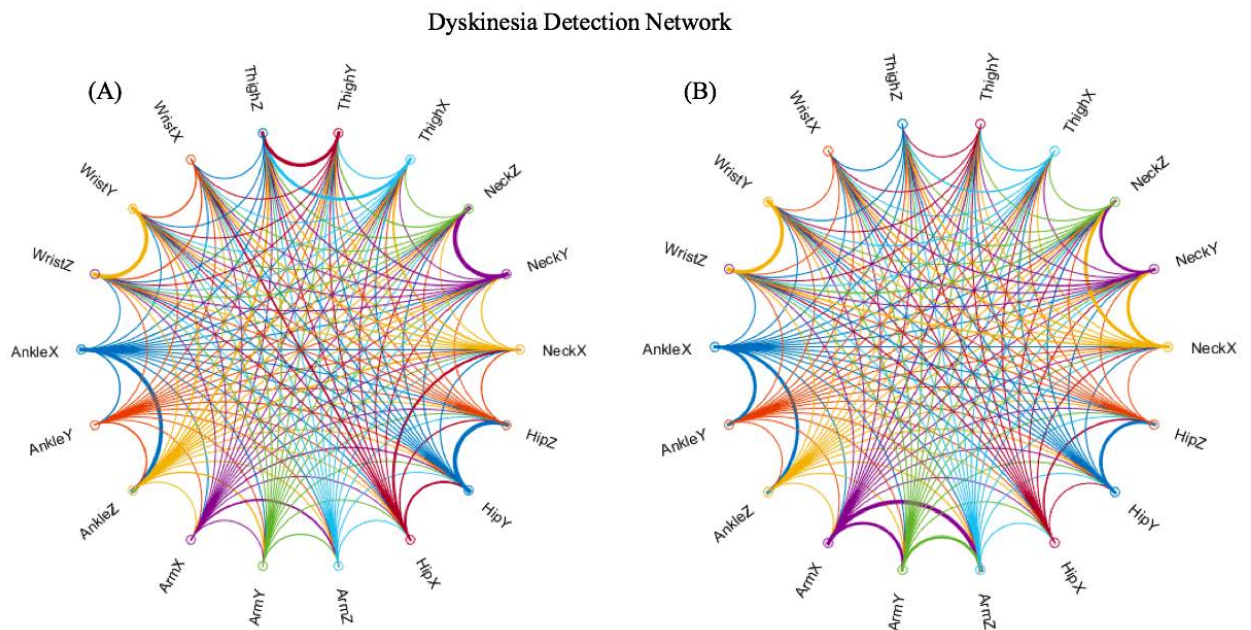


Figure V.8 – Example of the circular graph visualisation for the Dyskinesia Detection Network taken from the same PD patient while performing the same activity of Lying in the absence of LID (A), and in the presence of LID (B).

accurate and global representation of the network. This distribution is most commonly characterised by its mean, which becomes essential in distinguishing between different classes of networks. Therefore, in order to proceed with the classification process based on the computed network measures, the mean connectivity matrix for each subject's data in each specific category is first calculated. The following network measures are computed for each subject's mean connectivity matrix:

- **Degree:** the degree of a node is defined to be the number of links connected to it. This quantity represents the connectivity property of a node, revealing information on how it links to the rest of the network, or more specifically, revealing the importance of the individual node in the network. Assuming that a_{ij} is the connection status between nodes i and j such that $a_{ij} = 1$ if the link (i,j) exists and $a_{ij} = 0$ otherwise, then the degree of a single node i is computed as:

$$d_i = \sum_j a_{ij} \quad (\text{V.3})$$

- **Strength:** the strength of a node is defined as the sum of weights of the links connected to it. Assuming that r_{ij} is an element of the undirected weight (connectivity) matrix, then the strength of a single node i is computed as:

$$s_i = \sum_j r_{ij} \quad (\text{V.4})$$

- **Density:** the density of a node is defined as the ratio of present links to a node over the total number of possible links. Assuming that N is the total number of nodes in the network, and L is the number of links present in the individual node, then the density is computed as:

$$den_i = \frac{L}{\frac{N^2 - N}{2}} \quad (\text{V.5})$$

- **Clustering Coefficient:** the clustering coefficient of a node is the quantification of the number of connections a node has with its nearest neighbours as a proportion of the total number of possible connections. If the neighbouring nodes to an individual node also form connections between themselves, then they appear to form a cluster. For a weighted connectivity matrix, the clustering coefficient is the average intensity of triangles around a network and is computed as:

$$C = \frac{1}{N} \sum_i \frac{2t_i}{d_i(d_i - 1)} \quad (\text{V.6})$$

where t_i is the weighted geometric mean of the triangles around node i .

- **Modularity:** this value measures the density of links inside communities to links outside communities. In large scale networks, the optimal community structure is a subdivision of the

network into non-overlapping groups of nodes, such that the number of "within-group links" is maximised and the number of "between-group links" is minimised. For a weighted connectivity matrix, the Modularity is computed as:

$$Q = \frac{1}{l} \sum_{i,j} (r_{ij} - \frac{d_i d_j}{l}) \delta_{m_i, m_j} \quad (\text{V.7})$$

where m_i is the module containing node i , and $\delta_{m_i, m_j} = 1$ if $m_i = m_j$, and 0 otherwise.

- **Community Structure:** this property is based on a fast and accurate multi-iterative generalisation of the Louvain community detection algorithm [17]. It is considered that the optimal community structure is obtained when the network is subdivided into non-overlapping groups of nodes, such that the number of within group links is maximised and the number of between-group links is minimised. The Louvain community detection algorithm is used to extract communities from large networks and aims to optimise the value of Modularity as the algorithm progresses.

The computation of the listed network measures results in a total of 108 measures (18 nodes x 6 IMUs) for the entire network, in both the Activity Classification and Dyskinesia Detection Networks. In other words, the feature set is composed of 108 measures for each observation, as opposed to the previously computed 576 features in the pattern recognition based analysis of Chapter IV.

3.4 Statistical Significance and Classification

Each individual networks is a representation of the global and local connectivity of the system of monitoring. The computed network measures reveal aspects of functional and structural connectivity between the different IMUs, quantify the importance of individual IMUs, and characterise the relationships between the IMUs under different conditions.

However, the values of many network measures are influenced by network characteristics, and in certain cases are considered to be irrelevant or highly correlated, which could affect the classification process. As such, statistical significance methods are commonly implemented in order to test the importance of the computed measures.

In this case, the Kruskal-Wallis statistical test [18] was implemented. The Kruskal-Wallis test is a rank based non-parametric test which is also referred to as "one way ANOVA on ranks". This method allows to test whether samples originate from the same distributions without relying on specific distributions. This ensures the accuracy of the obtained significance even if the network fails to meet parametric conditions of validity.

In the case of the Activity Classification Network, the test is implemented by comparing the computed measures of each node with respect to the different activity classes. The resulting p-value leads to assuming one of two hypotheses:

- Null Hypothesis H0: The observations belong to the same population.

- Alternative Hypothesis H_a : The observations belong to different populations.

Where the population in this case represents the activity class.

In the case of the Dyskinesia Detection Network, the test is implemented by comparing the computed measures of each node with respect to the different motor states, which are dyskinetic or non-dyskinetic. The resulting p-value leads to assuming one of two hypotheses H_0 or H_a , where the population in this case represents the motor state class.

Based on the obtained results, only the network measures considered to be statistically significant in each case are retained for the classification process. This, in turn, results in minimising the feature set, removing noise in order to ensure better classification, and finally allows for the reduction of the number of IMUs in the monitoring system.

The reduced feature set of statistically significant network measures is then introduced for the classification phase using a RF classifier. This type of classifier was retained for this analysis since it provided the best performance in the pattern recognition based analysis applied in Chapter IV.

4 Results

4.1 Activity Classification Network

Healthy Subjects Dataset

The data collected from the same nine healthy individuals, and that was used for the analysis in Chapter IV, is also used in this case. The HS performed the acquisition protocol on two separate days, resulting in two sessions per subject. However, due to data loss, the data collected from the first sessions of subjects #6 and #9, as well as the data collected from the second session of subject #8 are discarded. Hence, the total number of recordings per activity over the 2 sessions is 15 (2 sessions x 9 subjects - 3 sessions).

The mean correlation matrix is computed for each subject's activity data per session and represents the Activity Classification Network's connectivity matrix. Therefore, a total of 15 connectivity matrices (18 x 18) were obtained per type of activity. Following that, the network measures for each connectivity matrix are computed. The resulting feature matrix consists of 60 observations x 108 measures (4 activities x 15 observations x 108 measures).

Statistical Significance

Prior to moving on with the classification process, the computed network measures are tested for statistical significance. In the Kruskal-Wallis H test, significance level α is set at 0.05 and the p-value is obtained for each of the network measures. This results in a subset of 22 network measures having p-values lower than the significance level α and are considered to be statistically significant.

However, when considering methods that deal with multiple comparison such as the Kruskal-Wallis method, it is common to adjust the significance level α in order for the probability of obtaining at least one significant result due to chance is lower than the desired significance level. For that, we apply a Bonferroni correction [19] on the significance level α by dividing the original value by the total number of comparisons performed, which is equal to 18, the total number of nodes. The new significance level is $\alpha_{corrected} = 0.0028$ and the surviving subset of measures with p-values lower than $\alpha_{corrected}$ consists of 10 measures instead of the original 22 (Table V.1). Measures corresponding to the Strength, Clustering Coefficient, Structure and Modularity were found to be statistically significant prior to the Bonferroni correction, while after the correction, only measures corresponding to the Strength and Clustering Coefficient were retained.

Table V.1 – Statistically Significant Network Measures for Activity Classification.

Measure	Statistically Significant compared to α	Statistically Significant compared to $\alpha_{corrected}$
Strength	AnkleY, NeckY, NeckZ, ThighX, ThighY, ThighZ, WristX, WristY, WristZ	NeckX, NeckZ, ThighX, ThighY, ThighZ
Clustering Coefficient	AnkleX, AnkleY, AnkleZ, ArmX, ArmY, HipY, NeckZ, ThighX, ThighY, ThighZ, WristZ, ArmY,	AnkleX, AnkleY, ThighX, ThighY, ThighZ
Modularity	ThighZ	
Structure	ArmY	

Ranking of Network Measures and Reduction of Modules

In order to explore the relative importance of the subset of measures, ReliefF feature selection method is used for ranking. The weights of the subset of measures are ranked in decreasing order in Figure V.9.

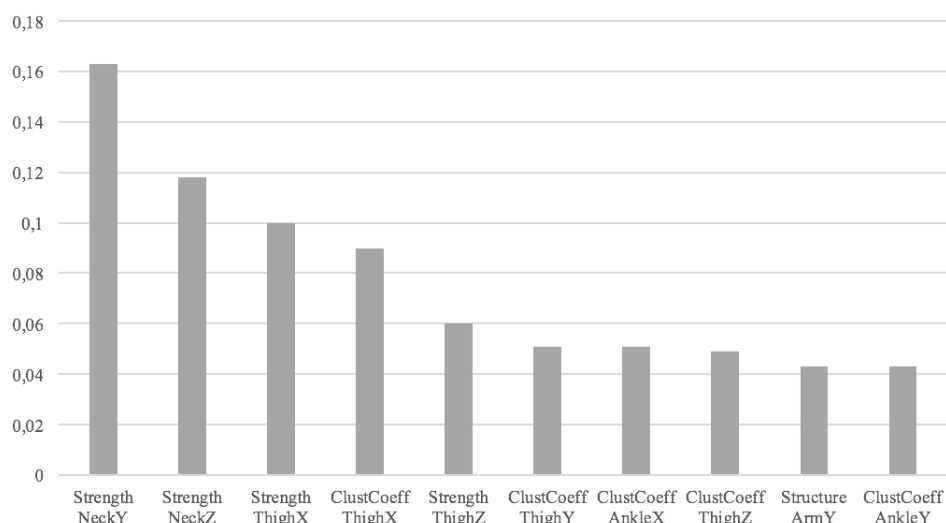


Figure V.9 – Ranking of network measures computed for the Activity Classification Network in decreasing order using the ReliefF feature selection method.

In order to determine a suitable subset of measures while minimising the number of modules, principal component analysis (PCA) was performed on different combinations of the listed measures.

PCA is a statistical procedure that aims to identify strong patterns in a dataset and is often used to visualise the data in an easily interpretable way [20]. This procedure is mainly used when dealing with high dimensional data, in which visualisation can be difficult. Its major advantage is reducing the dimensionality of the data by transforming it into a new coordinate system of a smaller number of uncorrelated variables, called principal components. In turn, this allows the identification of meaningful underlying variables. A common way of visualising the data after performing PCA is through a biplot, which is a plot that shows the principal components, represented by the axes, and the observed variables, represented by vectors. This plot allows the visualisation of the magnitude and sign of each variable's contribution to the first two components, and how each observation is represented in terms of those components.

According to the results of the ReliefF feature selection, it was observed that measures corresponding to the Neck and Thigh IMUs held greater importance in this case for distinguishing between the different activity classes. Therefore, the projection of observations was done while using different combinations of the highest ranked measures and the obtained clusters were observed. In Figure V.10, the projection of individuals shows grouping into distinct clusters belonging to each category of activities. Based on this representation, the first five ranking network measures are considered for

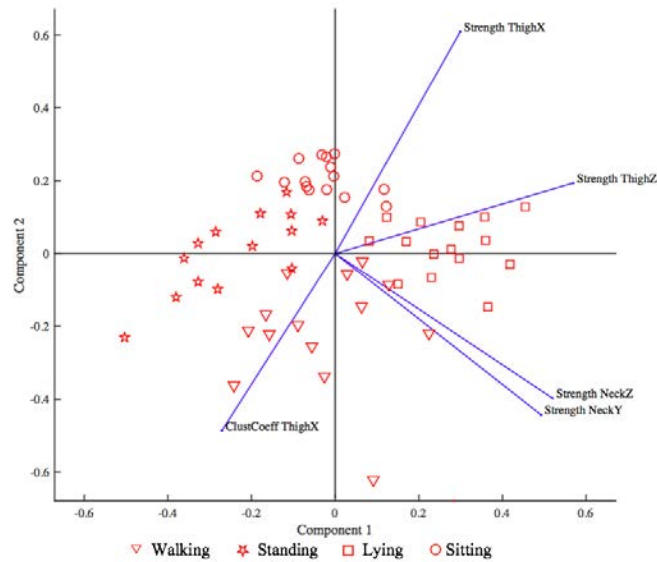


Figure V.10 – Biplot showing the projection of observations belonging to the four activity classes along with the selected network measures. Each group of observations belonging to the same category forms a distinct cluster.

classification. This signifies the reduction of the total number of modules in the system to the Neck and Thigh modules only.

Activity Classification

The classification strategy applied in this analysis method is based on splitting the HS data into a training and a testing set. The reduced feature set matrix is composed of 60 observations x 5 measures, and the HS data corresponding to Day 01 is used as the training set (TrainSet), while the data corresponding to Day 02 is used as the testing set (TestSet). A bootstrap validation method is applied with 100 repetitions in order to ensure robustness of results.

As a measure of performance, sensitivity, specificity and accuracy for each class of activities is computed similar to Chapter IV. Table V.2 shows an example of the contingency table obtained for one iteration, while Table V.3 shows the obtained performance for this iteration.

Table V.2 – An Example of the Contingency Table Obtained for the TestSet.

Activity	Walking	Standing	Lying	Sitting
Walking*	6	1	0	0
Standing*	1	6	0	1
Lying*	1	0	8	0
Sitting*	0	1	0	7

Table V.3 – Performance Measures Obtained for the TestSet.

Activity	Walking	Standing	Lying	Sitting
TP	6	6	8	7
FP	1	2	1	1
FN	2	2	0	1
TN	23	22	23	23
Sensitivity	75.0	75.0	100	87.5
Specificity	95.8	91.6	95.8	95.8
Model Accuracy	84.3			

The overall performance of the classifier is shown in Table V.4. The mean accuracy for activity classification was obtained at 84.6% with sensitivity and specificity values ranging from 73.6 – 97.3% and 93.3 – 95.8%. Although this performance is quite promising, it is however weak compared to the 98.5% overall accuracy obtained using the initial method of analysis presented in Chapter IV.

Table V.4 – Overall Performance Measures (%) Obtained for the Activity Classification Network.

Activity	Walking	Standing	Lying	Sitting
Sensitivity	73.6	75.1	97.3	92.6
Specificity	95.0	93.3	95.3	95.8
Model Accuracy	84.6			

4.2 Dyskinesia Detection Network

PD Patients Dataset

Each of the PD patients had performed the protocol session at least twice, ensuring the acquisition of one dyskinetic and one non-dyskinetic session. In order to have data in both motor states for each of

the three PD patients, the four classes of activities were combined. Only one of the patients did not perform the activity of Standing in one of the sessions. The total number of observations for the PD patients is therefore 23 (3 patients x 2 sessions x 4 activities - 1).

The mean correlation matrix is computed for each PD patient's session data and represents the Dyskinesia Detection Network's connectivity matrix. A total of 23 connectivity matrices (18 x 18 nodes) were obtained, of which 7 are labeled as dyskinetic and 16 are labeled as non-dyskinetic. The network measures for each connectivity matrix are then computed resulting in a feature matrix of dimension 23 observations x 108 measures.

Statistical Significance

Similar to the first network, the computed network measures are also tested for statistical significance. In this case, however, the network measures are being tested for their ability to distinguish between dyskinetic and non-dyskinetic observations.

The significance level α of the Kruskal-Wallis H test is initially set at 0.05 and the p-value is obtained for each of the computed network measures. This results in a subset of 6 network measures having p-values lower than α and therefore considered to be statistically significant. However, after applying the Bonferroni correction, none of the measures' p-values survived the new significance level $\alpha_{corrected} = 0.0028$. This is common in complex network analysis, since the Bonferroni correction forces harsh standards. As such, the obtained subset of 6 network measures (Table V.5) is retained for the following steps. The selected measures correspond to the Strength attribute of different IMUs.

Table V.5 – Statistically Significant Network Measures for Dyskinesia Detection.

Measure	Statistically Significant compared to α
Strength	ArmZ, HipY, NeckY, ThighY, ThighZ, WristY

Ranking of Network Measures and Reduction of Modules

The ReliefF feature selection method is then applied in order to rank the subset of remaining measures by importance, as seen in Figure V.11. Since the ranking of the selected measures does not imply a reduction of the number of modules, PCA is again used in order to visually identify the best combination of measures that results in grouping of observations into two clusters, a dyskinetic and a non-dyskinetic one. In Figure V.12, two separate clusters are formed by the dyskinetic and non-dyskinetic observations when considering only the first three ranked measures. Therefore, based on this representation, only these measures which correspond to the Arm, Hip and Thigh, are considered for the classification phase. These results are complementary to those obtained in the previous chapter, where the most important module positions for the detection of dyskinesia were determined to be the Ankle, Hip and Thigh modules. This shows that the relationship between the modules could be exploited to reinforce the decision process and produce better dyskinesia detection outcome.

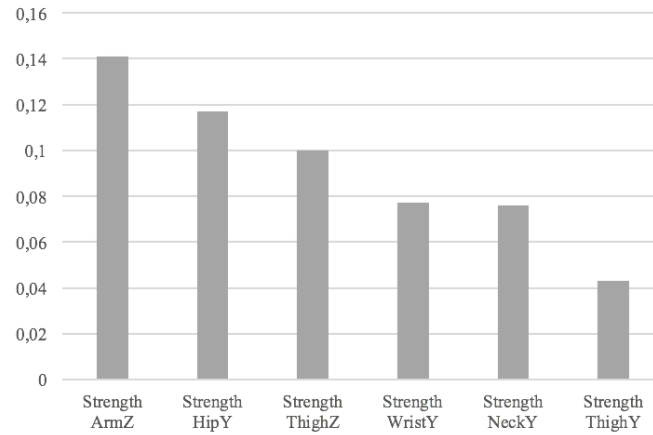


Figure V.11 – Ranking of network measures computed for the dyskinesia detection network in decreasing order using the ReliefF feature selection method.

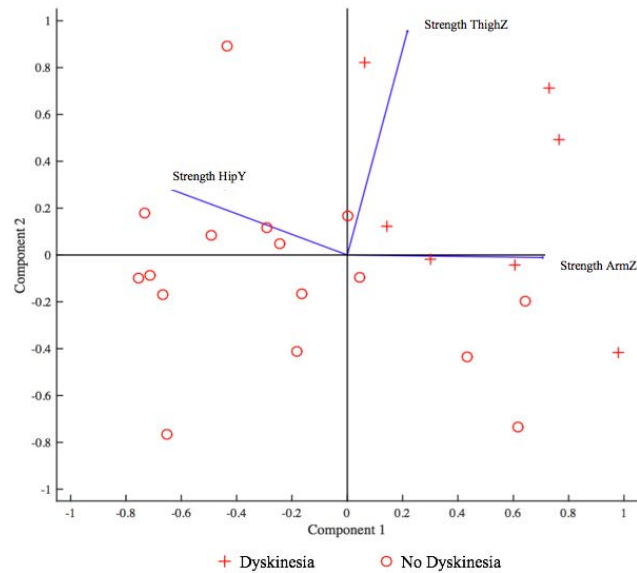


Figure V.12 – Biplot showing the projection of observations belonging to the two motor states, dyskinetic and non-dyskinetic, along with the selected network measures. Each group of observations belonging to the same category forms a somewhat distinct cluster.

Dyskinesia Detection

Due to the low number of observations, training and testing of the classifier is done by splitting the dataset into 80% – 20% for the training set (TrainSet) and testing set (TestSet) respectively. Although the low number of observations introduces limitations that might affect the classification outcome, the analysis done here is considered to be preliminary and is to be validated by a larger number of patients.

The performance of the classifier is assessed by computing the sensitivity, specificity and accuracy as in the previous section. An example of the contingency table for the TestSet and its corresponding performance measures is shown in Table V.6.

Table V.6 – An Example of the Contingency Table Obtained for the TestSet and the Computed Performance Measures.

Motor State	Dyskinesia	No Dyskinesia
Dyskinesia*	2	0
No Dyskinesia*	1	2
Sensitivity	66.6	
Specificity	100	
Model Accuracy	80.0	

The overall accuracy of the classifier in detecting dyskinetic instances is 78.6%, with sensitivity and specificity values at 58.6% and 87.8%. In comparison to the initial method of analysis presented in Chapter IV, the performance obtained here has also diminished. This performance can be explained by the low sample size which can greatly affect the classifier’s learning. As such, these results can be considered as encouraging, but further testing must be done in order to validate this method.

4.3 Overcoming the Limitation of a Low Number of Observations

One of the main issues faced with this type of analysis is the low number of observations in both the Activity Classification Network and the Dyskinesia Detection Network. The large difference in the size of the datasets corresponding to the HS and PD patients’ data, when compared to the previous analysis of Chapter IV, is due to the computation of the connectivity matrix as the mean of the total number of correlation matrices obtained for each subject per category (whether the category is the activity being performed or the motor state of the patient)¹.

In order to overcome this limitation, we propose increasing the obtained number of observations by computing the connectivity matrix as the mean of the correlation matrices obtained per minute for each subject per category. In this case, the processing method applied is modified with an additional step, as seen in Figure V.13.

¹The number of observations is increased in this case. However, we are aware that there exists bias due to the fact that inevitable correlation might exist between the segments coming from the same patient.

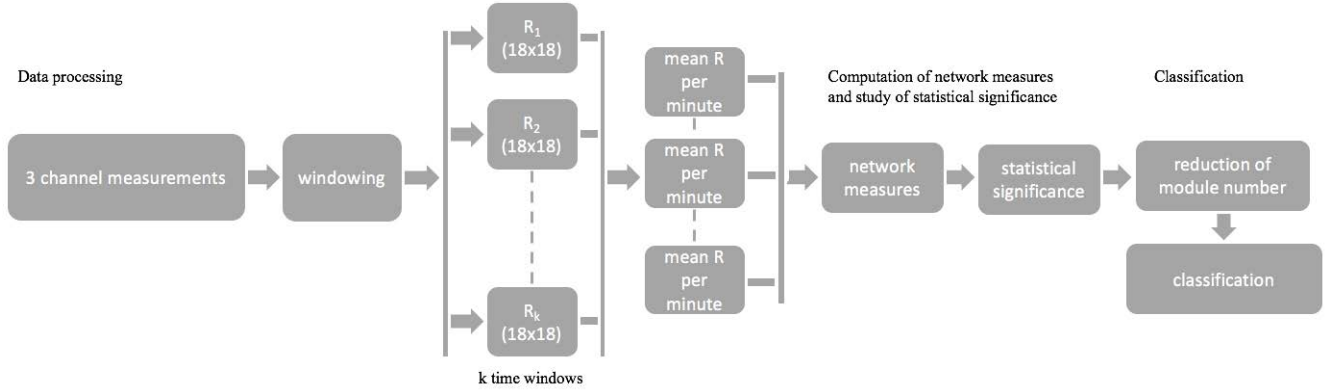


Figure V.13 – Flow chart representing the steps carried out in order to classify the activities performed by HS in the case of Activity Classification Network, or to detect presence of LID in PD patients in the case of Dyskinesia Detection Network. In this case, the total number of observations is increased by computing the mean correlation per minute instead of the the mean correlation of the total number of observations.

Activity Classification Network

The computation of connectivity matrix in this case is based on computing the mean correlation per minute of activity for each subject. As mentioned earlier, each subject performed a single type of activity for an average duration of 2 minutes. However, certain activities were repeated at the beginning and end of the protocol. Hence, the total number of observations obtained in this case is increased to 271 observations (Table V.7), as opposed to the 60 observations obtained originally.

Table V.7 – Number of Observations per Category for Healthy Subjects.

Connectivity Matrix	Walking	Standing	Sitting	Lying
Mean R	15	15	15	15
Mean R per Minute	53	45	84	89

The steps following the computation of the connectivity matrices were then repeated for the newly obtained connectivity matrices computed per minute of activity. The steps include the computation of the previously listed network measures and then performing the Kruskal-Wallis H test to determine a subset of measures considered to be statistically significant in distinguishing between the activities being performed.

By comparing the p-values obtained to a statistical significance level, $\alpha = 0.05$, we obtain a subset of 41 network measures that are considered to be statistically significant. However, by performing the Bonferroni correction, and comparing the obtained p-values to the corrected significance level $\alpha_{corrected} = 0.0028$, the subset of measures considered to be statistically significant is reduced to 29 network measures (Table V.8).

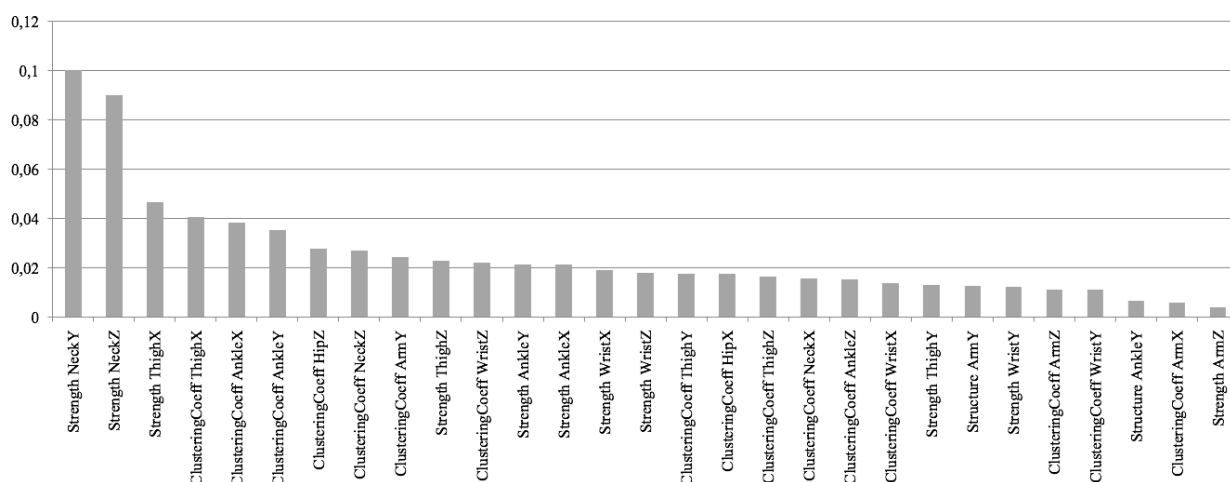
Similarly to the previous case, the remaining subset of 29 network measures considered to be statistically significant is then ranked by using the ReliefF feature selection method (Figure V.14). The results obtained show that the measures corresponding to the Neck and Thigh modules are the

Table V.8 – Statistically Significant Network Measures for Activity Classification for MeanR per Minute.

Measure	Statistically Significant compared to α	Statistically Significant compared to $\alpha_{corrected}$
Strength	AnkleX, AnkleY, AnkleZ, ArmX, ArmZ, HipY, HipZ, NeckY, NeckZ, ThighX, ThighY, ThighZ, WristX, WristY, WristZ	AnkleX, AnkleY, ArmZ, NeckY, NeckZ, ThighX, ThighY, ThighZ, WristX, WristY, WristZ
Clustering Coefficient	AnkleX, AnkleY, AnkleZ, ArmX, ArmY, ArmZ, HipX, HipY, HipZ, NeckX, NeckY, NeckZ, ThighX, ThighY, ThighZ, WristX, WristY, WristZ	AnkleX, AnkleY, AnkleZ, ArmX, ArmY, ArmZ, HipX, HipZ, NeckX, NeckZ, ThighX, ThighY, ThighZ, WristX, WristY, WristZ
Modularity	AnkleY, NeckY, ThighX, WristY	
Structure	AnkleY, AnkleZ, ArmY, WristX	AnkleY, ArmY

highest ranking measures in terms of distinguishing between the activities being performed. Therefore, classification was done using the first four highest ranked measures only, using the RF classifier.

The data corresponding to the HS was split into a training set (TrainSet) and a testing set (TestSet), which correspond to Day01 and Day02 sessions respectively. The results obtained in this case are shown in Table V.9. The mean accuracy of activity classification, using the mean correlation per minute as the connectivity matrix, decreased slightly, reaching 81.6%. Nevertheless, this result confirms the interest of applying this method of analysis.

**Figure V.14** – Ranking of network measures computed for the Activity Classification Network in decreasing order using the ReliefF feature selection method: case of MeanR per minute.**Table V.9** – Overall Performance Measures (%) Obtained for the Activity Classification Network: Case of MeanR per Minute.

Activity	Walking	Standing	Lying	Sitting
Sensitivity	75.7	68.6	88.0	84.6
Specificity	96.8	96.1	90.5	90.3
Model Accuracy	81.6			

Dyskinesia Detection Network

In the case of PD patients, the number of observations previously obtained also presents a serious limitation for the classification process. Therefore, we also attempted to increase the total number of observations by computing the mean correlation matrix per minute of motor state class for each patient. The obtained distribution of dyskinetic versus non-dyskinetic observations in this case is shown in Table V.10.

Table V.10 – Number of Observations per Category for PD patients.

Connectivity Matrix	Dyskinetic	Non-Dyskinetic
Mean R	7	16
Mean R per Minute	19	52

Following that, the network measures are again computed and the Kruskal-Wallis H test is performed to determine the set of measures considered to be statistically significant in distinguishing between the motor states of the patients. By comparing the obtained p-values to a statistical significance level $\alpha = 0.05$, we are left with a subset of nine network measures that are considered to be statistically significant (Table V.11). Similar to the previous case of dyskinesia detection, none of the network measures survived the Bonferroni correction and the new significance level of $\alpha_{corrected} = 0.0028$. ReliefF feature selection was therefore performed on the entire subset of statistically significant measures, when compared to α . The rankings of the measures in this case are presented in

The data corresponding to the PD patients was again split into 80% - 20% for the training set (TrainSet) and testing set (TestSet), respectively. The classification was redone using the RF classifier using different combinations of the selected network measures. The best compromise between classifier performance and number of considered modules was found when taking into account only the first five ranked measures according to the ReliefF method. These measures correspond to the Hip and Ankle modules and produced the performance shown in Table V.12. Figure V.15.

Table V.11 – Statistically Significant Network Measures for Dyskinesia Detection for MeanR per Minute.

Measure	Statistically Significant compared to α
Strength	AnkleX, HipZ
Clustering Coefficient	HipX, HipY, NeckX, NeckZ
Modularity	AnkleY, HipY, HipZ

Table V.12 – Overall Performance Measures (%) Obtained for the Dyskinesia Detection Network: Case of MeanR per Minute.

Motor State	Dyskinetic
Sensitivity	35.0
Specificity	85.3
Model Accuracy	70.2

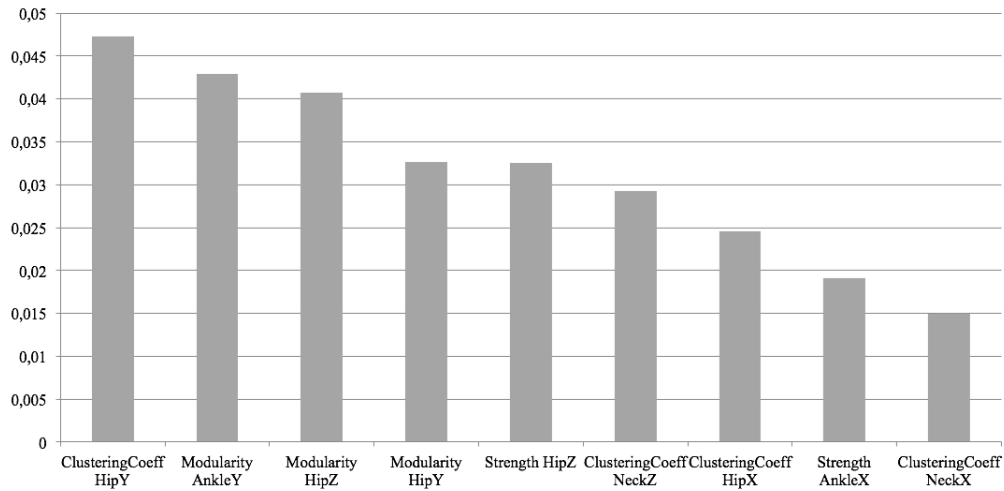


Figure V.15 – Ranking of network measures computed for the Dyskinesia Detection Network in decreasing order using the ReliefF feature selection method: case of MeanR per minute.

5 Conclusion

Many real-life networks are formed of large, complex connections that are neither uniformly random nor ordered. This principle led to the development of complex network analysis and its application on a wide range of connectivity data in several domains. However, to the extent of our knowledge, this type of analysis has not yet been applied in the area of wearable sensors for the evaluation of movement.

The designed ambulatory monitoring system is composed of a set of wearable sensors placed at different positions of the body, naturally taking on a network-like structure. Networks are characterised by anatomical or functional connections. In this case, the natural correlation occurring between different body parts during movement, whether corresponding to a specific activity or motor state, represents a functional connection between the monitoring system's IMUs. This led to the interest of pursuing complex network analysis for this application.

The first network, labeled Activity Classification Network, was constructed based on the data collected from healthy individuals. In this case, the overall accuracy of activity classification for the TestSet was obtained at 84.6%, using network measures belonging to the Neck and Thigh modules only. The second network, labeled Dyskinesia Detection Network, was constructed based on the data collected from PD patients. In this case, the overall accuracy of dyskinesia detection was obtained at 78.6%, using network measures belonging to the Arm, Hip and Thigh modules only. These results show that module positions carry certain importance and the method of analysis applied has an impact on the choice of modules that are considered to be of higher importance. In the previous chapter, and using a more conventional method of analysis based on pattern recognition, we saw that the modules positioned at the Ankle, Hip and Thigh presented the highest results in terms of accuracy of dyskinesia detection. As the results here seem to be complementary, we might consider an approach

that combines the two analysis methods, in which the relationship between the different modules is taken into account.

A major limitation for the classification process in both the Activity Classification and Dyskinesia Detection networks is the small number of observations. This relates directly to the learning capabilities of the classifiers and affects the performance obtained. As such, we attempted to increase the total number of observations, in both the HS and PD patients' case, by computing the connectivity matrices of the networks as the mean correlation per minute of category (whether the category is activity being performed or motor state), instead of mean correlation per category for each subject. This resulted in more than doubling the total number of observations obtained in both the HS and PD patients' cases.

For the Activity Classification Network, the ReliefF feature selection results showed measures corresponding to the Neck and Thigh modules to be of higher relevance in distinguishing between the activity classes, which is consistent to the results obtained using the first Activity Classification Network. In this case, and using the measures corresponding to the Neck and Thigh modules only, the overall accuracy of activity classification decreased to 81.6%.

For the Dyskinesia Detection Network, the ReliefF feature selection results showed measures corresponding to the Ankle and Hip modules to be of higher relevance in distinguishing between the motor states of the patients. These results are not entirely consistent with those obtained using the first Dyskinesia Detection Network, which consisted of measures corresponding to the Arm, Hip and Thigh modules. By performing the classification using the measures corresponding to the Ankle and Hip modules only, the overall accuracy of dyskinesia detection decreased significantly, reaching 70.2%. This shows that the variation of the number of observations has a significant effect on the classification outcome.

The low number of observations in this analysis, which is due to the short duration of activities and the low number of patients included, offers a certain limitation. The results obtained here, although promising, must therefore be considered as preliminary. Further exploration of this method of analysis must be done with a larger database that ensures the robustness of the classification process. More experiments need to be performed from a methodological point of view, such as taking into consideration the non-linear correlation coefficient between two observations x_1 and x_2 . The interest in doing that lies in the fact that $h_{x_1x_2} \neq h_{x_2x_1}$, which might offer some additional information.

Bibliography

- [1] L. EULER. *Solutio problematis ad geometriam situs pertinentis*. Commentarii academiae scientiarum Petropolitanae **8**, 128–140 (1741).
- [2] L. R. FOULDS. *Graph theory applications*. Springer Science & Business Media (2012).
- [3] K. RUOHONEN. *Graph theory; 2008*. Tampere University of Technology.
- [4] D. B. WEST ET AL. *Introduction to graph theory* , **2**. Prentice hall Upper Saddle River (2001).
- [5] C. GODSIL AND G. F. ROYLE. *Algebraic graph theory* , **207**. Springer Science & Business Media (2013).
- [6] B. BOLLOBÁS. *Modern graph theory* , **184**. Springer Science & Business Media (2013).
- [7] M. RUBINOV AND O. SPORNS. *Complex network measures of brain connectivity: uses and interpretations*. Neuroimage **52**(3), 1059–1069 (2010).
- [8] X. F. WANG AND G. CHEN. *Complex networks: small-world, scale-free and beyond*. IEEE circuits and systems magazine **3**(1), 6–20 (2003).
- [9] L. D. F. COSTA, F. A. RODRIGUES, G. TRAVIESO, AND P. R. VILLAS BOAS. *Characterization of complex networks: A survey of measurements*. Advances in physics **56**(1), 167–242 (2007).
- [10] E. BULLMORE AND O. SPORNS. *Complex brain networks: graph theoretical analysis of structural and functional systems*. Nature Reviews Neuroscience **10**(3), 186–198 (2009).
- [11] R. MILO, S. SHEN-ORR, S. ITZKOVITZ, N. KASHTAN, D. CHKLOVSKII, AND U. ALON. *Network motifs: simple building blocks of complex networks*. Science **298**(5594), 824–827 (2002).
- [12] A. TRUSINA, S. MASLOV, P. MINNHAGEN, AND K. SNEPPEN. *Hierarchy measures in complex networks*. Physical review letters **92**(17), 178702 (2004).
- [13] K. ANAND AND G. BIANCONI. *Entropy measures for networks: Toward an information theory of complex topologies*. Physical Review E **80**(4), 045102 (2009).
- [14] A.-L. BARABASI AND Z. N. OLTVAI. *Network biology: understanding the cell’s functional organization*. Nature reviews genetics **5**(2), 101–113 (2004).
- [15] S. BOCCALETTI, V. LATORA, Y. MORENO, M. CHAVEZ, AND D.-U. HWANG. *Complex networks: Structure and dynamics*. Physics reports **424**(4), 175–308 (2006).
- [16] J. SPINRAD. *Recognition of circle graphs*. Journal of Algorithms **16**(2), 264–282 (1994).
- [17] V. D. BLONDEL, J.-L. GUILLAUME, R. LAMBIOTTE, AND E. LEFEBVRE. *Fast unfolding of communities in large networks*. Journal of statistical mechanics: theory and experiment **2008**(10), P10008 (2008).

BIBLIOGRAPHY

- [18] W. H. KRUSKAL AND W. A. WALLIS. *Use of ranks in one-criterion variance analysis*. Journal of the American statistical Association **47**(260), 583–621 (1952).
- [19] E. W. WEISSTEIN. *Bonferroni correction*. (2004).
- [20] I. JOLLIFFE. *Principal component analysis*. Wiley Online Library (2002).

Part III

Evaluation of the Ambulatory Monitoring System

Unsupervised, At-Home Patient Monitoring

The objective of the developed system is to provide reliable and accurate detection of LID in PD patients in an unsupervised daily life environment. As such, the monitoring system's ability to properly identify dyskinetic periods is evaluated here under real-life conditions. In this chapter, we present an unsupervised, long-duration acquisition that was conducted at one of the PD patients' home, patient M01.

First, the protocol of acquisition that took place at the patient's home is described, providing context of the measurement method and activities performed. Then, the data processing method applied is presented. Detection of dyskinesia experienced by the patient over the course of the day is performed with and without the classification of activities, as described in *App1* (without activity classification) and *App3* (for automatically separated activity sets) of Chapter IV.

In addition, two strategies are explored for the training step. The first approach is labeled as the global approach, and consists of utilising all of the PD patients' data previously collected. The second approach is labeled as the subject-specific approach, and consists of utilising only patient M01's collected data.

The results obtained using the global and subject-specific approaches are then presented and a comparison of the performances is done. Finally, a conclusion regarding the performance of the monitoring system in an unsupervised home environment is drawn.

1 Protocol and Measurement Method

This acquisition was performed at patient M01's home, using the entire system of acquisition consisting of the 6 Shimmer3 IMUs. During this session, the patient was encouraged to go about her day as per usual and to maintain Levodopa intake as prescribed. Figure VI.1 shows some of the activities performed by the patient during this acquisition, which lasted approximately five and a half hours in total.

The configuration of the IMUs was done exactly as in the previous short duration acquisition sessions. However, due to a software error, data was lost from all IMUs with the exception of the IMU placed at the ankle. As a result, we perform the processing approaches presented in the following



Figure VI.1 – Some of the daily life activities performed by the patient at her home during the long duration, free acquisition.

section using only the data collected from the ankle modules in the previous short duration acquisition sessions. It is important to note, however, that although data loss is unfortunate, the ankle module did provide satisfying results during the single module assessment presented in Chapter IV section 2.4, making it one of the top three most important modules for this application.

2 Data processing

In order to keep track of the patient's motor condition, a small survey was filled out at 30 minute intervals during the acquisition session in which the patient was asked to rate her motor symptoms as absent, moderate or severe. The rating given by the patient was verified by the members of the study present during the acquisition. Starting from the first dose of Levodopa at 7h30, the patient reported experiencing dyskinesia in the morning, prior to the start of the acquisition session at 10h30. The second dose of Levodopa was taken at 10h30 and LID began manifesting shortly after. The next dose of Levodopa, taken by the patient at 13h30, did not seem to be effective, according to the patient's own reporting. The patient did not experience LID after this dose, but seemed to be quite fatigued and experienced difficulty moving. The evaluation of LID severity as well as other symptoms given by the patient is shown in Figure VI.2.

Symptom	10h30	11h00	11h30	12h00	12h30	13h00	13h30	14h00	14h30	15h00	15h30	16h00
Akinesia	++	-	-	-	-	+	+	++	++	+/++	+/++	++
Rigidity	+	-	-	-	-	+	+	++	++	+/++	+/++	+
Tremor	-	-	-	-	-	-	-	-	-	-	-	-
Dyskinesia	-	+	+	+	+/++	-	-	-	-	-	-	-
Dystonia	-	-	-	-	-	-	*	*	-	-	-	-

A - M + S ++ * Pain in right shoulder

Figure VI.2 – Self-evaluation survey taken by the patient to assess her motor symptoms.

During this acquisition, the activities performed by the patient were not annotated for practicality reasons and to minimise the intrusion on the patient. Consequently, the process of LID detection for this dataset is done as described in *App1* and *App3* of Chapter IV, where *App1* refers to dyskinesia detection for the entire collected dataset without separation of activities and *App3* refers to dyskinesia detection for automatically separated activity datasets. The two training strategies tested for LID detection were:

- The Global Approach, which is aimed towards testing the accuracy of dyskinesia detection when considering a global population including PD patients with varying LID severity and manifestation in the training set.
- The Subject-Specific Approach, where only the data collected from patient M01 is considered in the training set. This approach is aimed towards testing the effect of personalising the classifier to a specific patient's data on the accuracy of LID detection.

2.1 Dyskinesia Detection Using the Global Approach

In the global approach, data collected from the three PD patients' ankle module in previous acquisition sessions is considered. Therefore, the population used to train the classifiers can be considered as a heterogenous one, since it contains data from patients that manifested different severities of LID as well as in different body parts. Similar to what was detailed in Chapter IV, the processing steps of segmentation and feature extraction are performed. The long duration acquisition data was first segmented into 7 second time windows and the following features were computed: mean, mobility, complexity, peak cross correlation, energy, mean frequency and median frequency (detailed in Chapter IV section 1.1). Considering that only the data collected from the ankle module is available, the feature set size is diminished from the original 576 features corresponding to 6 module positions, to 96 features corresponding to a single module position.

For the first approach, *App1*, dyskinesia detection is performed directly on the entire dataset without separation of activities. While for the third approach, *App3*, activity classification is first performed on the entire dataset, separating the data into four classes of activities: Walking, Standing, Lying, and Sitting. Following that, dyskinesia detection is performed on each separated activity dataset.

The training set (TrainSet) is defined to be the data collected from the three PD patients during the short duration acquisitions. The testing set (TestSet) is defined as the data collected from patient M01's long duration acquisition. The patient data split and the number of instances to be classified are shown in Table VI.1.

Table VI.1 – Patient Data Split: Global Approach.

Data	Subjects	Size
TrainSet	3 patients Day01&Day02	2121 instances x 96 features
TestSet	patient M01 long duration acquisition	2830 instances x 96 features
Total	3 patients	4951 instances x 96 features

2.2 Dyskinesia Detection Using the Subject-Specific Approach

In the subject-specific approach, only the data collected from patient M01's ankle module during the previous short duration acquisitions is considered. Patient M01 had previously participated in the short duration acquisitions on two different days, performing four sessions on the first day and two sessions on the second day. An example of the collected signals in the dyskinetic and non-dyskinetic cases for a period five minutes during Day01, Day02 and the long-duration acquisition is shown in Figure VI.3. The signals correspond to the triaxial gyroscope of the Ankle module.

Considering that the patient followed a protocol of defined activities during the short duration acquisitions of Day01 and Day02, the periods of different activities can be clearly observed. For example, in the non-dyskinetic case of Figure VI.3, one can clearly distinguish between the periods of static activities (such as sitting) and dynamic activities (such as walking) of Day01 and Day02 data. During

the static activities, the patient refrained from performing any movement and focused on performing the task asked of her, which is reflected in the signals. However, during the long-duration acquisition, the patient was not following a predefined protocol and as such was moving in a natural way without refraining from random voluntary movements even when performing static activities such as sitting down. The patient would repeatedly perform voluntary gestures and movements as she conversed in a natural way without restricting herself. As such, in the non-dyskinetic case of the long-duration acquisition, one can observe the presence of small variations in the signals when compared to Day01 and Day02. However, a visual distinction can still be made between static and dynamic activities (for example the periods of 50-150 seconds and 150-300 seconds).

On the other hand, a clear difference is present between the dyskinetic and non-dyskinetic signals of Day01 and Day02. Although the patient was performing the same protocol and attempting to refrain from movement during the static activities, the presence of dyskinesia made that task extremely difficult. The signals shown in the dyskinetic case of Figure VI.3 during Day01 and Day02 display higher variance and the periods of different activities are hard to discern. The same can be noted for the signals collected in the long-duration acquisition during the periods in which the patient reported experiencing dyskinesia. The presence of dyskinesia does therefore introduce a certain random characteristic to the signals regardless of the activity being performed, even during periods of free undirected movement.

This case reflects a more personalised approach for dyskinesia detection, in which the classifiers are learned based on a specific activity pattern or dyskinesia pattern related to a single subject. The same processing methods were applied on the long duration acquisition data in this approach as well, with respect to segmenting the data into 7 second time windows and computing the features. Similarly to the global approach, both *App1* and *App3* were applied in this case in order to evaluate how activity classification affects the accuracy of dyskinesia detection when considering data corresponding to a single patient.

As previously mentioned, patient M01 performed short duration acquisitions on two previous days, and as a result different conditions of training were considered:

- First condition: the training set (TrainSet1) is defined to be the data collected from patient M01 during the sessions performed on Day01 only.
- Second condition: the training set (TrainSet2) is defined to be the data collected from patient M01 during the sessions performed on Day01 and Day02 combined.

For each of these conditions, the testing set is always defined as the data collected from patient M01's long-duration acquisition. The data split corresponding to this approach and the number of instances to be classified are shown in Table VI.2. Data collected during Day02 showed very short periods of dyskinesia. Testing the described classification techniques using this data resulted in very low accuracies, possibly due to the number of observations in the dyskinetic state. Therefore, performing dyskinesia detection using only the data collected on Day02 is not pursued.

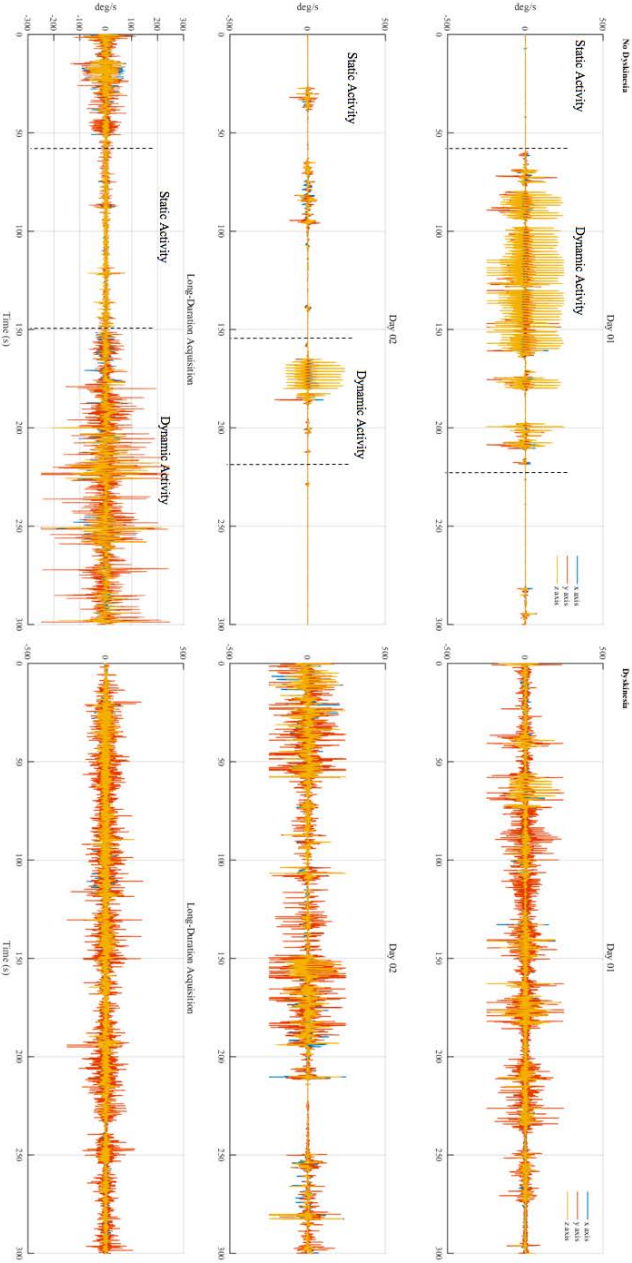


Figure VI.3 – Triaxial gyroscope signals collected from the Ankle module of patient M01 during Day 01, Day 02 and the long-duration acquisitions.

Table VI.2 – Patient Data Split: Subject-Specific Approach.

Data	Subjects	Size
TrainSet1	patient M01 Day01	425 instances x 96 features
TrainSet2	patient M01 Day01&Day02	1058 instances x 96 features
TestSet	patient M01 long duration acquisition	2830 instances x 96 features

3 Results

The performance evaluation of dyskinesia detection in each of the described approaches is done by comparing the output of the dyskinesia detector to the self-evaluation survey filled out by the patient during the long duration acquisition. Seeing as the activities performed during this session were not annotated, the performance of the activity classifier in *App3* will not be evaluated. The main interest here is to compare the accuracy of dyskinesia detection under *App1* and *App3*, when considering the different training approaches.

If we were to assign the instances obtained from patient M01’s long duration acquisition during the period of 11h00 and 13h00 a class of dyskinesia, and the instances outside that period the class of no dyskinesia, then we obtain a distribution of 1028 dyskinetic instances and 1802 non-dyskinetic instances to be considered as the testing set.

For comparison purposes, we recall the performance of the dyskinesia detector in both *App1* and *App3* using the data collected from the Ankle module only for the short-duration acquisitions presented in Chapter IV (Table VI.3).

Table VI.3 – Overall Performance of Dyskinesia Detection For Short Duration Acquisition Data Using the Ankle Module Only.

Method	Sensitivity	Specificity	Accuracy
<i>App1</i>	81.77	96.51	92.12
<i>App3</i>	83.51	95.46	92.41

3.1 Dyskinesia Detection Using the Global Approach

For the global approach, the training set was comprised of data collected from the three PD patients’ previous short duration acquisitions, while the testing set was comprised of patient M01’s long duration acquisition data. The distribution of dyskinetic and non-dyskinetic instances in the training and testing sets are presented in Table VI.4.

Figure VI.4 shows the classification results of the global approach in both *App1* and *App3* with respect to time, versus the patient’s self-evaluation survey.

Using *App1* (Figure VI.4, Top), in which dyskinesia detection was performed without the separation of activities, the output of the classifier is somewhat consistent with the patient’s self-evaluation

Table VI.4 – Global Approach: Number of Instances per Motor State.

Motor State	Dyskinesia	No Dyskinesia
TrainSet	630	1491
TestSet	1028	1802
Total	1658	3293

showing dyskinesia presence starting from 11h00 till approximately 13h00. However, during the period approximately between 14h20 and 15h40, there exists some false alarms¹ in which the dyskinesia detector indicates presence of dyskinesia while the patient reported absence of dyskinesia.

Similar results can be viewed when using *App3* (Figure VI.4, Bottom), in which dyskinesia detection was performed after automatically classifying the patient's activities. Dyskinesia detection is also consistent with the patient's self-evaluation. The period between 11h00 and 13h00, during which the patient reported experiencing dyskinesia of varying severities is almost entirely identified by the dyskinesia detector. However, more false alarms are detected in this case than in the case of *App1*, as can be observed in the graph. It is also important to note that the entire data collected from patient M01's long duration acquisition was classified as the activity of "Sitting". The fact that the activity classifier in this case was trained using PD patients' data limited to only the ankle module could be the reason behind the misclassification of other activities performed by the patient during the day.

When comparing the graphs of *App1* and *App3*, it is observed that *App3* identifies the dyskinetic instances in the period between 11h00 and 13h00 with higher sensitivity than *App1*. However, *App1* generates less false alarms, hence being more consistent with the patient's self-evaluation outside of that period. Although *App1* has higher specificity than *App3*, the sensitivity of dyskinesia detection in *App1* is clearly much lower than *App3*.

The performance measures of *App1* and *App3* of the global approach are computed based on the distribution of Table VI.4. The sensitivity, specificity and accuracy values obtained in each method are shown in Table VI.5.

Table VI.5 – Global Approach: Performance Measures Obtained for the TestSet. "*" Indicates Predicted State.

	Motor State	Dyskinesia	No Dyskinesia
<i>App1</i>	Dyskinesia*	244	1768
	No Dyskinesia*	784	34
	Sensitivity	24.45	
<i>App1</i>	Specificity	98.11	
	Model Accuracy	71.32	
<i>App3</i>	Dyskinesia*	744	1759
	No Dyskinesia*	284	43
	Sensitivity	72.21	
<i>App3</i>	Specificity	97.05	
	Model Accuracy	88.62	

¹It is worth noting that the false alarms are in comparison to the patient's self-evaluation.

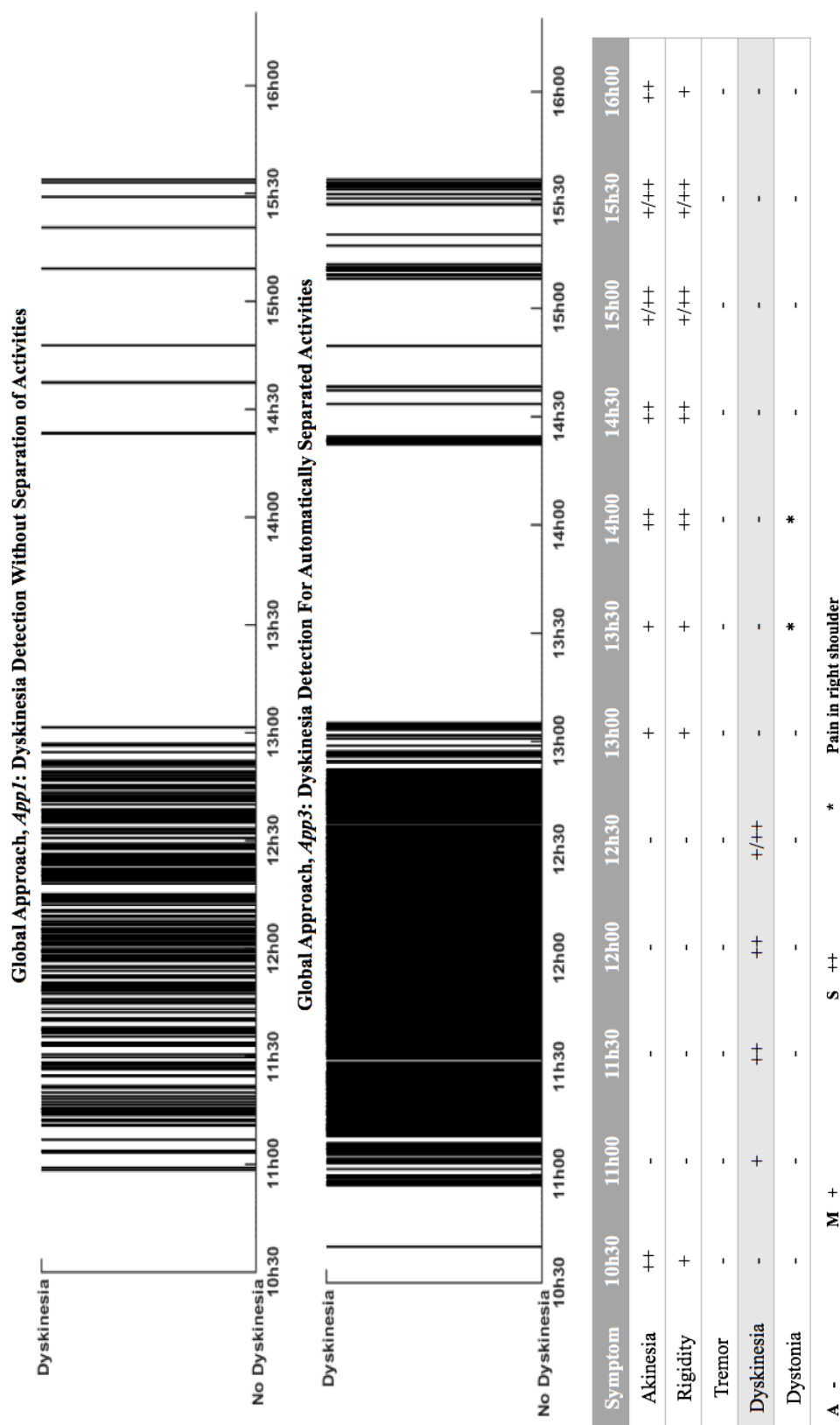


Figure VI.4 – Global approach results for dyskinesia detection in *App1* and *App3* versus the patient's self-evaluation survey. Each spike represents one instance, which is a 7 second time window.

3.2 Dyskinesia Detection Using the Subject-Specific Approach

For the subject-specific approach, the data collected during patient M01's short-duration sessions is used to provide two different training conditions (Table VI.2). It is important to note that this approach projects us towards the real utilisation of the developed system. The first condition consists of using the data collected from patient M01's Day01 sessions only, and the training set in this case is labeled as TrainSet1. The distribution of instances per motor state in this condition is shown in Table VI.6.

Table VI.6 – Subject-Specific Approach (TrainSet1): Number of Instances per Motor State.

Motor State	Dyskinesia	No Dyskinesia
TrainSet1	301	124
TestSet	1028	1802
Total	1329	1926

Similar to the global approach, the classification results using TrainSet1 in both *App1* and *App3* with respect to time are displayed versus the patient's self-evaluation survey in Figure VI.5.

The period between 11h00 and 13h00, which is defined as dyskinetic by the patient, is somewhat identified in *App1*, with a number of instances clearly misclassified as non-dyskinetic. However, in *App3*, this period appears to be entirely identified as dyskinetic. This leads to higher sensitivity in *App3* than in *App1*, when using TrainSet1. On the other hand, there is an evidently larger number of false alarms in *App3* than in *App1*, leading to better specificity in the latter, but with a significant decrease in sensitivity. The performance evaluation obtained in this case is shown in Table VI.7.

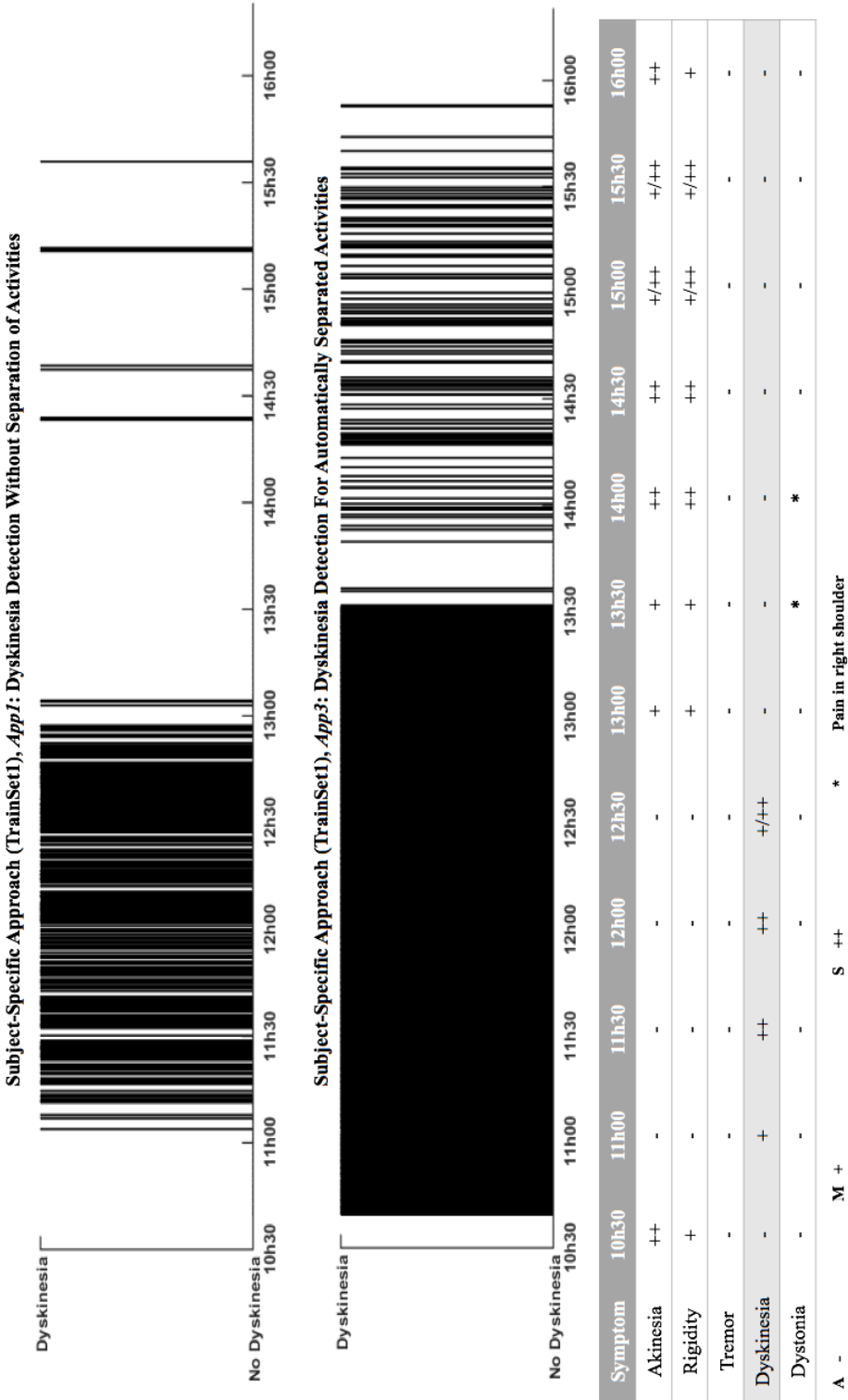


Figure VI.5 – Subject-specific approach results for dyskinesia detection in *App1* and *App3* versus the patient’s self-evaluation survey, using TrainSet1 as the training set. Each spike represents one instance, which is a 7 second time window.

Table VI.7 – Subject-Specific Approach: Performance Measures Obtained for the TestSet When Using TrainSet1. "*" Indicates Predicted State.

	Motor State	Dyskinesia	No Dyskinesia
<i>App1</i>	Dyskinesia*	557	1774
	No Dyskinesia*	471	28
<i>App1</i>	Sensitivity	54.55	
	Specificity	98.21	
	Model Accuracy	82.35	
<i>App3</i>	Dyskinesia*	844	1503
	No Dyskinesia*	184	299
<i>App3</i>	Sensitivity	82.98	
	Specificity	83.73	
	Model Accuracy	82.61	

For the second training condition, the data collected during both Day01 and Day02 are combined to comprise TrainSet2, which is used to train the classifier. In this case, the total number of instances per motor state is the sum of those during each day of short-duration acquisitions, while the TestSet remains to be the data collected during the patient's long duration acquisition (Table VI.8).

Table VI.8 – Subject-Specific Approach (TrainSet2): Number of Instances per Motor State.

Motor State	Dyskinesia	No Dyskinesia
TrainSet2	513	545
TestSet	1028	1802
Total	1541	2347

Figure VI.6 shows the results obtained and the corresponding performance measures are given in Table (VI.9) for both *App1* and *App3*. Similarly to the previous results, the sensitivity of dyskinesia detection between the period of 11h00 and 13h00 is higher in *App3* than in *App1*. However, when considering *App1*, the number of false alarms generated using TrainSet2 as the training set is higher than that obtained when using TrainSet1. The same can be observed when considering the output of *App3* as well. The period in which the patient reports presence of dyskinesia is almost entirely identified, but the number of false alarms has increased substantially. The overall accuracy of dyskinesia detection dropped from 82.35% and 82.61%, in *App1* and *App3* respectively, when using TrainSet1 to 68.11% and 46.91% when using TrainSet2, also in *App1* and *App3* respectively. This suggests that the data introduced from Day02 acquisitions have produced some difficulties with regards to the specificity of the detector. Therefore, we consider the optimal condition for learning in the subject-specific approach to be the use of TrainSet1 only.

As such, a summary of the obtained results for *App1* and *App3* are presented in Tables VI.10 and VI.11, respectively. In this summary we compare the performances obtained for the short-duration protocol of Chapter IV, the long-duration global approach and the long-duration subject-specific approach.

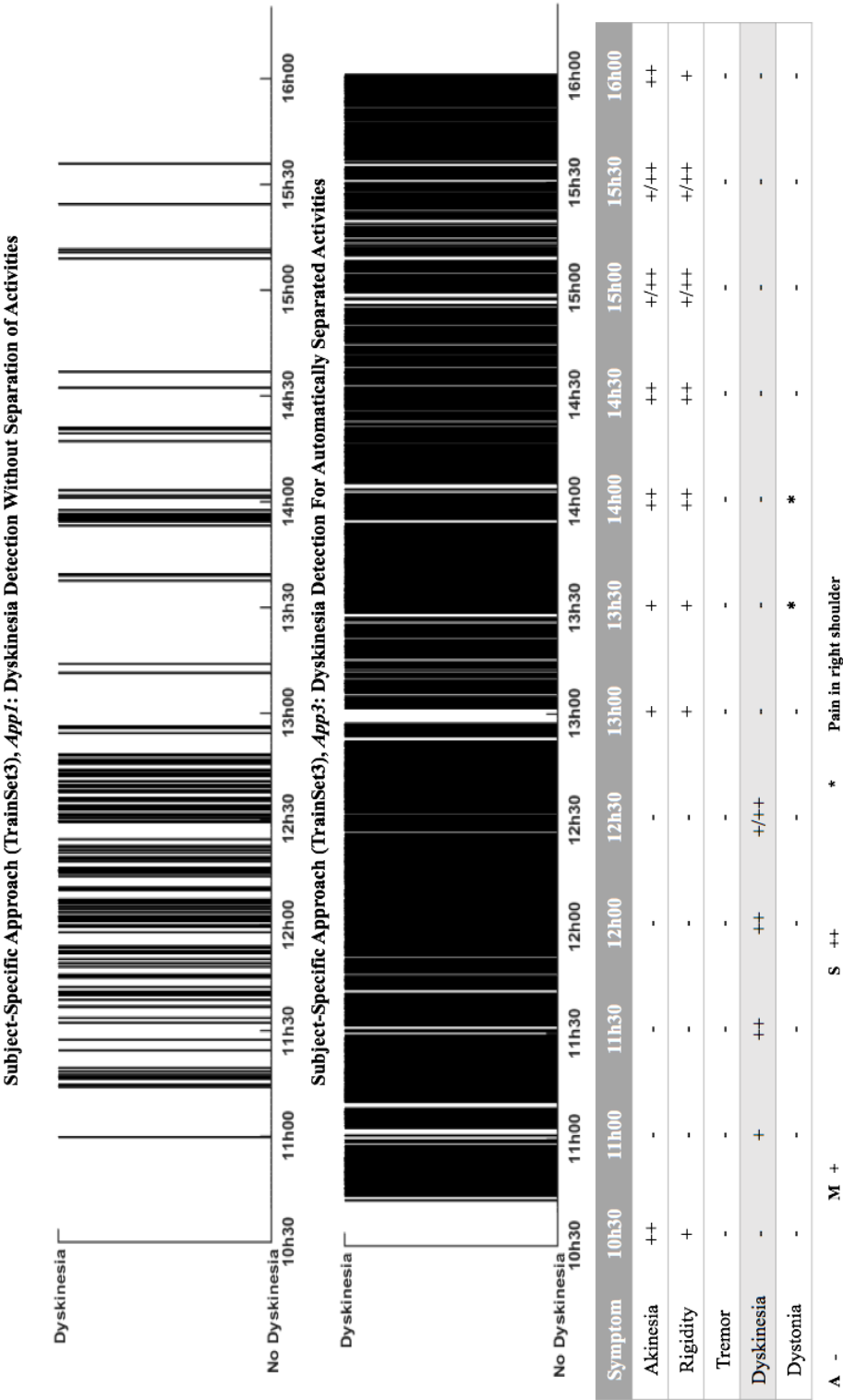


Figure VI.6 – Subject-specific approach results for dyskinesia detection in *App1* and *App3* versus the patient’s self-evaluation survey, using TrainSet3 as the training set. Each spike represents one instance, which is a 7 second time window.

Table VI.9 – Subject-Specific Approach: Performance Measures Obtained for the TestSet When Using TrainSet2.
"*" Indicates Predicted State.

	Motor State	Dyskinesia	No Dyskinesia
<i>App1</i>	Dyskinesia*	196	1733
	No Dyskinesia*	832	69
<i>App1</i>	Sensitivity	19.21	
	Specificity	96.23	
	Model Accuracy	68.11	
<i>App3</i>	Dyskinesia*	354	949
	No Dyskinesia	674	853
<i>App3</i>	Sensitivity	34.41	
	Specificity	52.78	
	Model Accuracy	46.91	

Table VI.10 – Performance of Dyskinesia Detection in *App1* Using the Short-Duration Protocol Data vs. Global and Subject-Specific (TrainSet1) Approaches Using Short and Long-Duration Acquisition Data.

Performance	Short-Duration Protocol	Global Approach	Subject-Specific Approach
Sensitivity	81.77	24.45	54.55
Specificity	96.51	98.11	98.21
Accuracy	92.12	71.32	82.35

Table VI.11 – Performance of Dyskinesia Detection in *App3* Using the Short-Duration Protocol Data vs. Global and Subject-Specific (TrainSet1) Approaches Using Short and Long-Duration Acquisition Data.

Performance	Short-Duration Protocol	Global Approach	Subject-Specific Approach
Sensitivity	83.51	72.21	82.98
Specificity	95.46	97.05	83.73
Accuracy	92.41	88.62	82.61

4 Conclusion

Based on the obtained results, it appears that generally, the detection of dyskinetic instances in *App1* is less accurate than that in *App3*. The overall accuracy of dyskinesia detection in *App1* for the global approach is 71.32% as opposed to 88.62% in *App3*. For the subject-specific approach, the global accuracies in *App1* and *App3* are close, at 82.35% and 82.61% respectively, while the sensitivity in *App3* is significantly higher.

Introducing the activity classification phase in *App3* appears to increase the accuracy of properly detecting dyskinetic instances. However, this process leads to over-sensitivity of the classifier, where an increase in the false alarms occurs. This can also be observed by the lower specificity values obtained in *App3* in both the global and subject-specific approaches, and under the different training conditions. This issue could very much be attributed to the error in activity classification occurring during *App3*.

Since the activities performed during the long duration acquisition have not been annotated, the performance measures corresponding to the activity classification phase of *App3* are not computed. However, during the activity classification phase of *App3*, misclassification of activities was observed. In the global approach, using TrainSet, and in the subject-specific approach, using TrainSet2, the activities performed by the patient are being classified solely as sitting. While in the subject-specific approach, using TrainSet1, the activities are being classified as either lying or sitting. In this case, the error in classifying the activities can be associated to the fact that the classifier is being trained using the data collected during the predefined protocol, in which the activities were more structured. During the long duration acquisition, the patient moved freely without instructions, which resulted in a more natural sequence of activities as well as the occurrence of several activities simultaneously. For example, when instructed to perform the activity of sitting during the short-duration protocol, patients would subconsciously refrain from performing other movements. On the other hand, during the long-duration acquisition, the patient would simultaneously perform different natural gestures while sitting, such as standing up shortly or moving around reaching for objects. Also, during the

long-duration acquisition, the patient did not perform the activity of walking for more than a few seconds at a time, which is normal considering that the acquisition occurred at the patient's home and the walking activity consisted of simply moving from one room to another.

The results obtained during this analysis are therefore considered as preliminary, and might vary when considering data from the six IMU positions initially included in the monitoring system. The best compromise between the sensitivity and specificity of dyskinesia detection was obtained when using the subject-specific approach, and while using TrainSet1 in *App3*, where the sensitivity and specificity values were obtained at 82.98% and 83.73% respectively, and the overall accuracy was obtained at 82.61%.

Nevertheless, this experiment is considered to be important in the scope of our work and lead to significant conclusions. It allowed us to assess the possibility and the issues related to performing at-home acquisitions with patients. The monitoring system proved to be simple to mount and dismount from the patient, and did not appear to cause any obstacles with her natural movement. Collecting data while preserving the patient's freedom in performing every day activities is a crucial factor in ensuring patient compliance for future long term monitoring. In order to overcome some of the issues faced, we consider asking the patient to perform a number of defined activities (in both the dyskinetic and non-dyskinetic states) in their natural environment. This process could possibly enhance the activity classification phase, and as such minimise the error in the dyskinesia detection phase. This leads us to propose an adaptive system, in which the data collected from a patient is used to refine the classification and could possibly be included into a continuous subject-specific training process, where the classifier adapts in real time to the training data provided.

PARADYSE : Platform of Activity Recognition and Dyskinesia Evaluation

This chapter introduces a Graphical User Interface (GUI) developed as part of the final ambulatory monitoring system proposed. Considering that this study is funded by an industrial contract, the development of a user interface for use by the company is required. The GUI, called PARADYSE (Platform of Activity Recognition and Dyskinesia Evaluation), serves as a complete platform embedding the previously applied analysis methods.

The objective of this platform is to provide a simple and efficient user interface for the manipulation of data collected using the monitoring system. Its purpose is also to rapidly perform tests on the selected features, the influence of patient-specific and global learning approaches, as well as provide a representation of the patient profile in terms of dyskinesia prevalence throughout the day.

In this chapter, we begin by introducing the different elements that comprise the platform. The objectives of the platform are then detailed and the general scheme of operation is presented. Following that, each element is explained while providing examples of the tests performed using the platform. Finally, we present the future prospects envisioned for this platform in order to further advance the monitoring system as a whole.

1 Introduction to PARADYSE

1.1 Objectives

The main objective of PARADYSE is to advance the analysis of data collected by the developed monitoring system, which is achieved through the ability to perform the following:

- Examine raw data collected from each module positioned at different places on the body and determine the sensors whose signal variations are more evident.
- Extract, plot and save segments of interest from the collected data. These segments can correspond to specific activities or to dyskinetic periods in the signals.

- Perform preprocessing on the collected signals, such as segmentation with or without overlap and remove zero crossing noise.
- Evaluate the significance of computed features by performing classification while varying the feature set.
- Export the computed feature set for either activity classification, dyskinesia detection or both.
- Explore the effect of training the classifier using pre-existing data, by incorporating a percentage of the new data along with the pre-existing data, or by performing subject-specific training in both the activity classification and the dyskinesia detection phases.
- Allow user-defined parameters for inclusion criteria in the classification process in order to create different scenarios that allow for further evaluation of the monitoring system as a whole.

1.2 Development

The GUI is developed using the MATLAB[®] GUIDE (GUI Development Environment) [1], an environment that provides tools for designing custom user interfaces. Since all of the algorithm coding is implemented in MATLAB[®] [2], creating a GUI offers the option of containing these programs into an interface and introducing GUI front-ends to automate tasks or calculations. Figure VII.1 shows the elements that comprise the platform along with the main function of each of them.

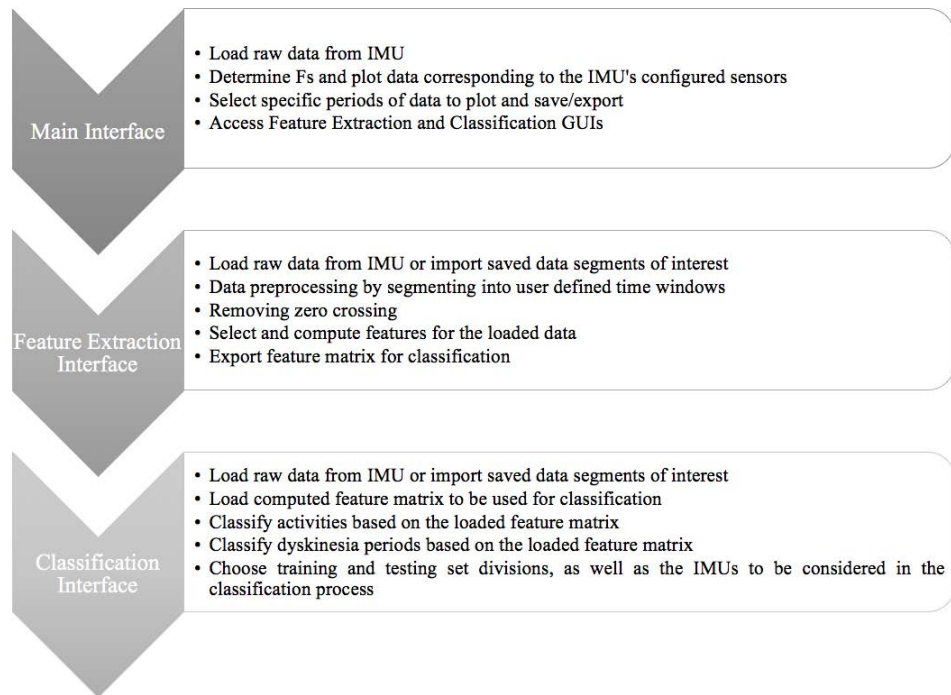


Figure VII.1 – Diagram of the elements comprising the developed platform.

1.3 Elements

The platform is intended to act as a means to facilitate the processing of data collected from the monitoring system's IMUs. The developed algorithms and processing techniques introduced in the previous chapters of this thesis were grouped into three different elements and integrated into the GUI. The elements are:

- **Main Interface:** includes the ability to load and view an IMUs raw data, specify sensor plots, choose sampling frequency, extract and plot specific segments from the total collected signals, and save segments of interest.
- **Feature Extraction Interface:** includes preprocessing methods such as segmenting raw data, as well as computing and saving some or all of the features used in the applied algorithms.
- **Classification Interface:** includes the ability to plot the raw data and view its corresponding feature matrix. This section includes the activity classification and dyskinesia detection algorithms.

The platform is designed to allow the implementation of a complete analysis, beginning with uploading and examining the raw collected data in the Main Interface, performing the required processing in the Feature Extraction Interface, and finally classifying the data based on the computed features in the Classification Interface. Each of these elements will be detailed in the following sections.

2 Main Interface

The main interface is shown in Figure VII.2. This is the main GUI in which the raw data can be examined, sensor signals can be plotted and segments of data can be extracted. From this GUI, the following steps of data processing can be accessed.

In Figure VII.3, a sample dataset collected from the IMU positioned at the ankle of a healthy individual is loaded into the interface by clicking the "**Load File**" button, and the file path is automatically displayed in the text box on its right. The IMUs are configured to record with a sampling frequency $F_s = 512$ Hz. Therefore in order to plot the raw data, this sampling frequency is chosen from the drop down menu labeled "**Sampling Frequency**", where the user has the ability to choose one of the predefined sampling frequencies displayed in Figure VII.4 (A). The three dimensional data collected from each sensor located in the IMU can be plotted separately in the first plot zone, as seen in Figure VII.4 (B).

Certain segments of data can be deemed as interesting and might require further exploration. For example a certain period in a healthy individual's activity data, or a dyskinetic phase in a PD patient's acquisition data. As such, these specific areas of interest can be plotted separately in the second plot zone by specifying the start and end times of the period of interest (Figure VII.5). The data

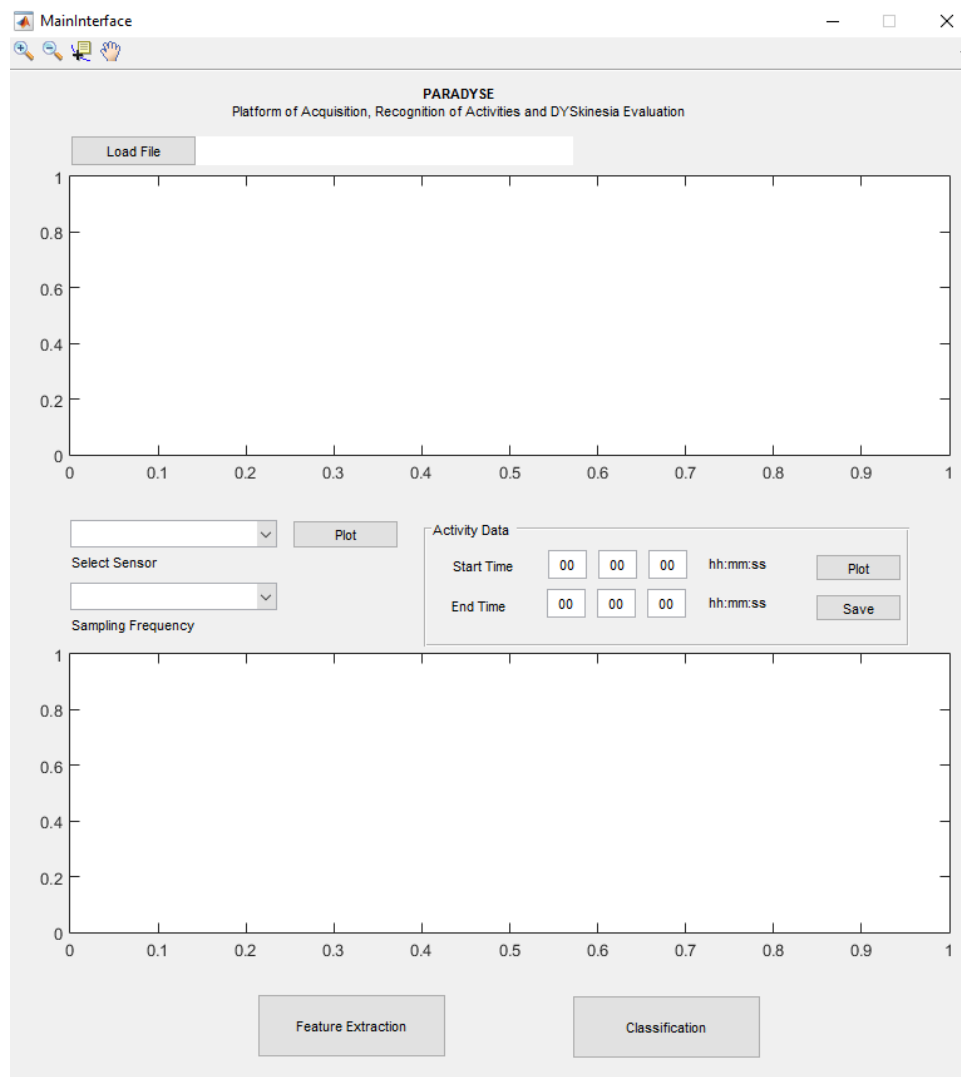


Figure VII.2 – Main interface of the GUI.

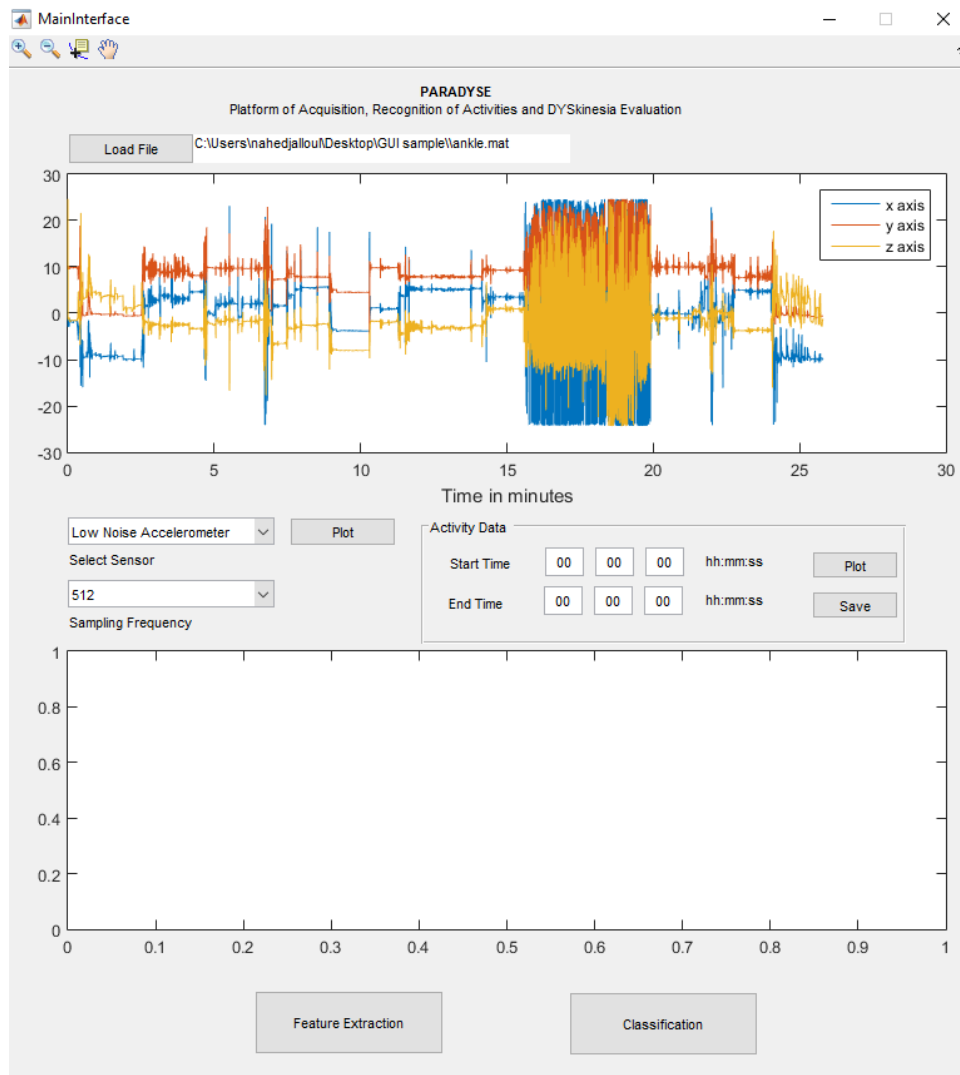


Figure VII.3 – Main interface of the GUI: Load raw data and plot example.

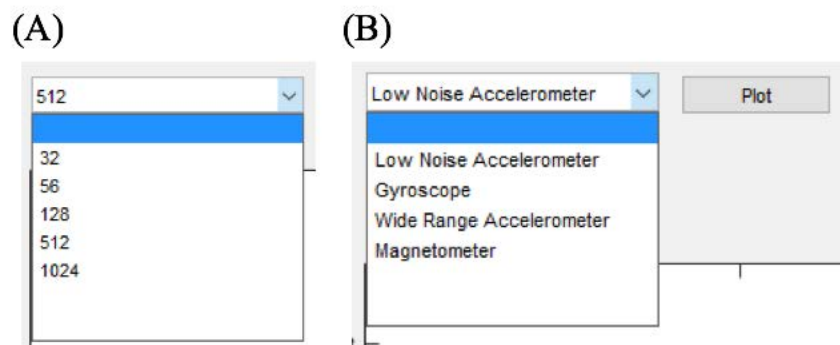


Figure VII.4 – Main interface of the GUI: (A) selection of sampling frequency, (B) selection of sensor data.

corresponding to the selected period of interest can be extracted and saved by clicking the "Save" button.

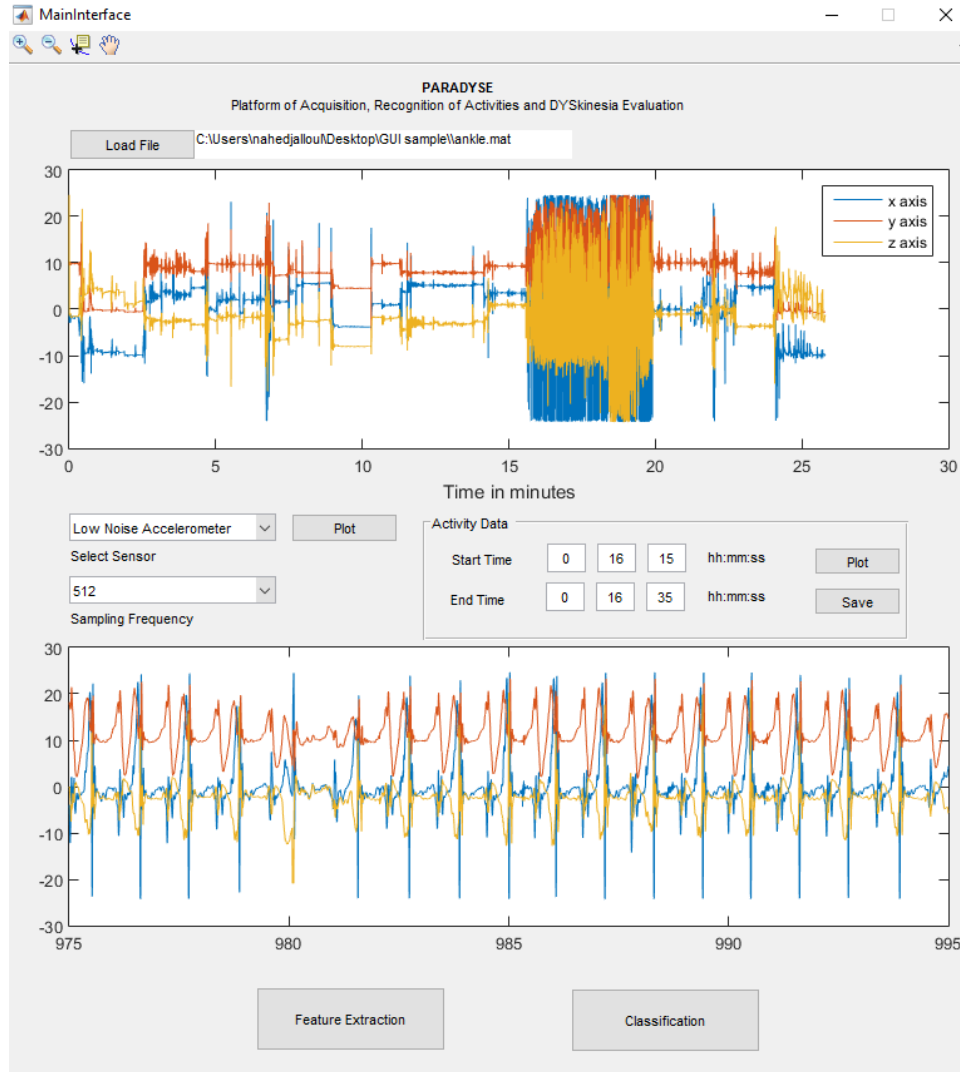


Figure VII.5 – Main interface of the GUI: Extraction and plot of a segment of data.

Based on the operations done in this general interface, a set of variables are automatically exported to MATLAB's workspace. These variables are listed in detail in Table VII.1 and allow the user freedom for further manipulation or analysis. From this interface, the user can access both the Feature Extraction and the Classification applications through the buttons at the bottom.

3 Feature Extraction Interface

The following steps applied in the algorithm described in Chapter IV consist of preprocessing the data prior to computing the features. In Figure VII.6, the file consisting either of the entire data collected

or a previously extracted segment of data is loaded into this application by clicking the "**Load File**" button. The corresponding file path is shown in the text box on the right and the raw data chosen is displayed in the table object below it.

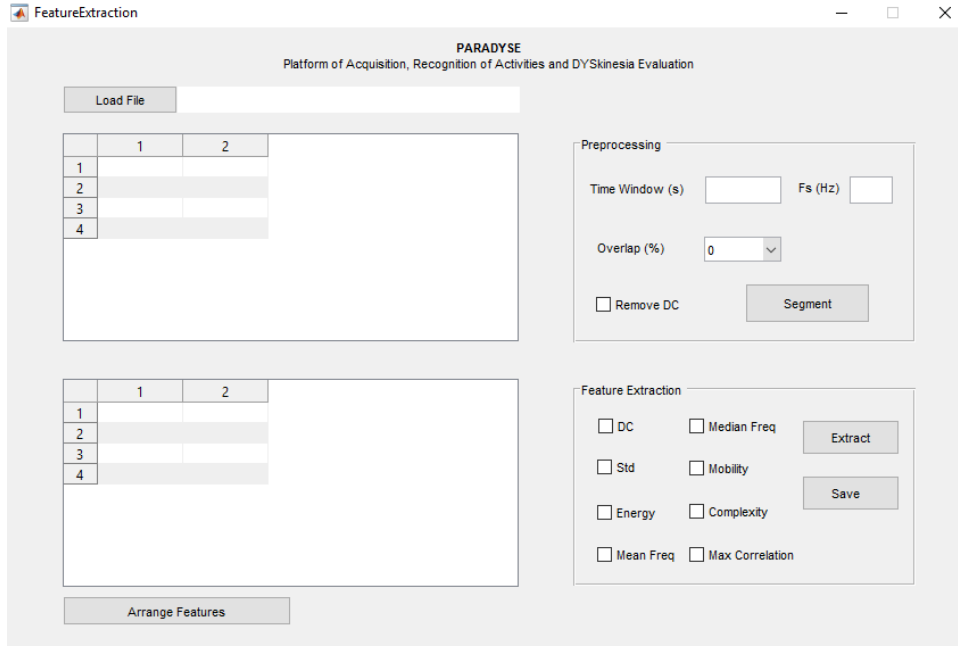


Figure VII.6 – Feature Extraction Interface.

To the right is a group of control objects labeled "**Preprocessing**", in which the user can input the size of time window in seconds and the percentage of overlap for the segmentation process based on the inputted sampling frequency. A checkbox object is also found that allows the user to proceed with or without removing the zero crossing error, otherwise known as "**DC**". An example of the preprocessing user inputs is shown in Figure VII.7.

By clicking the "**Segment**" button in this group, the variable containing the segmented data, labeled "windowed_data" will be exported to the MATLAB workspace (Table VII.1). The features to be extracted will be computed based on this variable and not the raw data file loaded into the GUI.

In another group of control objects, labeled "**Feature Extraction**", all the features used in the developed algorithm previously described are listed. These features appear as a checkbox selection and the user has the option to select all or a combination of the features simply by checking the box next to them and clicking "**Extract**". Once this button is clicked, a popup user input window appears to indicate the column order of the configured sensors in the IMU. The default order of columns appears first, and the user has the ability to modify the input in case the configuration of the IMU is custom (Figure VII.8).

The set of computed features then appears in the table object to the left. The computed features appear in the table in order of selection, as seen in Figure VII.9 (A). However, in many cases, it might be of interest to keep the order of columns since it represents the sensor and sensor axes included in the

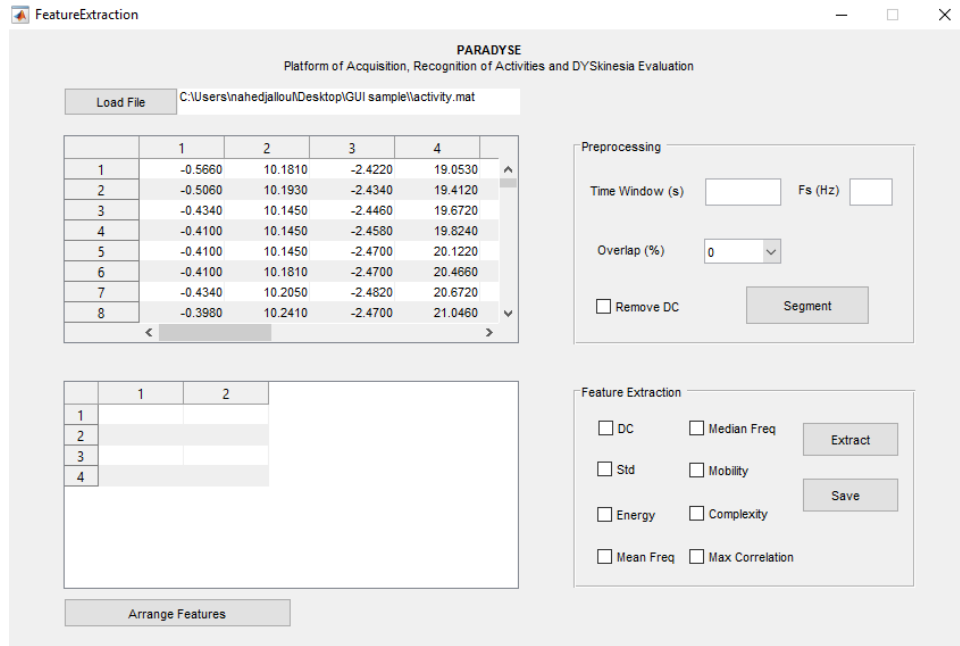


Figure VII.7 – Feature Extraction Interface: Preprocessing user input.

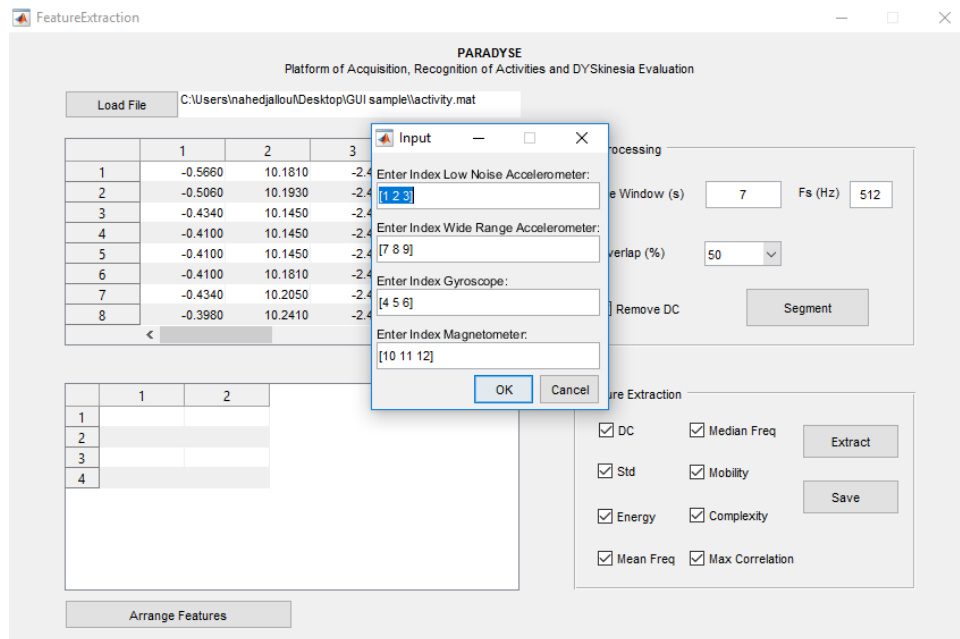


Figure VII.8 – Feature Extraction Interface: Feature extraction and sensor order based on the IMU's configuration.

IMU. Therefore, another option of arranging the features based on the order of sensors is presented by clicking the "Arrange Features" button. In this case, all the computed features for $sensor_i$, $axes_j$ are grouped together, as seen in Figure VII.9 (B). The ordered feature matrix can then be saved by clicking the "Save" button, and is labeled as "FM_arranged" (Table VII.1).

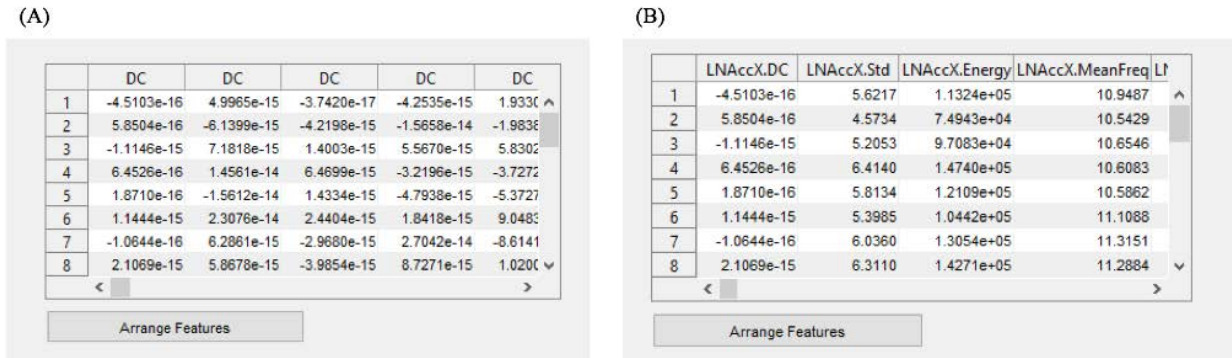


Figure VII.9 – Feature Extraction Interface: Arranging features by sensor order.

Table VII.1 – Variables Exported to MATLAB Workspace.

Interface	Name	Class	Description
Main Interface	rawdata	double	raw data file loaded into the general interface
	sensor_data	double	data corresponding to the three axes of the sensor chosen to be plotted in the first plot zone of the general interface
	act_data	double	segment of data extracted from the entire data for processing or examination
	act_time	double	vector containing the time stamps of the extracted segment of data
Feature Extraction Interface	windowed_data	cell	segmented data based on the chosen length of time window and percentage of overlap
	FM	double	feature matrix composed of the computed features by order of their selection
	FM_arranged	double	ordered feature matrix based on the index of configured sensors according to the user
Classification Interface	AC1, AC2, AC3, AC4	double	data extracted from the original data file which is classified as activities 1=walking, 2=standing, 3=lying, and 4=sitting
	AC_confusion_matrix	double	confusion matrix for the activity classification, where the columns represent the true class and the rows represented the predicted class
	Dys, NoDys	double	data extracted from the original data file which is classified as Dys=dyskinetic, and NoDys=non-dyskinetic
	DD_confusion_matrix	double	confusion matrix for dyskinesia detection, where the columns represent the true class and the rows represented the predicted class

4 Classification Interface

Following the feature extraction process, a classification interface (Figure VII.10) is available for both activity classification and dyskinesia detection based on the computed features from the previous interface.

In this interface, the user can load a raw data file or a previously extracted segment of data, using the "**Load Raw Data**" button, and plot that file's chosen sensor data based on the specified options in the "**Select Sensor**" and "**Sampling Frequency**" drop down menus (Figure VII.11).

Assuming that the loaded data file is the same one whose features had been computed and saved in the feature extraction interface, then the user can load the corresponding feature matrix variable (FM_arranged) by clicking the "**Load Features**" button. The file path is then displayed in the text box to the right and the computed features are displayed in the table object below. In the "**Feature Matrix**" object group, the number of observations and variables are automatically displayed

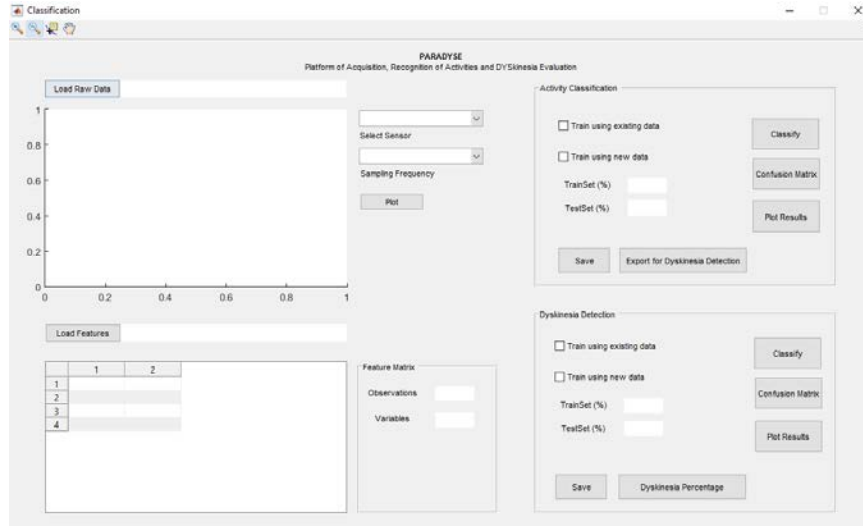


Figure VII.10 – Classification Interface.

representing the total number of instances to be classified and the features included respectively (Figure VII.11).

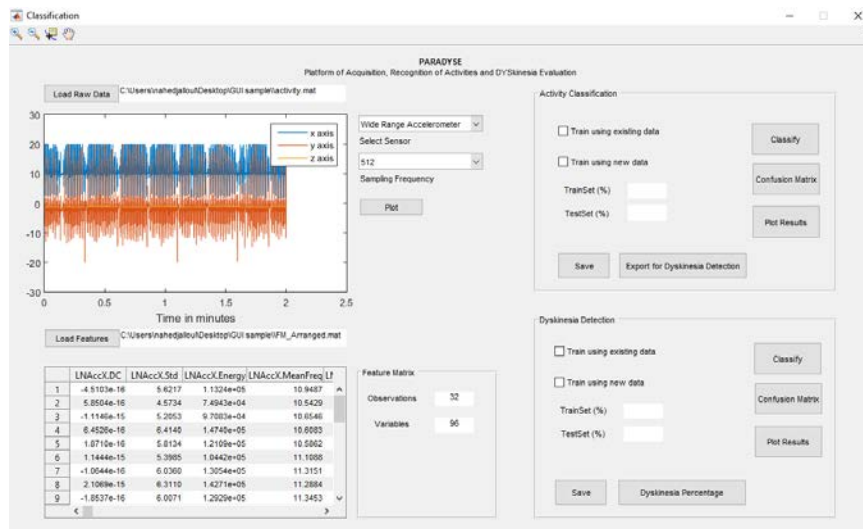


Figure VII.11 – Classification Interface: Load and plot data, and load corresponding feature matrix.

4.1 Activity Classification

In order to allow for more advanced analysis, several user defined options are introduced. Firstly, an object group labeled "**Activity Classification**" is created for the activity classification phase, and includes the user defined parameters. For this phase, the user can choose to train the built-in RF activity classifier described in Chapter IV with the pre-existing data included in the GUI by selecting

the **"Train using existing data"** checkbox (Figure VII.12). This data corresponds to the activities performed by both the HS and the PD patients during the acquisitions performed in this study.

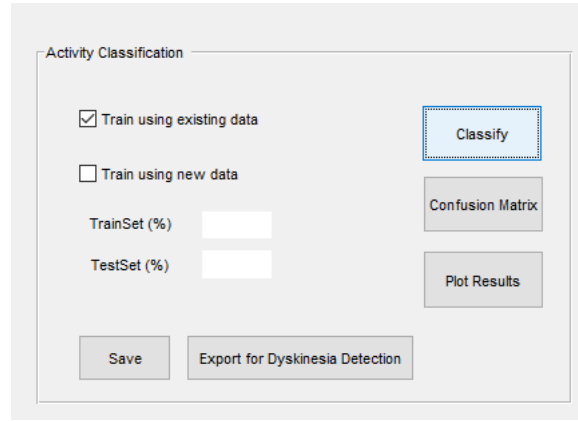


Figure VII.12 – Classification Interface: Activity classification options.

By clicking the **"Classify"** button, a popup window appears that introduces several inclusion criteria to the user (Figure VII.13). The inclusion criteria are categorised as "Subjects", "Sessions" and "Modules". The user can then select which subject's data (HS and PD subjects), which session performed by the selected subjects and the module positions to which the data corresponds, to be included in the training. For example, in Figure VII.14, the user chose to include in the training the data collected from three healthy subjects (HS04, HS05, & HS07) and two PD patients (PD02 & PD03), during only the first day of acquisition (Day01), and corresponding to the ankle, hip and thigh modules alone. The file containing the observations to be classified, FM_arranged, is therefore used as the test set.

The user can also choose to select the **"Train using new data"** checkbox in order to train the classifier using the newly introduced data. The purpose of this procedure is to enrich the database included in the GUI or, for an independent analysis, allow the user the ability to perform subject-specific training and testing. The objective here is to give the user the option of incorporating a portion of the newly acquired data with the pre-existing HS and PD patients datasets in the GUI for classifier training, and the remaining portion of newly acquired data is used for classifier testing. The second option is for an independent subject-specific analysis. In this case the user defines a portion of the newly acquired data to act as the training set for the classifier, and the remaining portion would be considered as the testing set. This analysis could be very interesting when comparing the classification performance obtained when considering a global approach and that obtained when considering a personalised subject-specific approach.

Once the activity classification technique is decided and performed by the user, four variables are automatically exported to the MATLAB workspace. These variables, labeled "AC1, AC2, AC3 & AC4" (Table VII.1), represent the output of the classifier. Each variable contains the raw data that is classified as one of the four activities extracted from the dataset used for testing. The user therefore

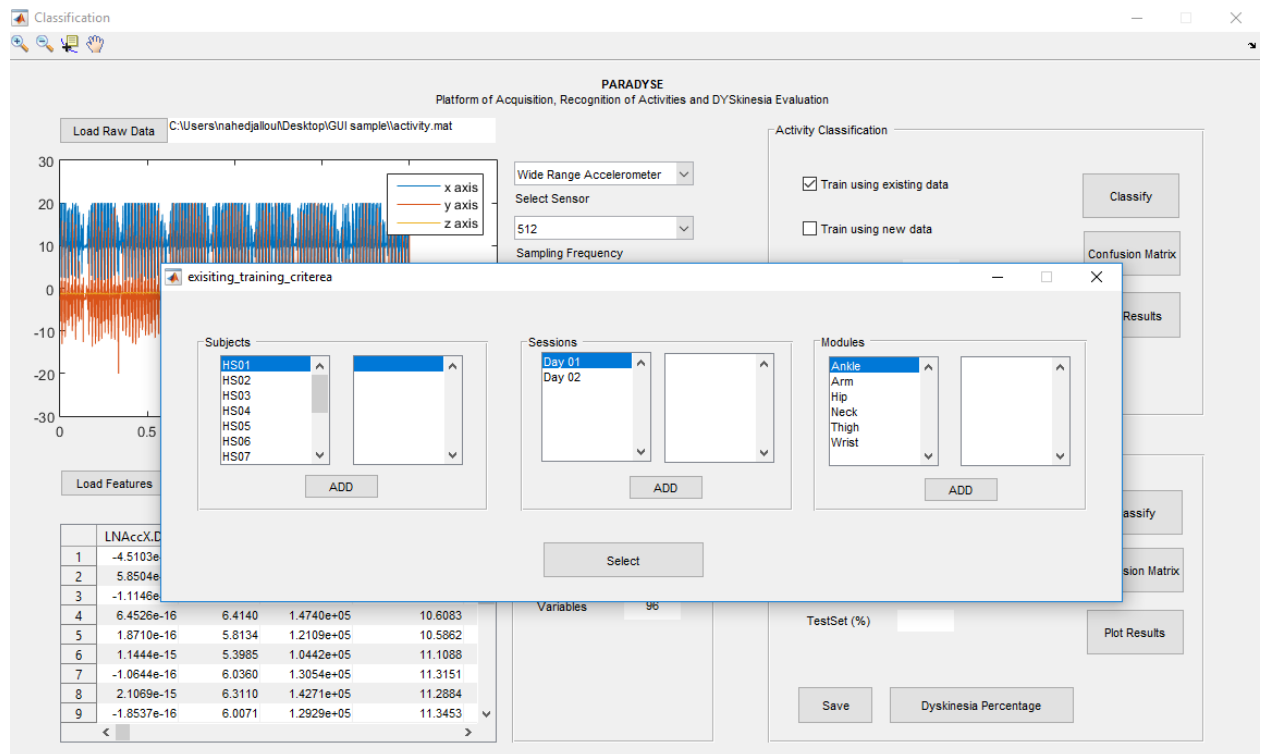


Figure VII.13 – Classification Interface: Activity classification train using existing data.

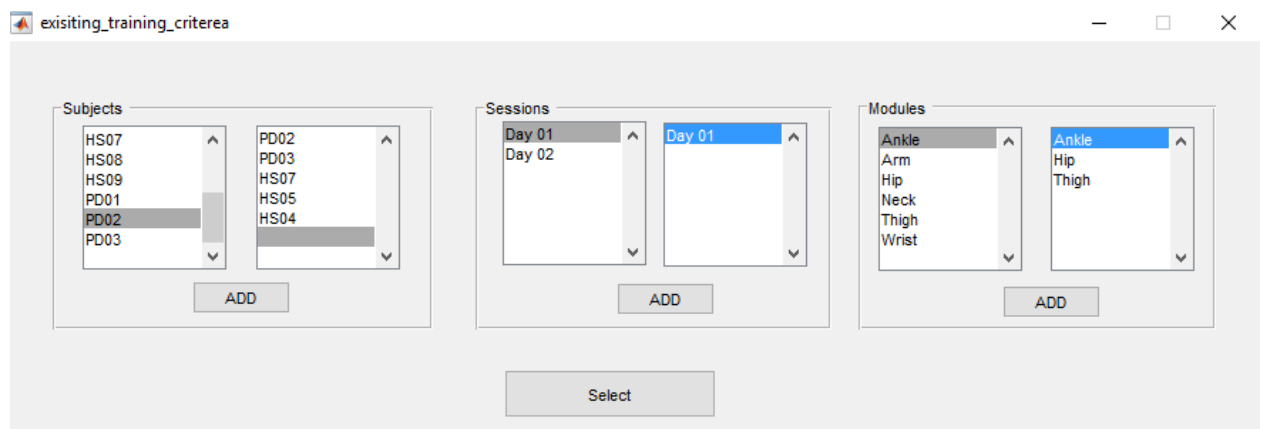
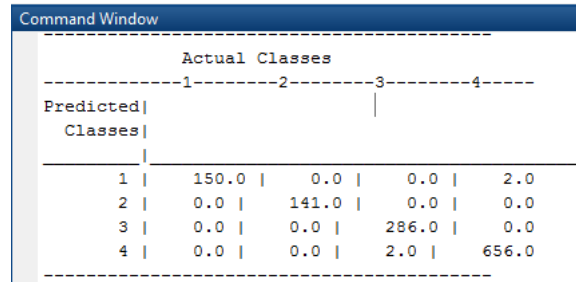


Figure VII.14 – Classification Interface: Activity classification example for training criteria using existing data.

has the liberty to perform further analysis on these classified activities, or automatically export the classified activities for dyskinesia detection by clicking on "**Export for Dyskinesia Detection**" which would be the application of *App3* as described in Chapter IV.

The "**Confusion Matrix**" button in this object group, on the other hand, outputs a variable labeled "AC_confusion_matrix", which shows the ratio of correctly classified activities if the test set's true activity classes are provided. An example of this output variable is shown in Figure VII.15.



		Actual Classes			
		1	2	3	4
Predicted Classes	1	150.0	0.0	0.0	2.0
	2	0.0	141.0	0.0	0.0
	3	0.0	0.0	286.0	0.0
	4	0.0	0.0	2.0	656.0

Figure VII.15 – Classification Interface: Confusion matrix variable output to the command window.

The "**Plot Results**" button in this object group is aimed to show the performance of the activity classifier for the selected training and testing data. This part of the GUI is still currently being developed and therefore will not be detailed in this thesis.

4.2 Dyskinesia Detection

Another object group is also created for the dyskinesia detection phase. This process was separated from the activity classification phase in order to provide the user with the ability to perform dyskinesia detection on the collected data without performing activity classification, in other words similar to *App1*, described in Chapter IV.

If the user chooses to perform classification on manually separated activity datasets, similar to *App2*, then the feature matrix loaded into the Classification GUI should be the one corresponding to each separate activity data.

On the other hand, if the user chooses to perform dyskinesia detection on the automatically classified activity datasets using the Activity Classification object group, similar to *App3*, then the automatically exported feature matrices corresponding to each classified activity should be loaded into the Classification GUI.

Similar to the activity classification phase, several training options are also provided to the user in this case. Figure VII.16 shows an example in which the user selected the "**Train using existing data**", which signifies training the built-in RF classifier for dyskinesia detection using the pre-existing datasets. These datasets correspond only to the three PD patients and do not include the data collected from the healthy individuals.

Once the user clicks the "**Classify**" button in this case, another popup window will appear indicating the inclusion criteria to be defined. The user can choose to include data from all or any of the pre-

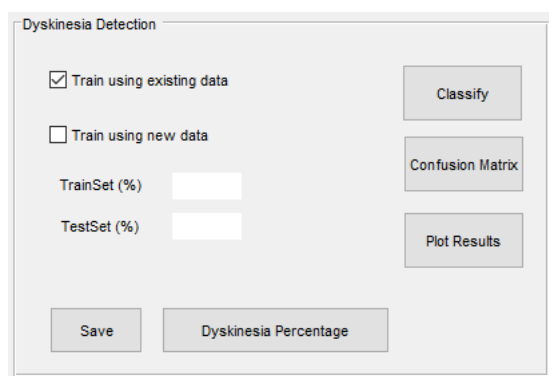


Figure VII.16 – Classification Interface: Dyskinesia detection example for training criteria using existing data.

existing PD patients' datasets labeled as "PD01, PD02 & PD03", specify the session to be included by choosing "Day01, Day02 or both", and select the modules to which the data corresponds (Figure VII.17).

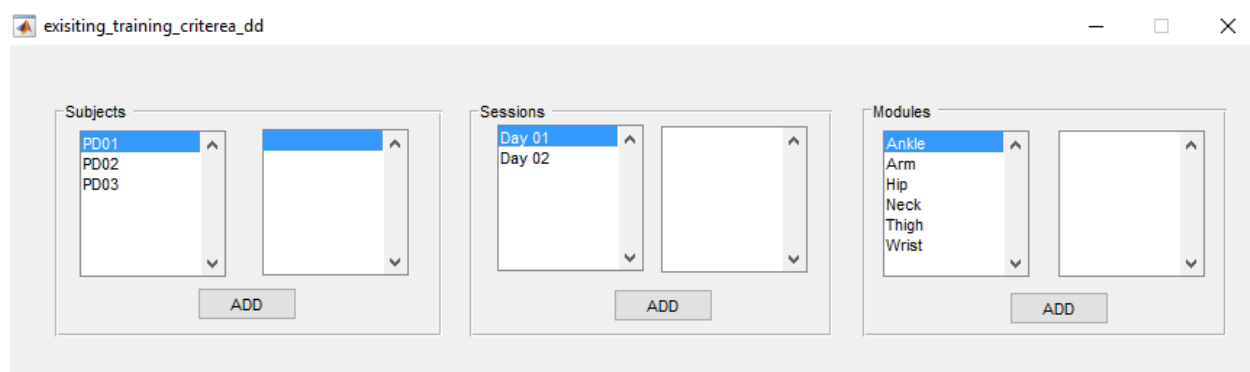
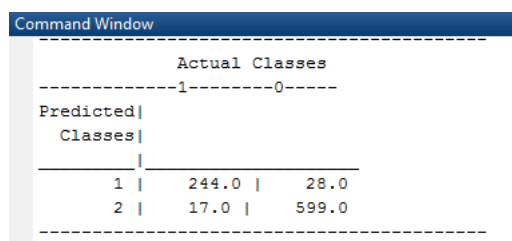


Figure VII.17 – Classification Interface: Selection of data to include in the training set for dyskinesia detection.

On the other hand, the user can select the "**Train using new data**". In this case, the user must also define a percentage of the data to act as the training set and the remaining percentage to act as the testing set.

Following the detection of dyskinesia, two variables are automatically exported into the workspace, which are labeled "Dys" and "NoDys" (Table VII.1). These variables contain the raw data classified as dyskinetic and non-dyskinetic, respectively, from the dataset used for testing. The user can then click on the "**Confusion Matrix**" button to view the confusion matrix showing the ratio of correctly classified dyskinetic instances, in the case where the test set's true dyskinesia classes are provided (Figure VII.18). The confusion matrix is also exported to the workspace as a variable labeled "DD_confusion_matrix".

The "**Plot Results**" and "**Dyskinesia Percentage**" options are still under development. However, the objective is to be able to show the the performance of the classifier in detecting dyskinetic instances for the selected training and testing instances using the "**Plot Results**" button. It is also interesting, from a clinical point of view, to be able to quantify the percentage of time spent in a dyskinetic state



		Actual Classes	
		1	0
Predicted Classes	1	244.0	28.0
	2	17.0	599.0

Figure VII.18 – Classification Interface: Confusion matrix variable output to the command window.

during the total period of acquisition. This purpose is going to be achieved using the "**Dyskinesia Percentage**" button, and will provide further information into the tested patient's overall motor condition.

5 Future Prospects

A clear view of the objectives in terms of signal acquisition, analysis and processing have provided a global understanding of the required functions of this platform. The processing methods applied in this study have been incorporated in a way that provides the user with liberty in performing the analysis under different conditions. The user-defined options are aimed towards driving the advancement of the monitoring system.

The importance of such an interface is attributed to the need for providing a straightforward and time-efficient method to perform the analyses. More acquisitions are envisioned in the scope of this project, and new data will be collected from both healthy individuals and PD patients. As such, the database will be enriched and there is interest in performing the previously tested methods for a larger, and more heterogeneous population. PARADYSE therefore provides a user-friendly and standardised means of performing the required analysis to further refine the accuracy of the results and the monitoring system as a whole.

Some additional developments in the GUI include the incorporation of the methods described in Chapter V, which are based on graph connectivity. Certainly enriching the database in terms of HS and PD patients data from additional acquisitions will provide insight into the validity of this method and its advantage in providing a visual interpretation of the relationship between the modules considered in the monitoring system.

Finally, the prospects of this project include implementing the proposed monitoring system in research efforts aimed towards detecting LID in PD patients and improving the understanding of this phenomenon. In order to achieve that, the system must provide output in ways that are interpretable from a clinical standpoint. The development of a GUI able to output such results therefore promotes the advancement towards this goal. The following steps include finalising the developed platform and applying for a software licence in order to launch the platform as part of the monitoring system.

Bibliography

- [1] S. T. SMITH. *MATLAB: advanced GUI development*. Dog ear publishing (2006).
- [2] I. MATHWORKS. *MATLAB: the language of technical computing. Desktop tools and development environment, version 7 , 9*. MathWorks (2005).

Conclusion and perspectives

Parkinson's disease is one of the most common and devastating neurological diseases and the absence of a cure for the disease has directed treatment towards minimising the symptoms of PD. As such, Levodopa remains to be the gold standard in terms of medication dealing with PD's motor symptoms. Despite the deterioration of the drug's positive effect after a few years, Levodopa is still considered to be the most effective drug in relieving PD motor symptoms. The main side effect of Levodopa manifests as dyskinesia and a diminishing period of time in which the drug is considered to be effective. The objective is to prolong the therapeutic window of Levodopa while delaying and minimising the prevalence of dyskinesia. In order to do that, the prescribed dose and frequency of Levodopa must be adjusted and managed according to the patient's responsiveness and the prevalence of LID. Therefore, an accurate, objective and automated method for the detection of LID is necessary.

The objective of this work was to develop a complete system of acquisition and movement analysis for the automated and objective detection of LID in PD patients. The work described in this thesis was funded by the drug development and pharmaceutical research company, Biotrial. The project focuses on the detection of LID in PD patients as part of the evaluation of Levodopa and the enhancement of the therapeutic plan. The aim of this conclusion is not to come back to main quantified results obtained throughout this thesis. These results can be found at the end of each chapter. We would prefer to insist on several interesting contributions that this thesis has provided:

- The development and implementation of an automated system for the recording of movements of PD patients suffering from LID. The system is composed of six Shimmer3 IMUs, each containing two accelerometers, a gyroscope and a magnetometer. A pilot system was designed on the subject's body at the following positions: ankle, hip, thigh, wrist, arm and neck. A protocol of simple daily life activities was setup for the data acquisition process, which took place in a laboratory setting setup to resemble a home environment.
- The proposition of a reliable and objective method for the detection of LID phases in PD patients based on a pattern recognition scheme. Following the data collection and processing steps, several approaches for the detection of dyskinesia were pursued. The purpose of these different approaches was to evaluate the accuracy of dyskinesia detection for a dataset that contained data corresponding to different activities versus that containing data that corresponded to a single activity. As such, we designed an activity classifier able to distinguish between the activities

performed during the protocol. The activity classifier, first evaluated on healthy individuals, was trained to distinguish between four classes of activities (walking standing, lying and sitting), which encompassed the activities performed during the protocol. After comparing the performance obtained using a number of different classifiers, the results showed that a Random Forest classifier yielded the best results for our application.

- The proposition of a system with a minimum number of sensor units. As mentioned in the objectives of this thesis, the aim is to develop an ambulatory system using a minimal number of modules, in order to ensure accurate detection of LID while minimising patient discomfort. Therefore, the significance of each module position with respect to detecting dyskinesia is assessed. The results showed that the modules positioned at the ankle, hip and thigh were most important for detecting dyskinesia, since classification using the data collected from each of these modules showed higher overall accuracies.
- The implementation of a new approach based on complex network analysis. The system of body worn IMUs is represented as a network structure, where each IMU represents a node and the correlation between them represents the links of the network. An activity classification network was constructed to evaluate the relationship between the different IMUs with respect to different activities performed by healthy individuals, and a dyskinesia detection network was constructed to evaluate the same relationship with respect to the prevalence of dyskinesia in PD patients. However encouraging, these results are considered as preliminary and further testing is necessary in order to validate this method.
- The performance of a prior validation test through a long duration, unsupervised acquisition at one of the PD patients' home. The purpose of this acquisition was to validate the developed system in a real-world environment. Unfortunately, due to a software error, only the data collected from the ankle module was preserved, and as such the evaluation was performed using this data. The patient was recorded at her home for a period of around 5.5 hours while she performed various daily life activities. Two separate training approaches were evaluated in this case. The first, labeled as the global approach, consisted in using the data collected from the PD patients in the previous short duration acquisitions as the training set. The second approach, labeled as the subject-specific approach, consisted in using the data collected from the patient herself during the previous short duration acquisitions as the training set. Data collected from the patient during the long duration acquisition would act as the testing set. The results show that, as previously, the activity classification phase helps to increase the accuracy of dyskinesia detection. While the subject-specific approach does offer acceptable results, it is very sensitive to the patient's conditions. The global approach appears to yield a better performance in terms of dyskinesia detection. One explanation for this might be that in pathology, states are perhaps less reproducible. Therefore, considering a global approach, while less precise, maybe privileged at first in order to progressively refine the classification by continuous adaptively and auto-learning.

- The development of Platform of Activity Recognition and DYSkinesia Evaluation (PARADYSE) as part of the final system to be delivered to Biotrial. This platform is intended to serve as interface for the processing and analysis of data collected using the developed system. The proposed methods of analysis are incorporated into the platform providing the system with a simple user interface to evaluate collected data and further advance the system as a whole.

This work has prompted several perspectives. The first of which includes the elaboration of a protocol that permits the evaluation of the system using a larger and more comprehensive database projected to consist of thirty patients. The objective here is to resume the simplified protocol and perform the acquisitions on patients while leaving room for sufficient autonomy that would allow simulating real life conditions. These new acquisitions will follow the conclusions drawn out during this study regarding the methodology applied, and will include:

- The pattern recognition method with extraction of features, described in Chapter IV, has so far been based on a global approach regarding the modules. In other words, all the modules comprising the system of acquisition have been attributed equal weights in terms of the decision making process. We might apply, as in other projects pursued in our laboratory [1], an approach in which the decision making process for dyskinesia detection is distributed over the modules based on weights attributed for each module depending on that module's individual performances.
- The complex network method applied has resulted in some interesting outcomes however, based on the results obtained, lacks in achieving the desired accuracy. As such, exploring the relationship between the different modules under new conditions will help clarify their impact on the results. This pursuit, which has been discussed in Chapter V, along with the principle evoked in the previous point could offer a new perspective on this approach.
- Last but not least, the long-duration acquisition performed has permitted to reveal the impact of the learning strategy on the classification phase. As presented in our conclusions, a global strategy is preferred. The next envisioned step is to refine the learning process through newly acquired data, iteratively and in real-time. This process aims to render the classification more specific to the patient, while being based on initial data acquired from a diverse PD population.
- Finally, a technique for validating the obtained results must be thought out. Current studies base their validation on annotations given by independent experts. Seeing as this is the only available method of confirming results up to this point, it is included as an initial assessment for our study. However, a method based on long-term monitoring of patients and progressive evaluation is envisioned as means to eliminate the factor of subjectivity introduced by the current validation techniques, as described in [2].

The ensemble of these developments constitute new scientific challenges that might also be integrated into PARADYSE in order to provide a somewhat autonomic station that is specific to each patient.

Conclusion

These challenges motivate us to further explore the aspects of this work in hopes to provide an answer to the problem invoked by Levodopa therapy. The purpose here remains to pursue an accurate, objective and cost-conscious method that will aid in providing PD patients with efficient and successful treatment through Levodopa.

Bibliography

- [1] A. I. HERNANDEZ, G. CARRAULT, F. MORA, L. THORAVALE, G. PASSARIELLO AND J. M. SCHLEICH. *Multisensor fusion for atrial and ventricular activity detection in coronary care monitoring*. IEEE Transactions on Biomedical Engineering vol. 46, no. 10, pp. 1186-1190, (1999).
- [2] ESPAY, A. J., BONATO, P., NAHAB, F. B., MAETZLER, W., DEAN, J. M., KLUCKEN, J., ESKOFIER, B. M., MEROLA, A., HORAK, F., LANG, A. E., REILMANN, R., GIUFFRIDA, J., NIEUWBOER, A., HORNE, M., LITTLE, M. A., LITVAN, I., SIMUNI, T., DORSEY, E. R., BURACK, M. A., KUBOTA, K., KAMONDI, A., GODINHO, C., DANEALD, J. F., MITSU, G., KRINKE, L., HAUSDORFF, J. M., BLOEM, B. R., PAPAPETROPOULOS, S.. *Technology in Parkinson's disease: Challenges and opportunities* Mov Disordorders, 31: 1272-1282. doi:10.1002/mds.26642 (2016).

List of publications

International journals

1. **N. Jalloul**, F. Porée, G. Viardot, P. L'Hostis, and G. Carrault. Activity Recognition Using Multiple Inertial Measurement Units. *IRBM, Elsevier* 37(3), 180–186, (2016).

International conferences

1. **N. Jalloul**, F. Porée, G. Viardot, P. L'Hostis, and G. Carrault. Detection of Levodopa Induced Dyskinesia in Parkinson's Disease Patients Based on Activity Recognition In *37th Annual International Conference of the IEEE Engineering in Medicine and Biology Society, (EMBC)*, Milan 2015, pp.5134-5137.
2. **N. Jalloul**, F. Porée, G. Viardot, P. L'Hostis, and G. Carrault. Feature selection for activity classification and Dyskinesia detection in Parkinson's disease patients In *International Conference on Advances in Biomedical Engineering (ICABME), IEEE*, Beirut 2015, pp.146–149.
3. **N. Jalloul**, F. Porée, G. Viardot, P. L'Hostis, and G. Carrault. Activity Recognition Using Multiple Inertial Measurement Units In *Recherche en Imagerie et Technologies pour la Santé (RITS)*, Dourdan 2015.

Reduction by Feature Selection

This appendix provides complementary information on the strategy of reducing the total number of modules included in the monitoring system through feature selection. This strategy is described in Chapter IV section 2.4 and focuses on testing different feature selection methods in order to determine a subset of features that provides reliable classification while corresponding to a lower number of modules.

Initially, Cfs is used to extract a subset of features that is considered to be highly correlated with the class while having low intercorrelation. Two separate experiments are performed:

- Experiment I: the data collected from the nine HS is used to determine the features most relevant to the different activity classes.
- Experiment II: the data collected from PD patients is used to identify the features most relevant to the dyskinesia class.

In Experiment I, concerning the data collected from healthy subjects only, the classes are defined as the seven activity groups performed during the protocol {Walking, Standing, Lying, Sitting, Writing, Reading, and Eating}. Using the Cfs evaluation method, we obtained a subset of 50 features selected from the original feature set that are considered to be highly correlated to the activity classes. The following feature selection methods were also applied and only the first 50 highest ranked features were retained: Chi-Squared, Gain Ratio, Information Gain, OneR, and ReliefF Figure A.1 shows the distribution of the selected features with respect to the six module positions. Based on the feature rankings obtained, the most pertinent module positions appear to be the Ankle, Hip and Thigh. In order to evaluate the performance of the RF classifier, activity classification was performed using the previously listed feature selection methods. We then proceed to evaluate the classification performance by decreasing the sizes of the selected feature subsets in order to achieve a minimum size that corresponds to a reduced number of modules. The overall accuracy of classification obtained in each case is presented in Figure A.2.

The overall accuracy of classification obtained when considering the seven activity classes, and the entire feature set computed based on the data collected from the six module positions, was obtained at 87.95%. After applying the feature selection methods, it was noted that the highest overall accuracy of classification obtained at 88.05%, occurred when applying the Information Gain method with a subset of the five highest ranked features. These features corresponded to the Ankle, Neck and Thigh modules. However, the difference in overall accuracies obtained when using the feature selection methods, and when varying the size of the subset, is less than 1%. While on the other hand the ranking of the features delivered by each of the feature selection methods was inconsistent. Thus, determining the most relevant module positions through feature selection proved to be difficult.

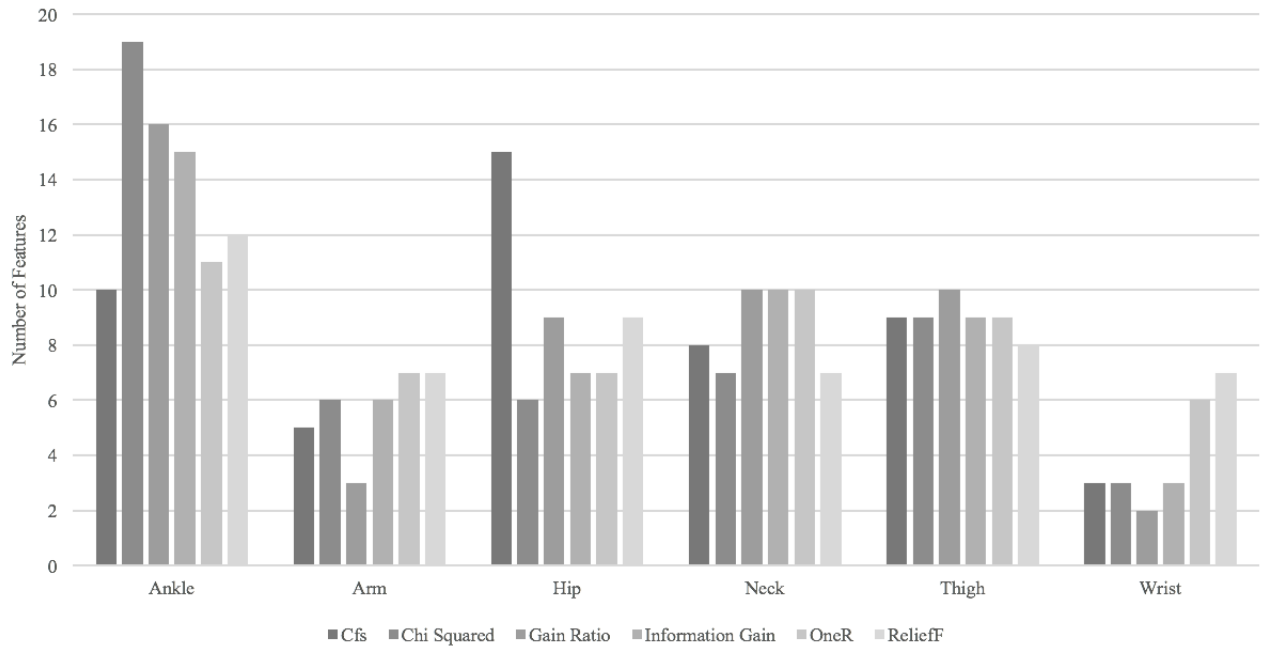


Figure A.1 – The distribution of selected features with respect to the module position by each method for the data collected from HS.

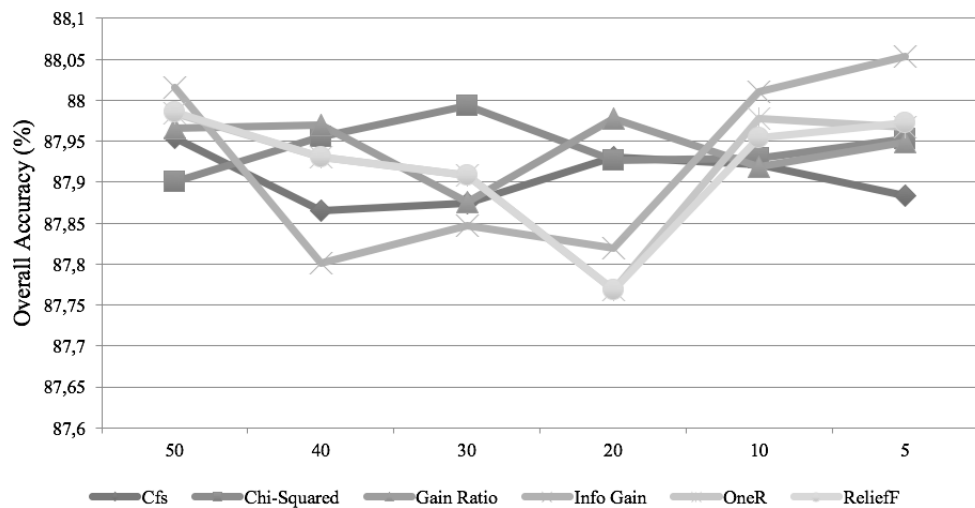


Figure A.2 – Overall accuracy of activity classification obtained using the different feature selection methods, and by reducing the size of the selected subset of features.

In Experiment II, concerning the data collected from PD patients only, the classes are defined as the motor states experienced by the patients {Dyskinetic, and Non-Dyskinetic}. Using the Cfs evaluation method, a subset of 100 features considered as highly correlated to the presence or absence of dyskinesia is chosen from the original feature set. Similarly to before, the listed feature selection methods are also applied and only the first 100 ranked features are retained. Figure A.3 shows the distribution of the selected features with respect to the six module positions. Based on the obtained rankings, the modules positioned at the Ankle and Thigh seem to be most relevant to the patients' motor state.

In this case, dyskinesia detection was done using a KNN classifier. When considering the entire feature set corresponding to the six module positions, the overall accuracy for dyskinesia detection was obtained at 86.44%. Dyskinesia detection was repeated using the subset of selected features by each feature selection method, and by decreasing the sizes of the subsets in order to achieve a minimum size that corresponds to a reduced number of modules. The overall accuracy of dyskinesia detection obtained in each case is presented in Figure A.4. The Information Gain feature selection method provided the highest overall accuracy of dyskinesia detection at 84.5% when considering a subset of the first fifty ranked features. These features corresponded to all module positions and hence could not offer a reduction of the total number of modules.

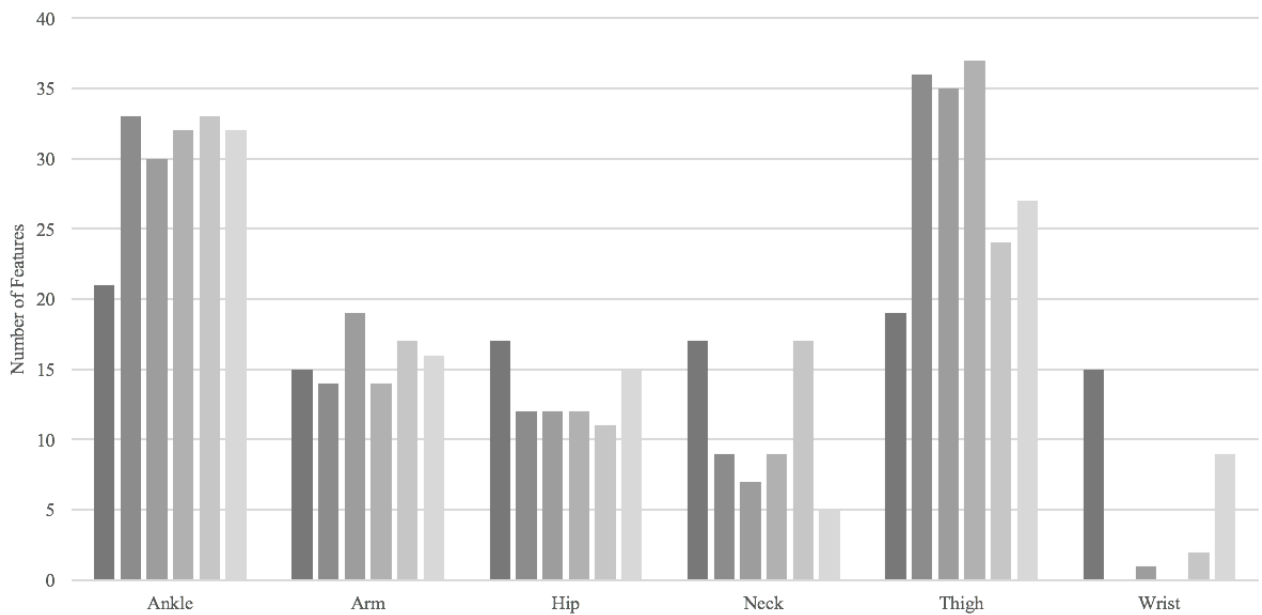


Figure A.3 – The distribution of selected features with respect to the module position by each method for the data collected from PD patients.

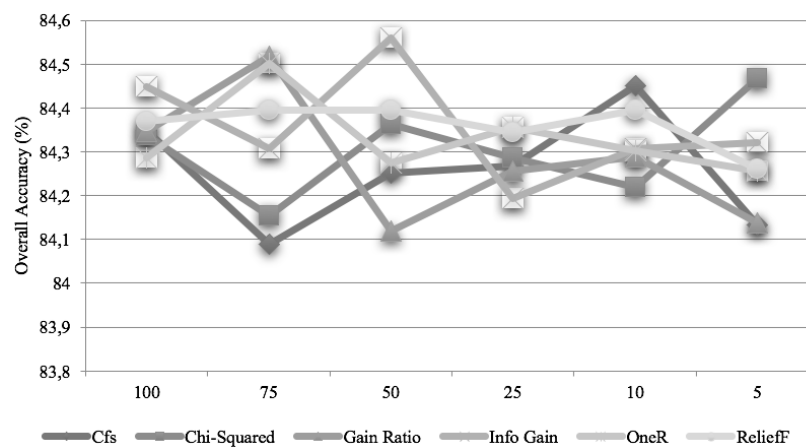


Figure A.4 – Overall accuracy of dyskinesia detection obtained using the different feature selection methods, and by reducing the size of the selected subset of features.